E-ISSN: **2636-7688**

year **2026**
volume **33**
issue **8**

ANNALS OF MEDICAL RESEARCH

The Official Journal of the Inonu University Faculty of Medicine

Original Articles

İNÖNÜ UNIVERSITY PRESS

ANN MED RES

ANN MED RES

ANNALS OF MEDICAL RESEARCH

The Official Journal of Inonu University Faculty of Medicine

Editorial Board

| Volume: 33 | Issue: 8 | August 2026 |

ANN MED RES

ANNALS OF MEDICAL RESEARCH

The Official Journal of Inonu University Faculty of Medicine

| Volume: 33 | Issue: 8 | August 2026 |

Editorial Advisory Board

ANN MED RES

ANNALS OF MEDICAL RESEARCH

The Official Journal of Inonu University Faculty of Medicine

Table of Contents

| Volume: 33 | Issue: 8 | August 2026 |

Original Articles

Ann Med Res

Current issue list available at Ann Med Res

Annals of Medical Research

journal page: annalsmedres.org

Strain-dependent differences in neuroplasticity markers related to memory

Ilknur Dursun [a], Ertugrul Kilic [b], Birsen Elibol [c,*]

[a] Istanbul Health and Technology University, Faculty of Medicine, Department of Physiology, Istanbul, Türkiye
[b] Istanbul Medeniyet University, Faculty of Medicine, Department of Physiology, Istanbul, Türkiye
[c] Istanbul Medeniyet University, Faculty of Medicine, Department of Medical Biology, Istanbul, Türkiye
*Corresponding author: elibolbirsen@gmail.com (Birsen Elibol)

MAIN POINTS

- Hippocampal-dependent spatial memory deficits are a core feature of several neurological and psychiatric disorders, and rodent strain differences may influence the translational relevance of preclinical findings.
- Although Wistar, Sprague Dawley, and Long Evans rats all acquired spatial memory under identical conditions, strain-specific differences in behavioral performance suggest that cognitive outcomes may be differentially interpreted depending on the animal model used.
- Strain-dependent variations in hippocampal BDNF and DCX expression indicate that baseline neuroplasticity profiles differ between commonly used rat strains, which may critically affect the interpretation of therapeutic and biomarker studies targeting learning and memory dysfunction.

Cite this article as: Dursun I, Kilic E, Elibol B. Strain-dependent differences in neuroplasticity markers related to memory. *Ann Med Res*. 2026;33(8):362–368. doi: 10.5455/annalsmedres.2026.01.011.

ABSTRACT

Aim: Spatial learning and memory both rely critically on hippocampal plasticity which are a core feature of several neurological and psychiatric disorders; but commonly used different rat strains might exhibit differences in these processes which may influence the translational relevance of preclinical findings Herein, we examined the long-term spatial memory of adult Wistar (n=5), Sprague Dawley (n=6), and Long Evans (n=5) rats, and their hippocampal expression of two plasticity markers: brain-derived neurotrophic factor (BDNF) and doublecortin (DCX).

Materials and Methods: The animals were trained in the Morris water maze for four days, followed by a probe trial with no platform. Hippocampal BDNF and DCX protein levels were quantified by Western blotting.

Results: All strains learned the task, as indicated by a decrease in escape latency and swim distance over time. Sprague Dawley rats swam faster than the other strains, suggesting that swim distance evaluates learning independently of speed. On the first training day, Wistar rats swam the shortest distances, whereas by the final day Long Evans rats did. In the probe trial, Sprague Dawley rats spent a greater proportion of time in the target quadrant than Wistar rats did. Long Evans rats displayed an intermediate pattern. At the molecular level, Sprague--Dawley rats had higher hippocampal BDNF levels than Wistar and Long-Evans rats. DCX levels were higher in Sprague Dawley and Long Evans rats than in Wistar rats.

Conclusion: These findings suggest that although all three strains can acquire and retain spatial memory under identical conditions, they differ in behavioral strategies and hippocampal plasticity. Therefore, strain background should be carefully considered when designing and interpreting rodent studies of learning and memory.

Keywords: BDNF, DCX, Morris water maze, Rat strains, Spatial learning and memory

Received: Jan 14, 2026 **Accepted:** May 22, 2026 **Available Online:** Aug 25, 2026

INTRODUCTION

The capacity for spatial learning and memory is critical for living beings to develop proper relationships with their environments and to move about them. In mammals, the hippocampus is the primary brain region associated with learning and memory. The hippocampus is involved in the experience-dependent synaptic plasticity that determines the formation and reorganization of synaptic connections [1,2]. The association of spatial memory and hippocampal plasticity is the reason that tasks that involve movement (like the Morris Water Maze) are commonly used to study the cognitive abilities and its cellular mechanisms in rodents [3,4].

At the cellular level, brain-derived neurotrophic factor (BDNF) is regarded as a key molecule for the survival and differentiation of neurons. Besides its basal functions, BDNF also plays a role in activity-dependent synaptic plasticity, especially in hippocampal circuits. BDNF contributes directly to several forms of hippocampus-dependent learning and memory functions by regulating synaptic strength and connectivity [5,6]. The induction and expression of long-term potentiation (LTP), the physiological basis of memory, also depend on BDNF. Furthermore, increased expression of BDNF in

the hippocampus is associated with training on spatial navigation tasks while BDNF signaling impairment disrupts spatial learning and memory [7-10].

Doublecortin (DCX), one of the microtubule-associated proteins expressed by immature neurons, is another well-established marker of hippocampal plasticity [11]. In the adult brain, expression of DCX is primarily seen in the subventricular and subgranular zone [12]. These areas are responsible for the lifelong neurogenic process, as they ensure a steady supply of newly formed neurons [13]. Numerous studies have established the strong association of newly formed hippocampal neurons with adult learning and memory [14-17]. This indicates that the adult-generated hippocampal neurons tracked by DCX expression are a vital part of the circuitry underlying learning and memory. Thus, the number of DCX-positive cells and the morphological changes of these cells could account for differences in cognitive function. Moreover, in studies of hippocampal functions, DCX has served as a significant integrative tool at the molecular, cellular, and behavior levels [18]. Overall, BDNF and DCX are complementary markers of molecular and cellular processes underlying spatial long-term memory.

Behavioral neuroscience and neuropsychopharmacology have extensively utilized laboratory rodents [19,20]. Previous studies have demonstrated that different strains of rats (Wistar, Sprague Dawley, and Long Evans) exhibit distinct profiles of learning and memory abilities. Gokcek-Sarac and her colleagues investigated the performance of three strains of rats in a partially baited radial arm maze and found differences in spatial learning among strains [21]. The Sprague Dawley rats showed the worst performance in working and reference memory tasks, while Wistar rats and the outcrossed Wistar/Sprague-Dawley rats, who learned the task most rapidly, demonstrated better working memory. Long Evans rats exhibited an intermediate performance level [2]. In a different study, Long Evans rats also successfully learned a lever-press response in a two-object discrimination test. They demonstrated the only strain that exhibited clear short-term object recognition. However, albino Wistar and Sprague-Dawley rats showed relatively better performance in the swim maze but poorer discrimination learning [22]. Another study examined the effects of drugs. The rats were administered intracerebroventricular galanin and then tested in the Morris water maze. It was found that galanin clearly impaired the spatial learning and probe trial performance of Wistar and Sprague Dawley rats, while Long Evans rats were largely unaffected [23].

The present study aims to investigate strain-dependent differences in spatial long-term memory and hippocampal neuroplasticity markers in Wistar, Sprague Dawley, and Long Evans rats. Specifically, we compared their performance on a hippocampus-dependent spatial memory task and explored the relationship between this behavioral variability and hippocampal BDNF levels and DCX-defined immature neuron populations.

MATERIALS AND METHODS

Animals

In the present study, 4-month-old Wistar (W, n=5), Sprague Dawley (SD, n=6), and Long Evans Hooded (LE, n=5) rat strains were used. All animals were housed under standard laboratory conditions (22 ± 2 °C, 12 h light/dark cycle) with free access to food and water. All experimental procedures were conducted in accordance with the ethical principles of the ARRIVE Guidelines and were approved by the Istanbul Medeniyet University Animal Experiments Local Ethics Committee (İMÜ-HADYEK) (Approval no: 2025/3-1, Date: 26.03.2025).

Behavioral experiments

At the beginning of the experiment, the spatial learning and memory performance of all rats was assessed using the Morris Water Maze (MWM). The MWM apparatus consisted of a circular tank (125 cm in diameter and 60 cm in height) filled with opaque water, containing a hidden platform. To assess learning performance, rats were trained for 4 consecutive days, with 4 trials per day, to locate the hidden platform that remained in a fixed location using spatial cues. The rats were considered to have learned the task when the escape latency fell below 10 seconds. The latency to reach the hidden platform, the distance swum, and the swimming speed of the rats were monitored for 60 seconds using an automated video tracking system (EthoVision XT, Noldus Information Technology, Netherlands).

On the 5th day, a probe trial was applied to all rats. Therefore, the hidden platform was removed from the pool, and the time each rat spent in the target quadrant where the platform had previously been located was recorded using an automated video tracking system to evaluate spatial memory retention.

Sample collection and homogenization

At the end of the behavioral experiments, the rats were euthanized with ketamine (90 mg/kg, i.p.) and xylazine (10 mg/kg, i.p.) anesthesia. Their brains were removed and frozen on dry ice, and hippocampal tissues were dissected for molecular analysis. The samples were transferred to sterile tubes and stored at -80 °C until analysis.

Frozen tissues were homogenized using a lysis buffer containing 1M Tris-HCl (pH 6.8), 0.5 M EDTA, β-mercaptoethanol, 100% glycerol, bromophenol blue, distilled water, and a freshly added protease inhibitor. Homogenates were kept on ice for 20 min, then centrifuged at 14000 rpm for 15 min at 4 °C. The resulting supernatants were aliquoted into sterile tubes and stored at -20 °C until analysis.

Western blotting

First, total protein concentrations were determined using the Pierce BCA Protein Assay kit (Thermo Scientific, USA).

https://doi.org/10.5455/annalsmedres.2026.01.011

Equal amounts of protein were separated by SDS-PAGE and transferred onto PVDF membranes using the Trans Blot Turbo system (Bio-Rad Laboratories, California, USA). The membranes were blocked with 5% non-fat milk in 0.1% Tween 20/0.1 M Tris-buffered saline (TBST) for 1 h at room temperature. After rinsing with TBST, the membranes were incubated overnight at 4°C with the primary antibodies BDNF (1:1000; Santa Cruz, USA) and DCX (1:1000; Thermo Scientific, USA), both diluted in blocking solution. After washing with TBST, membranes were incubated for 1 h at room temperature with horseradish peroxidase-conjugated goat anti-rabbit (1:5000; Cell Signaling Technologies, USA) secondary antibodies, diluted in blocking solution. Protein loading was controlled by reprobing membranes with the β-tubulin antibody (1:1000; Cell Signaling Technologies, USA). Protein bands were visualized using enhanced chemiluminescence (Advansta, USA) and detected with a CCD camera on the Fusion FX7 imaging system (Vilber Lourmat, France). Densitometric analysis of protein levels was performed using ImageJ.

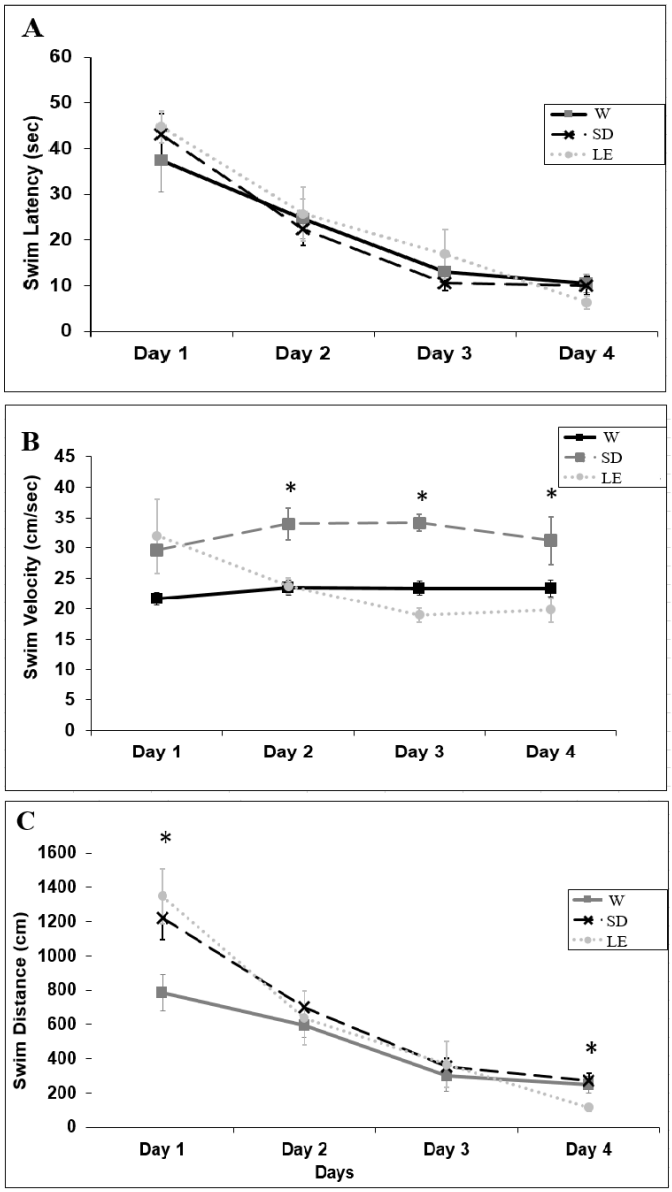

Figure 1. Acquisition of water-maze performance across four training days in three rat strains. (A) Swim latency (sec) to reach the hidden platform, (B) Swim velocity (cm/sec), and (C) Swim distance (cm) traveled to the platform are shown for Wistar (W), Sprague Dawley (SD), and Long Evans (LE) rats. Data are mean ± SD. Asterisks indicate significant differences at $p < 0.05$.

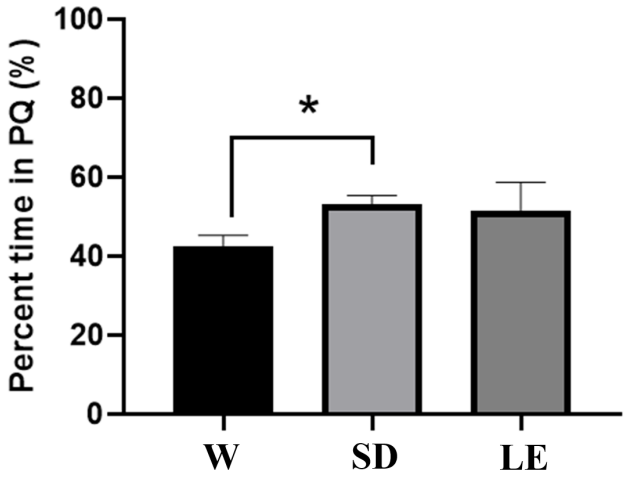

Figure 2. Probe trial performance in the water maze in three rat strains. Percent time spent in the platform quadrant (PQ) during the probe test is shown for Wistar (W), Sprague Dawley (SD), and Long Evans (LE) rats. Bars represent mean ± SD. Asterisks indicate significant differences at $p < 0.05$.

Statistical analysis

Statistical analyses were performed in GraphPad Prism 10 (GraphPad Software Inc., San Diego, CA). Data are reported as mean ± standard deviation (SD). A post hoc power analysis was performed using G*Power (version 3.1.9.7). Based on the observed effect size (0.332) and an alpha level of 0.05, the study's achieved statistical power was 0.74. Normality was assessed with the Shapiro-Wilk test. For statistical comparisons, the Kruskal-Wallis test with the Dunn-Bonferroni post hoc test, one-way ANOVA, and repeated-measures ANOVA with the LSD post hoc test were employed. In addition, Pearson's correlation test was used to assess linear correlations between probe data and molecular outcomes (BDNF and DCX values) within each group. Values of $p \leq 0.05$ were considered statistically significant.

RESULTS

Spatial learning and memory performances

Figure 1 shows the MWM acquisition performance across all rat strains. In the current study, according to two-way repeated measure ANOVA (strain X day), there were no between-group differences ($F(2,13) = 0.15$, $p = 0.86$) or day × group interactions ($F(6,39) = 0.83$, $p = 0.56$) for latency to

https://doi.org/10.5455/annalsmedres.2026.01.011

Table 1. The data of swim latency, swim velocity, and swim distance traveled to the platform in the Morris water maze for Wistar (n=5), Sprague Dawley (n=6), and Long Evans (n=5) rats.

Strain	Wistar		Sprague Dawley		Long Evans	
Swim latency (sec)						
DAYS	Mean	SD	Mean	SD	Mean	SD
1	37.4	15.3	43.1	11.4	44.8	7.8
2	24.6	9.7	22.3	8.7	25.7	13.1
3	13.1	9.1	10.6	3.9	16.9	12.2
4	10.4	4.4	9.9	5.0	6.3	3.3
Swim velocity (cm/sec)						
DAYS	Mean	SD	Mean	SD	Mean	SD
1	784.7	238.9	1222.1	308.2	1348.1	357.6
2	592.2	151.0	697.6	233.6	636.1	349.5
3	300.9	208.0	354.6	111.3	365.9	302.2
4	246.7	107.3	270.4	103.4	114.1	44.7
Swim distance (cm)						
DAYS	Mean	SD	Mean	SD	Mean	SD
1	21.7	2.5	29.7	1.3	27.7	7.1
2	23.5	2.8	33.9	6.4	23.7	2.9
3	23.4	2.5	34.1	3.6	18.9	2.6
4	23.4	3.1	31.2	6.7	19.8	4.6
Probe (% time in the Platform Quadrant)						
Median		(Min-Max)	Median	(Min-Max)	Median	(Min-Max)
43.0		33.0-49.0	51.5	47.0-62.0	45.0	35.0-77.0

Data are mean ± SD and median (minimum-maximum).

Table 2. The results of Pearson's correlation of Probe trial percent time correlations with BDNF and DCX values.

Probe trial percent time correlations with	Wistar (n=5)	Sprague Dawley (n=6)	Long Evans (n=5)
BDNF	r = 0.28, p = 0.81	r = 0.85, p = 0.35	r = -0.54, p = 0.64
DCX	r = -0.66, p = 0.54	r = 0.98, p = 0.12	r =- 0.80, p = 0.41

the escape platform. In addition, a significant decrease day by day in the latency to reach the hidden platform ($F(3,39) = 58.52$, $p < 0.001$) was observed in MWM training (Figure 1A). However, there were significant between-group differences ($F(2,13) = 23.23$, $p \leq 0.001$) and day × group interactions ($F(6,39) = 3.23$, $p = 0.01$) in the swim velocities of rat strains without any change day by day ($F(3,39) = 1.02$, $p = 0.39$) (Figure 1B). According to the post hoc LSD test, Sprague Dawley rats were faster than other rat strains ($p < 0.05$). Due to these differences in the swim velocities, swim distances were calculated to determine the more accurate learning performances [24]. According to two-way repeated measure ANOVA, while there was insignificant between-group differences ($F(2,13) = 1.6$, $p = 0.24$) among rat strains, there was a significant day × group interactions ($F(6,39) = 2.93$, $P = 0.02$) and day-effect ($F(3,39) = 64.27$, $p < 0.001$) for swim distance (Figure 1C). According to the post hoc LSD test, Wistar rats swam shorter distances than other strains on the first day of training ($p = 0.03$ for Sprague Dawley and $p = 0.01$ for Long Evans), whereas Long Evans rats swam shorter distances to reach the hidden platform on the fourth day of training ($p = 0.01$ for Sprague Dawley and $p = 0.04$ for Wistar) (Figure 1C). The corresponding descriptive statistics are provided in Table 1 to complement the graphical representations

For the MWM probe trial, which measures the time spent in the platform quadrant in the absence of an escape platform, strains differed slightly in the percentage of time spent there ($p = 0.08$) (Figure 2). As shown in Figure 2, a significant increase in the percentage of time spent in the platform quadrant was observed in Sprague Dawley rats compared with Wistar rats ($p = 0.03$). On the other hand, there was no significant difference in the percentage of time spent in the platform quadrant between Sprague Dawley rats and Long Evans rats ($p = 0.8$). While there was an increase in the percentage of time spent in the platform quadrant in the Long Evans rats compared to the Wistar rats, it did not reach the accepted significance level ($p = 0.2$) (Figure 2).

Molecular outcomes

To determine molecular mechanisms underlying strain-dependent differences in learning and memory, the relative levels of BDNF and DCX in hippocampal tissues from dif-

https://doi.org/10.5455/annalsmedres.2026.01.011

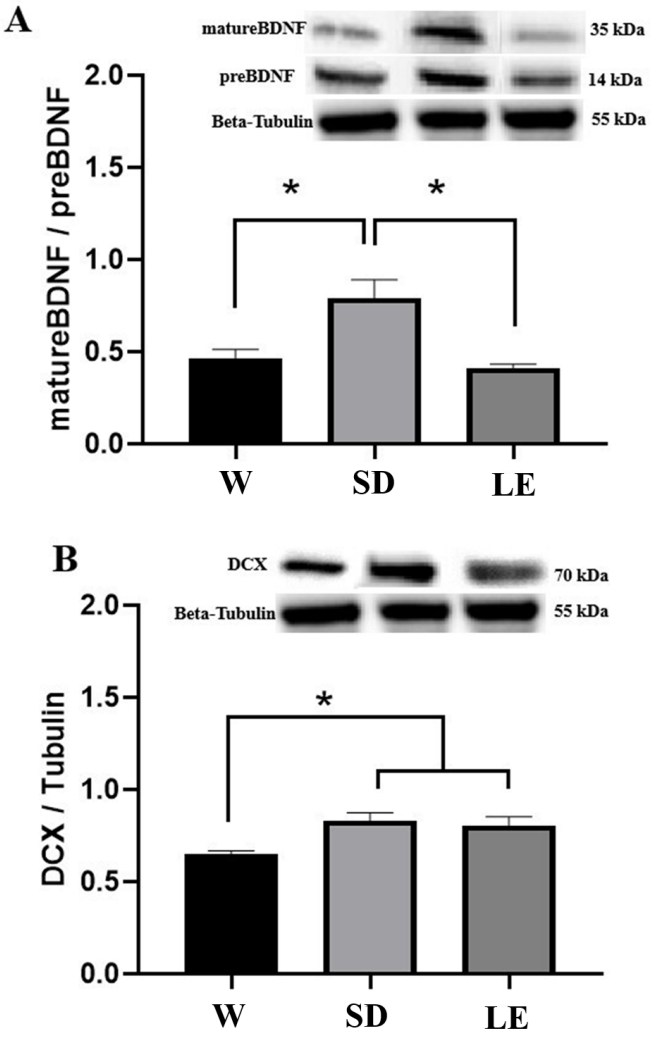

Figure 3. Hippocampal brain-derived neurotrophic factor (BDNF) and doublecortin (DCX) protein levels in three rat strains. (A) Representative Western blots and quantification of the ratio of matureBDNF to preBDNF in hippocampal tissue from Wistar (W), Sprague Dawley (SD), and Long Evans (LE) rats; β-tubulin served as a loading control. (B) Representative Western blots and quantification of DCX expression normalized to β-tubulin (DCX/tubulin) in the same samples. Bars represent mean ± SD for each strain. Asterisks indicate significant differences at $p < 0.05$. kDa: kilodalton.

ferent rat strains were evaluated (Figure 3). In the present study, there was a statistically significant increase in the mature BDNF levels of Sprague Dawley rats (0.79 ± 0.08) compared to the Wistar rats (0.46 ± 0.04) ($p = 0.01$) and Long Evans rats (0.41 ± 0.02) ($p = 0.006$) (Figure 3A). On the other hand, compared to that of the Wistar rats (0.65 ± 0.01), the DCX levels were significantly higher in the Sprague Dawley rats (0.83 ± 0.03) ($p = 0.01$) and Long Evans rats (0.81 ± 0.04) ($p = 0.03$) (Figure 3B).

Application of Pearson's correlation test to examine correlations between percent time spent in the target quadrant and BDNF and DCX values showed no correlation across strains (Table 2).

DISCUSSION

Variability in learning and memory performance among rat strains plays an important role in understanding and generalizing behavioral neuroscience findings. In a systematic comparison of seven male rat strains (Wistar, Wistar Kyoto, Sprague Dawley, Long Evans, LT, SHR, and BD-IX), Rybnikova and colleagues examined open-field behavior, anxiety- and depression-like behavior, circulating stress and thyroid hormones, and blood antioxidant capacity [25]. They found strain-specific differences rather than a single "standard" behavioral pattern. Locomotor and exploratory activity, anxiety scores, immobility in the forced swim test, the balance of glucocorticoids, thyroid-stimulating hormone and thyroxine levels, and total antioxidant activity significantly varied between strains [25]. Another comparative study examined Long-Evans and Sprague-Dawley rats housed in standard or enriched cages. Researchers used a broad behavioral battery, relevant to neuropsychiatric models, to conduct a detailed gene × environment study. The experiment demonstrated that both strain and environment influence behavior. Long Evans rats were more active, had lower prepulse inhibition, and learned operant tasks faster than Sprague-Dawley rats. Enriched housing reduced anxiety-like behavior and improved learning abilities, particularly in Long Evans rats. It slightly reduced prepulse inhibition in Sprague–Dawley rats. These findings overall highlight that strain and housing together affect cognitive and behavioral performance [26]. Therefore, this study compared long-term spatial memory and hippocampal plasticity markers (BDNF and DCX) among three commonly used rat strains: Wistar, Sprague Dawley, and Long Evans. Across all three strains, we observed a consistent learning pattern in the Morris water maze, indicated by decreases in escape latency and swim distance over the course of training. At the same time, we observed modest differences in swimming performance, probe trial results, and hippocampal BDNF and DCX protein expression levels that were clearly related to strain. These results support the hypothesis that both cognitive performance and learning- and memory-related molecular pathways are affected by genetic background and phenotypic characteristics of strains.

In the Morris water maze, escape latency is commonly used as a measure of learning. However, there are other factors besides spatial memory that may affect this measure, such as differences in swimming speed [24]. In this study, Sprague-Dawley rats swam faster than Wistar and Long-Evans rats. Although no significant difference in spatial learning ability was observed, their swim latencies were shorter. To address this, we also examined swim distance (path length) because it is less influenced by differences in swimming speed and represents how directly the rats swam toward the hidden platform. With this measure, we found that, on the first day of training, Wistar rats swam shorter distances, whereas, by the last day, Long Evans rats swam the shortest distances. These findings support the notion that Wistar rats demonstrated bet-

https://doi.org/10.5455/annalsmedres.2026.01.011

ter task acquisition, while Long Evans rats navigated the maze more efficiently by the end of training. This is likely more indicative of differences in the strains' learning strategies than of one strain having better performance than the other. Data from the probe trial provide information about spatial memory retention. In the probe trial, Sprague Dawley rats spend a higher percentage of time in the target quadrant than Wistar rats. Long Evans rats exhibited an intermediate pattern that did not differ significantly from the other two strains. Together with the acquisition data, these results indicate that all three strains demonstrated a degree of spatial memory for the location of the platform, but Sprague Dawley rats displayed marginally greater retention than Wistar rats under our experimental conditions. The absence of significant behavioral differences is not surprising, since all the animals were healthy, age-matched adults tested with the same standardized protocol. However, prior reports of the differences between Wistar, Sprague Dawley, and Long Evans rats are dependent to the specific types of learning and memory performance across various tasks [21-23].

While evaluating the results from the Morris water maze, researchers should also consider the role of visual function. Given that this task relies on distal visual cues, strain-related differences in vision may have affected performance, particularly when comparing the Wistar and Sprague Dawley albino strains with the Long Evans pigmented strain. Kumar et al. [27] found strain-specific variations in performance on visual and spatial tasks suggesting that pigmented rats probably have better visual acuity when compared with albino rats, and reduced vision can affect place learning in the water maze. Meanwhile, it should be mentioned that albino rodents are widely used in studies of behavior, including spatial learning tasks such as the Morris water maze [28]. In the present study, the visual cues, positioned at different locations around the maze, were clear and simple and were placed at distances designed to fall within the detection range of albino animals. Nevertheless, no additional visual examination has not been carried out, which should be considered a limitation. Therefore, the differences observed between strains should be interpreted with caution, as they may reflect not only variation in hippocampus-dependent memory processes but also, to some extent, differences in visual acuity.

The molecular results also provide evidence for these behavioral differences. In particular, hippocampal BDNF levels in Sprague-Dawley rats were significantly higher than in Wistar and Long-Evans rats. BDNF is important as a master regulator of synaptic plasticity, long-term potentiation, and the consolidation of memory, and as such it plays a crucial role [5-7]. In our study, Sprague-Dawley rats, which exhibited the highest BDNF levels, showed superior probe performance compared with Wistar rats. Although no direct correlation analyses were performed between BDNF and behavior, this pattern is consistent with the idea that higher levels of BDNF in the hippocampus may support more enduring retention of spatial memory. Additionally, baseline or experience-induced differences in BDNF levels between strains may indicate distinct sensitivities to training, stress, or environmental cues during the task.

DCX expression levels also differed by strain. DCX expression in the hippocampus is higher in Sprague Dawley and Long Evans rats than in Wistar rats. DCX is expressed in immature neurons in the neurogenic niches and is used as a marker for neurogenesis in the adult hippocampus [11,12,14]. The presence of higher levels of DCX in the Sprague Dawley and Long Evans rat strains likely indicates a greater number of newborn granule cells. Since adult-born hippocampal neurons play a role in learning and memory, particularly in tasks requiring pattern discrimination and adaptable spatial information processing [15,17,18], the lower DCX levels observed in Wistar rats might partially explain their poorer performance in the probe test and their swimming patterns during later training sessions. This finding is consistent with studies showing that spatial navigation experience increases the pool of DCX-positive neurons [12].

CONCLUSION

The study showed that all three rat strains, Wistar, Sprague Dawley, and Long Evans, acquired and retained spatial memory as assessed using the MWM. In particular, Sprague Dawley rats exhibited the greatest memory retention and the highest hippocampal levels of BDNF and DCX. Long-Evans rats exhibited the best search strategies by the end of the training sessions. This was, however, coupled with the Wistar rats consistently displaying poorer probe performance and lower expression of the plasticity markers. Although these gaps are relatively small, their consistent presence indicates that the particular rat strain is not an arbitrary variable. It is a principal component that dictates the behavior and the accompanying plasticity that the hippocampus undergoes. Thus, differences among rat strains are a key factor to consider when evaluating behavioral subfields. This must be done, especially in the field of behavioral neuroscience, when designing the experiment, interpreting results, and finalizing your findings from various studies.

Ethics Committee Approval: This study was approved by the Istanbul Medeniyet University Local Ethics Committee for Animal Experiments (İMÜ-HADYEK) (Approval no: 2025/3-1, Date: 26.03.2025).

Peer-review: Externally peer-reviewed.

Conflict of Interest: There is no conflict of interest

Author Contributions: Concept: ID, EK, BE; Design: ID, EK, BE; Supervision: BE; Materials: ID and EK; Data Collection and/or Processing: ID and BE; Analysis and/or Interpretation: BE and EK; Literature Search: ID; Writing Manuscript: ID; Critical Review: ID, EK, BE.

https://doi.org/10.5455/annalsmedres.2026.01.011

Financial Disclosure: The authors declare that this study received no financial support.

Artificial Intelligence Disclosure: ChatGPT (OpenAI, GPT-5.5 Thinking) was used only for English language editing and proofreading of the manuscript.

REFERENCES

1. Chandra S, Sharma S, Chaudhuri R, Fiete I. Episodic and associative memory from spatial scaffolds in the hippocampus. *Nature.* 2025;638(8051):739-751. doi: 10.1038/s41586-024-08392-y.
2. Broadbent NJ, Squire LR, Clark RE. Spatial memory, recognition memory, and the hippocampus. *Proc Natl Acad Sci U S A.* 2004;101(40):14515–14520. doi: 10.1073/pnas.0406344101.
3. Morris R. Developments of a water-maze procedure for studying spatial learning in the rat. *J Neurosci Methods.* 1984;11(1):47–60. doi: 10.1016/0165-0270(84)90007-4.
4. Olopade FE, Folarin OR, Gilbert TT, Olopade JO. Short- and long-term neurobehavioural impairments in mice offspring following chronic perinatal caffeine exposure and withdrawal. *BMC Neurosci.* 2025;26(1):63. doi: 10.1186/s12868-025-00981-5.
5. De Luca P, Mele M, Tanqueiro S, et al. Synaptic accumulation of GluN2B-containing NMDA receptors mediates the effects of BDNF–TrkB signalling on synaptic plasticity and hyperexcitability during status epilepticus. *J Biomed Sci.* 2025;32(1):82. doi: 10.1186/s12929-025-01164-4.
6. Miranda M, Morici JF, Zanoni MB, Bekinschtein P. Brain-derived neurotrophic factor: a key molecule for memory in the healthy and the pathological brain. *Front Cell Neurosci.* 2019;13:363. doi: 10.3389/fncel.2019.00363.
7. Cunha C, Brambilla R, Thomas KL. A simple role for BDNF in learning and memory? *Front Mol Neurosci.* 2010;3:1. doi: 10.3389/neuro.02.001.2010.
8. Park H, Poo MM. Neurotrophin regulation of neural circuit development and function. *Nat Rev Neurosci.* 2013;14(1):7–23. doi: 10.1038/nrn3379.
9. Rauti R, Cellot G, D'Andrea P, et al. BDNF impact on synaptic dynamics: extra- or intracellular long-term release differently regulates cultured hippocampal synapses. *Mol Brain.* 2020;13(1):43. doi: 10.1186/s13041-020-00582-9.
10. Toader C, Serban M, Munteanu O, et al. From synaptic plasticity to neurodegeneration: BDNF as a transformative target in medicine. *Int J Mol Sci.* 2025;26(9):4271. doi: 10.3390/ijms26094271.
11. Vukovic J, Borlikova GG, Ruitenberg MJ, et al. Immature doublecortin-positive hippocampal neurons are important for learning but not for remembering. *J Neurosci.* 2013;33(15):6603–6613. doi: 10.1523/JNEUROSCI.3064-12.2013.
12. Keith JR, Priester C, Ferguson M, Salling M, Hancock A. Persistent increases in the pool of doublecortin-expressing neurons in the hippocampus following spatial navigation training. *Behav Brain Res.* 2008;188(2):391–397. doi: 10.1016/j.bbr.2007.11.026.
13. Kim JS, Jung J, Lee HJ, et al. Differences in immunoreactivities of Ki-67 and doublecortin in the adult hippocampus in three strains of mice. *Acta Histochem.* 2009;111(2):150–156. doi: 10.1016/j.acthis.2008.05.002.
14. Deng W, Aimone JB, Gage FH. New neurons and new memories: how does adult hippocampal neurogenesis affect learning and memory? *Nat Rev Neurosci.* 2010;11(5):339–350. doi: 10.1038/nrn2822.
15. Jessberger S, Clark RE, Broadbent NJ, et al. Dentate gyrus-specific knockdown of adult neurogenesis impairs spatial and object recognition memory in adult rats. *Learn Mem.* 2009;16(2):147–154. doi: 10.1101/lm.1172609.
16. Kitamura T, Saitoh Y, Takashima N, et al. Adult neurogenesis modulates the hippocampus-dependent period of associative fear memory. *Cell.* 2009;139(4):814–827. doi: 10.1016/j.cell.2009.10.020.
17. Saxe MD, Battaglia F, Wang JW, et al. Ablation of hippocampal neurogenesis impairs contextual fear conditioning and synaptic plasticity in the dentate gyrus. *Proc Natl Acad Sci U S A.* 2006;103(46):17501–17506. doi: 10.1073/pnas.0607207103.
18. Simard S, Rahimian R, Davoli MA, et al. Spatial transcriptomic analysis of adult hippocampal neurogenesis in the human brain. *J Psychiatry Neurosci.* 2024;49(5):E319–E333. doi: 10.1503/jpn.240026.
19. McGraw CM, Ward CS, Samaco RC. Genetic rodent models of brain disorders: perspectives on experimental approaches and therapeutic strategies. *Am J Med Genet C Semin Med Genet.* 2017;175(3):368–379. doi: 10.1002/ajmg.c.31570.
20. Sare RM, Lemons A, Smith CB. Behavior testing in rodents: highlighting potential confounds affecting variability and reproducibility. *Brain Sci.* 2021;11(4):522. doi: 10.3390/brainsci11040522.
21. Gokcek-Sarac C, Wesierska M, Jakubowska-Doğru E. Comparison of spatial learning in the partially baited radial-arm maze task between commonly used rat strains: Wistar, Sprague-Dawley, Long-Evans, and outcrossed Wistar/Sprague-Dawley. *Learn Behav.* 2015;43(1):83–94. doi: 10.3758/s13420-014-0163-9.
22. Andrews JS, Jansen JH, Linders S, Princen A, Broekkamp CL. Performance of four different rat strains in the autoshaping, two-object discrimination, and swim maze tests of learning and memory. *Physiol Behav.* 1995;57(4):785–790. doi: 10.1016/0031-9384(94)00336-X.
23. Gleason TC, Dreiling JL, Crawley JN. Rat strain differences in response to galanin on the Morris water task. *Neuropeptides.* 1999;33(4):265–270. doi: 10.1054/npep.1999.0044.
24. Tomas Pereira I, Burwell RD. Using the spatial learning index to evaluate performance on the water maze. *Behav Neurosci.* 2015;129(4):533-539. doi: 10.1037/bne0000078.
25. Rybnikova EA, Vetrovoi OV, Zenko MY. Comparative Characterization of Rat Strains (Wistar, Wistar–Kyoto, Sprague Dawley, Long Evans, LT, SHR, BD-IX) by Their Behavior, Hormonal Level and Antioxidant Status *J Evol Biochem Physiol.* 2018;54(5):374–382. doi: 10.1134/S0022093018050058.
26. Turner KM, Burne TH. Comprehensive behavioural analysis of Long Evans and Sprague-Dawley rats reveals differential effects of housing conditions on tests relevant to neuropsychiatric disorders. *PLoS One.* 2014;9(3):e93411. doi: 10.1371/journal.pone.0093411.
27. Kumar G, Talpos J, Steckler T. Strain-dependent effects on acquisition and reversal of visual and spatial tasks in a rat touchscreen battery of cognition. *Physiol Behav.* 2015;144:26-36. doi: 10.1016/j.physbeh.2015.03.001.
28. Yavuz M, Dayanc ED, Merve Antmen F, et al. Relationships between trace elements and cognitive and depressive behaviors in Sprague Dawley and Wistar albino rats. *Front Pharmacol.* 2024;15:1367469. doi: 10.3389/fphar.2024.1367469.

https://doi.org/10.5455/annalsmedres.2026.01.011

Ann Med Res

Current issue list available at Ann Med Res

Annals of Medical Research

journal page: annalsmedres.org

HER2 IHC score as a predictor of pathologic complete response in HER2-positive breast cancer after neoadjuvant therapy

Mehmet Furkan Sagdic [a,*], Emre Tunc [a], Mahmut Onur Kulturoglu [a], Ozgen Ahmet Yildirim [b], Lutfi Dogan [a]

[a]Ankara Etlik City Hospital, Clinic of Surgical Oncology, Ankara, Türkiye
[b]Ankara Etlik City Hospital, Clinic of Medical Oncology, Ankara, Türkiye
*Corresponding author: m.f.sagdic@gmail.com (Mehmet Furkan Sagdic)

MAIN POINTS

- Patients with HER2 IHC 3+ tumors had substantially higher pCR rates than patients with HER2 IHC 2+/ISH+ disease, underscoring the prognostic significance of HER2 IHC scoring for neoadjuvant treatment response.
- Progesterone receptor (PR) negativity and HER2 IHC 3+ status emerged as independent predictors of pCR, highlighting the clinical utility of routine pre-treatment biopsy markers to identify patients most likely to benefit from neoadjuvant therapy.
- The higher prevalence of estrogen receptor (ER)/progesterone receptor (PR) positivity and the lower pCR rates observed in the HER2 IHC 2+/ISH+ subgroup suggest that this subgroup has a biologically less-responsive phenotype, reinforcing the need for careful therapeutic stratification within HER2-positive breast cancer.

Cite this article as: Sagdic MF, Tunc E, Kulturoglu MO, Yildirim OA, Dogan L. HER2 IHC score as a predictor of pathologic complete response in HER2-positive breast cancer after neoadjuvant therapy. *Ann Med Res*. 2026;33(8):369–374. doi: 10.5455/annalsmedres.2025.12.388.

ABSTRACT

Aim: To evaluate factors associated with pathologic complete response (pCR) in patients with human epidermal growth factor receptor 2 (HER2)-positive breast cancer receiving neoadjuvant therapy, with a specific focus on the prognostic relevance of HER2 immunohistochemistry (IHC) scores.

Materials and Methods: This retrospective study included 147 patients with HER2-positive breast cancer who underwent neoadjuvant chemotherapy (NAC) followed by surgery at a tertiary care center from late 2022 to early 2025. Patients were categorized into two groups based on their HER2 IHC status: IHC 2+/in situ hybridization-positive (ISH+) and IHC 3+. We compared patients' clinicopathological features and pCR rates. pCR was defined as the absence of residual invasive carcinoma in the breast and axillary lymph nodes (ypT0/is ypN0).

Results: The overall pCR rate was 54% (n=79). Among patients with HER2 IHC 3+ tumors, pCR was achieved in 73 of 121 cases (60%), compared with 6 of 26 cases (23%) in the IHC 2+/ISH+ group (p<0.001). In univariate analyses, HER2 IHC score (IHC 2+/ISH+ vs IHC 3, p<0.001), estrogen receptor negativity (p<0.001), and progesterone receptor negativity (p<0.001) were significantly associated with pCR. Multivariate analysis identified HER2 IHC 3+ status (p=0.035) and progesterone receptor-negative status (p=0.037) as independent predictors of achieving pCR.

Conclusion: Positivity for estrogen and progesterone receptors was more prevalent in the IHC 2+/ISH+ group than in the IHC 3+ group. HER2 IHC 3+ status and progesterone receptor negativity were identified as independent predictors of pCR.

Keywords: Breast cancer, Human epidermal growth factor receptor 2, Immunohistochemistry, Neoadjuvant, Pathological complete response

Received: Dec 10, 2025 **Accepted:** Feb 03, 2026 **Available Online:** Aug 25, 2026

INTRODUCTION

Human epidermal growth factor receptor 2 (HER2) overexpression is observed in approximately 15–20% of all breast cancer patients [1]. HER2 overexpression identifies a subgroup of breast cancer patients who are highly responsive to neoadjuvant therapy, with anti-HER2 treatment protocols yielding pathologic complete response (pCR) rates nearing 50% [2-7]. This is of particular clinical significance, as achieving pCR after neoadjuvant treatment was previously associated with improved disease-free survival (DFS) and overall survival (OS) [8,9]. Accurately determining which individuals are likely to respond with a complete pathological remission to preoperative chemotherapy is crucial for optimizing treatment outcomes.

Assessment of HER2 receptor status is typically performed using immunohistochemistry (IHC) and fluorescence in situ hybridization (FISH) techniques. As outlined in the ASCO/CAP recommendations, a tumor is considered HER2-positive if it receives an IHC score of 3+ or if a 2+ score is accompanied by evidence of gene amplification via FISH.

Interestingly, individuals whose tumors are scored as HER2 IHC 3+ have higher rates of pCR than those classified as IHC 2+in situ hybridization-positive (ISH+) [7,10-12].

In this context, identifying clinicopathological differences between HER2 IHC 2+ and IHC 3+ subgroups, as well as determining the patient profiles most likely to achieve pCR to NAC, holds significant clinical relevance. In this study, we aimed to identify factors influencing pCR by examining the clinical and pathological profiles of patients with HER2 IHC 2+ or 3+ expression. We anticipate that these insights could aid in predicting therapeutic outcomes and refining candidate selection for neoadjuvant treatment planning.

MATERIALS AND METHODS

A total of 147 patients diagnosed with HER2-positive breast cancer who underwent neoadjuvant chemotherapy (NAC) followed by surgical intervention at a tertiary medical institution between late 2022 and early 2025 were included in a retrospective analysis. Individuals lacking complete clinical records, those who failed to complete NAC, or those presenting with metastatic disease at the time of diagnosis were excluded from the study. Ethical approval for this research was granted by the institutional review board (Ankara Etlik City Hospital Scientific Research Evaluation and Ethics Committee No. 2, Decision no: AEŞH-BADEK2-2025-41, Date: 29.04.2025).

pCR was defined as the complete absence of invasive carcinoma in breast tissue and axillary lymph nodes, as determined by examination of surgical specimens. The pCR was defined as the absence of residual invasive carcinoma in both the breast and axillary lymph nodes (ypT0/is ypN0). The presence of residual ductal carcinoma in situ (DCIS) was permitted.

Accordingly, cases classified as Miller–Payne grade 5, indicating no residual invasive tumor cells in the breast, regardless of residual DCIS, were considered to have achieved pCR.

The dataset comprised variables such as patient age, HER2 IHC classification, clinical nodal status prior to NAC, tumor histology, initial T stage, histologic grade, expression status of ER and PR, Ki-67 proliferation index, tumor focality, and the specific neoadjuvant chemotherapy regimen administered. Neoadjuvant chemotherapy regimens were categorized as AC-TH and TCHP. AC-TH consisted of doxorubicin and cyclophosphamide, followed by a taxane combined with dual HER2-targeted therapy (trastuzumab and pertuzumab). TCHP consisted of docetaxel, carboplatin, trastuzumab, and pertuzumab.

Tumor staging was performed in accordance with the 8th edition of the American Joint Committee on Cancer (AJCC) Tumor-Node-Metastasis (TNM) classification system [13]. Positivity for ER and PR was defined as ≥1% nuclear staining, in accordance with the 2010 ASCO/CAP recommendations [14]. The Ki-67 proliferation index was assessed via immunostaining using the MIB-1 monoclonal antibody (1:1000 dilution) with the Dako EnVision+ Labeled Polymer detection kit.

HER2 positivity was defined as an IHC score of 3+ or an IHC score of 2+ validated by FISH. A 3+ IHC score indicated intense, uniform membranous staining in more than 10% of tumor cells. Conversely, a 2+ score reflected either weak-to-moderate complete membrane staining in more than 10% of the tumor cells or strong staining in 10% or fewer of the tumor cells.

All individuals completed the entire course of neoadjuvant chemotherapy. Every patient received combined HER2-targeted therapy with trastuzumab and pertuzumab. The neoadjuvant protocol began with four treatment cycles con-

Table 1. Patients' clinicopathological characteristics (IHC 3+ vs. IHC 2+).

Clinicopathological Variables	IHC 2+/ISH+ (%) n=26	IHC 3+ (%) n=121	p-value
Age (years)			0.672
<50	16 (61.5)	69 (57)	
≥50	10 (38.5)	52 (43)	
pCR			<0.001*
Yes	6 (23.1)	73 (60.3)	
No	20 (76.9)	48 (39.7)	
Pre-NAC Nodal Status			0.467
Negative	10 (38.5)	56 (46.3)	
Positive	16 (61.5)	65 (53.7)	
Histopathology			0.642
NST	26	120 (99.2)	
Others	0	1 (0.8)	
Pre-NAC T stage			0.023*
T1	11 (42.3)	33 (27.3)	
T2	8 (30.8)	75 (62)	
T3	5 (19.2)	10 (8.3)	
T4	2 (7.7)	3 (2.5)	
Grade			0.758
Grade 1	1 (3.8)	8 (6.6)	
Grade 2	9 (34.6)	47 (38.8)	
Grade 3	16 (61.6)	66 (54.6)	
Estrogen Receptor			0.023*
Negative	4 (15.4)	47 (38.8)	
Positive	22 (84.6)	74 (61.2)	
Progesterone Receptor			<0.001*
Negative	4 (15.4)	73 (60.3)	
Positive	22 (84.6)	48 (39.7)	
Ki-67			0.137
≤15	2 (7.7)	24 (20)	
>15	24 (92.3)	96 (80)	
Disease Focality			0.178
Unifocal	21 (80.8)	109 (90.1)	
Multifocal	5 (19.2)	12 (9.9)	
CT Regimen			0.338
TCHP	16 (61.5)	86 (71.1)	
AC-TH	10 (38.5)	35 (28.9)	

• NAC: Neoadjuvant Chemotherapy; • pCR: Pathologic Complete Response; • TCHP = Docetaxel/Carboplatin/Trastuzumab/Pertuzumab; • AC-TH = Doxorubicin/Cyclophosphamide Followed by Taxane+HER2 Blockade.

https://doi.org/10.5455/annalsmedres.2025.12.388

sisting of doxorubicin and cyclophosphamide, administered every three weeks. Subsequently, 102 patients underwent four cycles of docetaxel, also on a 21-day schedule, while the remaining 45 patients were treated with weekly paclitaxel over 12 sessions. Prior to each treatment cycle, complete blood counts and standard biochemical panels were reviewed. To prevent hypersensitivity reactions, patients routinely received premedication with 10 mg of intravenous hydrocortisone.

Statistical analysis

For cases with an IHC score of 2+, HER2 gene status and CEP17 (chromosome 17 enumeration probe) chromosomal changes were evaluated by FISH. Amplification of HER2 was defined as either a HER2/CEP17 ratio ≥2.0 or a mean HER2 gene copy number ≥6.0. To analyze the data, categorical variables were assessed using the Chi-square test, while continuous variables were evaluated using the independent samples t-test. Variables with p<0.05 in univariate analyses were subsequently included in a multivariable logistic regression model to identify independent predictors of pCR. Statistical significance was set at p<0.05, and all statistical analyses were performed using Jamovi (version 2.3.28).

RESULTS

The proportion of patients who reached pCR was 54% (n=79). The results showed that 18% of patients (n=26) had HER2 IHC 2+/ISH-amplified tumors, while 82% (n=121) had HER2 IHC 3+ tumors. All patients received taxane-based chemotherapy regimens: 69% received docetaxel-based regimens, and 31% received paclitaxel-based regimens. Among patients with HER2 IHC 3+ tumors, pCR was achieved in 73 of 121 cases (60%), compared with 6 of 26 cases (23%) in the IHC 2+/ISH+ group (p<0.001). Prior to NAC, nodal involvement was identified in 61% (n=16) of patients with IHC 2+ tumors and in 54% (n=65) of those with IHC 3+ expression. Among the IHC 2+ subgroup, T1 lesions were observed in 42% (n=11), T2 in 30.8% (n=8), T3 in 19% (n=5), and T4 in 7.7% (n=2). In contrast, within the IHC 3+ group, 27% (n=33) had T1 tumors, 62% (n=75) had T2 tumors, 8% (n=10) had T3 tumors, and 2.5% (n=3) had T4 tumors. (p=0.023). ER positivity was more prevalent in the IHC 2+ group (84%, n=22) than in the IHC 3+ group (61%, n=74).

Similarly, the rate of PR positivity was markedly higher in the IHC 2+ subgroup (85%; n=22) than in the IHC 3+ subgroup (40%; n=48); this difference was statistically significant (p<0.001). The Ki-67 index exceeded 15% in 92.3% (n=25) of patients in the IHC 2+/ISH+ group and 80.0% (n=96) of patients in the IHC 3+ group. Although no significant difference was observed in the distribution of neoadjuvant chemotherapy regimens between the groups, TCHP (docetaxel/carboplatin/trastuzumab/pertuzumab) was more frequently used than AC-TH in both cohorts (61% in the IHC 2+ group and 71% in the IHC 3+ group) Table 1 summarizes patients' clinicopathological characteristics.

Table 2. Patients' clinical and pathological characteristics (pCR vs. non-pCR).

Clinicopathological Variables	pCR (%) n=79	Non-pCR (%) n=68	p-value
Age (years)			0.574
<50	44 (55.7)	41 (60.3)	
≥50	35 (44.3)	27 (39.7)	
HER2			<0.001*
IHC 2+/ISH+	6 (7.6)	20 (29.4)	
IHC 3+	73 (92.4)	48 (70.6)	
Pre-NAC Nodal Status			0.132
Negative	40 (50.6)	26 (38.2)	
Positive	39 (49.4)	42 (61.8)	
Histopathology			0.279
NST	79 (100)	67 (98.5)	
Others	0	1 (1.5)	
Pre-NAC T stage			0.180
T1	28 (35.4)	16 (23.5)	
T2	41 (51.9)	42 (61.8)	
T3	6 (7.6)	9 (13.2)	
T4	4 (5.1)	1 (1.5)	
Grade			0.429
Grade 1	3 (3.8)	6 (8.8)	
Grade 2	30 (38)	26 (38.2)	
Grade 3	46 (58.2)	36 (53)	
Estrogen Receptor			<0.001*
Negative	38 (48.1)	14 (20.6)	
Positive	41 (51.9)	54 (79.4)	
Progesterone Receptor			<0.001*
Negative	56 (70.9)	23 (39.1)	
Positive	23 (39.1)	45 (66.2)	
Ki-67			0.777
≤15	14 (17.9)	11 (16.2)	
>15	64 (82.1)	57 (83.8)	
Disease Focality			0.944
Unifocal	70 (88.6)	60 (88.2)	
Multifocal	9 (11.4)	8 (11.8)	
CT Regimen			0.671
TCHP	56 (70.9)	46 (67.6)	
AC-TH	23 (29.1)	22 (32.4)	

• HER2: Human Epidermal Growth Factor Receptor 2; •NAC: Neoadjuvant Chemotherapy; • TCHP = Docetaxel/Carboplatin/Trastuzumab/Pertuzumab; • AC-TH = Doxorubicin/Cyclophosphamide Followed by Taxane+HER2 Blockade.

When classified by pCR status, 92% (n=73) of individuals who achieved pCR and 71% (n=48) of those who did not had IHC 3+ expression. The T-stage distribution in the pCR group was as follows: T1, 35% (n=28); T2, 52% (n=41); T3, 8% (n=6); and T4, 5% (n=4). In the non-pCR group, we detected T1 in 24% (n=16), T2 in 62% (n=42), T3 in 13% (n = 9), and T4 in 2% (n=1). A significantly higher rate of ER negativity was observed in the pCR group (48%, n=38), compared with 21% (n=14) in the non-pCR group (p<0.001). Similarly, PR negativity was more frequent among patients who achieved pCR (71%, n=56) than among those who did not (34%, n=23) (p<0.001). Although the distribution of NAC

https://doi.org/10.5455/annalsmedres.2025.12.388

Table 3. Multivariate analysis of the factors associated with pCR.

Predictor	Odds Ratio	Lower (95% CI)	Upper (95% CI)	p-value
Pre-NAC Her2 IHC 2+/ISH+- IHC 3+	3.12	1.09	8.98	0.035*
Progesterone Receptor Positive-Negative	2.86	1.07	7.61	0.037*
Estrogen Receptor Negative-Positive	0.664	0.24	1.84	0.430

regimens did not differ notably between the two groups, docetaxel-based chemotherapy was used in 71% (n=56) and 68% (n=46) of the pCR and non-pCR groups, respectively. Table 2 summarizes the clinical and pathological characteristics by pCR status.

Univariate analysis revealed that HER2 IHC score, ER expression, and PR status were significantly associated with achieving a pCR (p<0.001). Multivariate analyses demonstrated that pre-NAC HER2 IHC score (p=0.035) and PR negativity (p=0.037) were independent factors significantly associated with the outcome achieving pCR. PR negativity was associated with a higher likelihood of attaining pCR. Further details are provided in Table 3.

DISCUSSION

The aim of this study was to evaluate the clinicopathological characteristics and pCR rates in NAC patients with HER2 IHC 3+ or HER2 IHC 2+/ISH+ breast cancer. To the best of our knowledge, this is the first comprehensive study conducted in Türkiye to address this specific clinical distinction.

From a biological standpoint, higher HER2 IHC expression may reflect greater HER2 protein overexpression and, consequently, a higher likelihood of HER2-driven tumor biology. This may increase tumor dependence on the HER2 pathway and enhance sensitivity to HER2-targeted neoadjuvant therapy [10,11]. In addition, PR negativity is often associated with reduced hormone receptor signaling and may indicate diminished functional interaction between hormone receptor pathways and HER2-driven oncogenic signaling. Collectively, these features may contribute to a more HER2-dependent phenotype, rendering HER2 IHC 3+ and PR-negative tumors more responsive to dual HER2 blockade and cytotoxic chemotherapy, thereby increasing the probability of achieving pCR [6,15].

The membrane tyrosine kinase receptor HER2 is associated with aggressive tumor biology and poor prognosis in breast cancer [16]. Accurate assessment of HER2 receptor status is therefore critical for initiating NAC. As is well known, achieving pCR in HER2-positive breast cancer is one of the strongest prognostic indicators. In their cohort, Krystel-Whittemore et al. reported a pCR rate of 59% [7], while the largest series in the literature by Winer et al. demonstrated a pCR rate of 44.3% [17]. In our study, we identified a pCR rate of 54% in HER2-positive patients.

In determining HER2 positivity, both HER2 IHC 3+ and IHC 2+/ISH+ cases are classified as HER2-positive. In clinical practice, these subgroups are often combined under the HER2-positive category, and potential clinicopathological differences between them may be overlooked. However, patients with HER2 IHC 3+ status tend to exhibit higher pCR rates compared with those with HER2 IHC 2+/ISH+ status, suggesting that the IHC 3+ subgroup is more responsive to NAC [7, 18-24]. Krystel-Whittemore et al. reported a pCR rate of 67% in IHC 3+ patients versus 17% in IHC 2+/ISH+ patients [7]. Similarly, Wang et al. reported rates of 55.1% versus 17.6% [19]; Sun et al. found rates of 58.1% versus 26.7% for IHC 3+ and IHC 2+/ISH+ patients, respectively [24]. In our study, we observed pCR rates of 60.3% in the IHC 3+ group and 23.1% in the IHC 2+/ISH+ group.

Hormone receptor status also differed between the two subgroups. Previous research has shown that patients with IHC 2+/ISH+ exhibit higher ER positivity than IHC 3+ patients, whereas PR negativity is more frequent in the IHC 3+ subgroup [18,24]. Jia et al. reported ER positivity rates of 75% and 53%, and PR positivity rates of 49% and 41%, in the IHC 2+/ISH+ and IHC 3+ groups, respectively [18]. Consistent with these findings, our study revealed ER positivity in 84.6% of patients with IHC 2+/ISH+ tumors and 61.2% of patients with IHC 3+ tumors. PR positivity was observed in 84.6% of the IHC 2+/ISH+ group, whereas it was 39.7% in the IHC 3+ group.

Jung et al. confirmed that PR negativity (p=0.01) and preoperative HER2 IHC 3+ status (p=0.04) were independent predictors of pCR rates [15]. In their study, Krystel-Whittemore et al. identified dual blockade (p=0.001), high grade (p=0.04), HER2 IHC 3+ (p<0.001), and PR negativity (p=0.01) as independent predictors of pCR [7]. Katayama et al. also demonstrated that HER2 IHC 3+ and Grade 3 were independent predictors of pCR following neoadjuvant anti-HER2 therapy [20]. In our study, univariate analyses identified hormone receptor negativity (p<0.001) and IHC status as significant predictors of pCR. In multivariate analysis showed that PR negativity and HER2 IHC 3+ status were independent predictors of pCR. Therefore, the rate of complete response to NAC is likely higher in patients who are HER2 IHC 3+ and PR-negative.

https://doi.org/10.5455/annalsmedres.2025.12.388

Although the study's design and results are relatively straightforward, identifying, through routine pathological workups, patients likely to respond well or poorly to NAC is highly useful in clinical practice. It can guide the management of borderline cases, for example, by allowing upfront surgery for patients unlikely to benefit from NAC. Yet, novel predictive and prognostic markers are still needed.

Limitations

This study has several limitations that should be acknowledged. Its retrospective and single-center design may limit the generalizability of the findings. In addition, the relatively small size of the HER2 IHC 2+/ISH+ subgroup (n=26) may have reduced the statistical power of subgroup analyses and limited the precision of effect estimates. Therefore, the results, particularly those derived from subgroup comparisons, should be interpreted with caution. Furthermore, the limited follow-up period precluded the calculation of OS and DFS. Despite these constraints, we assert that evaluating the complete response using data readily available from routine pre-treatment biopsies holds substantial clinical value. Given that this represents the first comprehensive investigation of its kind in our country, it is expected to make a significant contribution to the existing literature. Additionally, our findings may provide a foundation for prospective studies with larger sample sizes that could offer further insights and enhance the generalizability of the results.

CONCLUSION

In summary, the present study compared clinicopathological characteristics and pCR rates between HER2 IHC 3+ and HER2 IHC 2+/ISH+ patients who received NAC. The IHC 2+/ISH+ group exhibited higher ER and PR positivity than the IHC 3+ group. HER2 IHC 3+ status and PR negativity was identified as an independent predictor of pCR. Considering the HER2 IHC score and PR status together may help guide clinical decision-making regarding neoadjuvant therapy.

Ethics Committee Approval: Ethical approval was obtained from the Ankara Etlik City Hospital Scientific Research Evaluation and Ethics Committee No. 2 (Decision no: AEŞH-BADEK2-2025-41, Date: 29.04.2025).

Informed Consent: It was not deemed necessary due to the retrospective nature of the study.

Peer-review: Externally peer-reviewed.

Conflict of Interest: The authors declare that they have no conflicts of interest to disclose.

Author Contributions: M.F.S.: Contributed to Conceptualization and Methodology, Performed Data Curation, Investigation, Formal Analysis, Validation, and Visualization, and Drafted and Revised the Manuscript; E.T. and M.O.K.: Contributed to Data Curation and Investigation and Provided Study Resources. Ö.A.Y.: Contributed to Conceptualization, Supervised the Study, and Critically Reviewed and Edited the Manuscript; L.D.: Contributed to Conceptualization and Methodology,

Financial Disclosure: None.

Artificial Intelligence Disclosure: The authors declare that no artificial intelligence tools were used in the preparation of this article.

REFERENCES

1. Sareyeldin RM, Gupta I, Al-Hashimi I, et al. Gene expression and miRNAs profiling: function and regulation in human epidermal growth factor receptor 2 (HER2)-positive breast cancer. *Cancers (Basel)*. 2019;11(5):646. doi: 10.3390/cancers11050646.
2. Broglio KR, Quintana M, Foster M, et al. Association of pathologic complete response to neoadjuvant therapy in HER2-positive breast cancer with long-term outcomes: a meta-analysis. *JAMA Oncol*. 2016;2(6):751–760. doi: 10.1001/jamaoncol.2015.6113.
3. Gianni L, Pienkowski T, Im YH, et al. Efficacy and safety of neoadjuvant pertuzumab and trastuzumab in women with locally advanced, inflammatory, or early HER2-positive breast cancer (NeoSphere): a randomised multicentre, open-label, phase 2 trial. *Lancet Oncol*. 2012;13(1):25–32. doi: 10.1016/S1470-2045(11)70336-9.
4. Buzdar AU, Ibrahim NK, Francis D, et al. Significantly higher pathologic complete remission rate after neoadjuvant therapy with trastuzumab, paclitaxel, and epirubicin chemotherapy: results of a randomized trial in human epidermal growth factor receptor 2-positive operable breast cancer. *J Clin Oncol*. 2005;23(16):3676–3685. doi: 10.1200/JCO.2005.07.032.
5. Buzdar AU, Valero V, Ibrahim NK, et al. Neoadjuvant therapy with paclitaxel followed by 5-fluorouracil, epirubicin, and cyclophosphamide chemotherapy and concurrent trastuzumab in human epidermal growth factor receptor 2-positive operable breast cancer: an update of the initial randomized study population and data of additional patients treated with the same regimen. *Clin Cancer Res*. 2007;13(1):228–233. doi: 10.1158/1078-0432.CCR-06-1345.
6. Gianni L, Eiermann W, Semiglazov V, et al. Neoadjuvant and adjuvant trastuzumab in patients with HER2-positive locally advanced breast cancer (NOAH). *Lancet Oncol*. 2014;15(6):640–647. doi: 10.1016/S1470-2045(14)70080-4.
7. Krystel-Whittemore M, Xu J, Brogi E, et al. Pathologic complete response rate according to HER2 detection methods in HER2-positive breast cancer treated with neoadjuvant systemic therapy. *Breast Cancer Res Treat*. 2019;177(1):61–66. doi: 10.1007/s10549-019-05295-9.
8. Burstein HJ, Curigliano G, Loibl S, et al. Estimating the benefits of therapy for early-stage breast cancer: the St. Gallen International Consensus Guidelines 2019. *Ann Oncol*. 2019;30(10):1541–1557. doi: 10.1093/annonc/mdz235.
9. Huober J, Holmes E, Baselga J, et al. Survival outcomes of the NeoALTTO study (BIG 1–06): updated results of a phase III neoadjuvant clinical trial. *Eur J Cancer*. 2019;118:169–177. doi: 10.1016/j.ejca.2019.04.038.
10. Yan H, Xiao H, Zhu J, Zhang J, Liu Z. Association between HER2 protein expression level and efficacy of neoadjuvant chemotherapy in HER2-positive breast cancer. *Cancer Manag Res*. 2020;12:12715–12722. doi: 10.2147/CMAR.S278694.
11. Xu B, Shen J, Zhang L, Zhao W, Wang L. HER2 protein expression level is positively associated with efficacy of neoadjuvant systemic therapy in HER2-positive breast cancer. *Pathol Res Pract*. 2022;234:153900. doi: 10.1016/j.prp.2022.153900.

https://doi.org/10.5455/annalsmedres.2025.12.388

12. Singer CF, Tan YY, Fitzal F, et al. Pathological complete response to neoadjuvant trastuzumab is dependent on HER2/CEP17 ratio in HER2-amplified early breast cancer. *Clin Cancer Res.* 2017;23(14):3676–3683. doi: 10.1158/1078-0432.CCR-16-2373.
13. Giuliano AE, Connolly JL, Edge SB, et al. Breast cancer—major changes in the AJCC eighth edition cancer staging manual. *CA Cancer J Clin.* 2017;67(4):290–303. doi: 10.3322/caac.21393.
14. Hammond MEH, Hayes DF, Dowsett M, et al. American Society of Clinical Oncology/College Of American Pathologists guideline recommendations for immunohistochemical testing of estrogen and progesterone receptors in breast cancer. *J Clin Oncol.* 2010;28(16):2784–2795. doi: 10.1200/JCO.2009.25.6529.
15. Jung YJ, Lee S, Kang SK, Kim JY, Choo KS, Nam KJ, et al. Clinicopathological factors predicting pathological complete response to neoadjuvant anti-HER2 therapy in HER2-positive breast cancer. *Oncology.* 2025;103(5):351–359. doi: 10.1159/000541019.
16. Suydam C, Chibane F, Brown N, et al. Are There More HER2 FISH in the Sea? An Institution's Experience in Identifying HER2 Positivity Using Fluorescent In Situ Hybridization in Patients with HER2 Negative Immunohistochemistry. *Ann Surg Oncol.* 2024;31(1):376–381. doi: 10.1245/s10434-023-14439-7.
17. Winer L, Ruth KJ, Bleicher RJ, et al. Immunohistochemical status predicts pathologic complete response to neoadjuvant therapy in HER2-overexpressing breast cancers. *Ann Surg Oncol.* 2025;32(2):931-943. doi: 10.1245/s10434-024-16470-8.
18. Jia M, Yang H, Pan L, Gao J, Guo F. Effect of Estrogen Receptor on the Relationship Between HER2 Immunohistochemistry Score and Pathological Complete Response to Neoadjuvant Treatment in HER2-Positive Breast Cancer. *Breast J.* 2024;2024:8851703. doi: 10.1155/2024/8851703.
19. Wang Y, Singh K, Dizon D, et al. Immunohistochemical HER2 score correlates with response to neoadjuvant chemotherapy in HER2-positive primary breast cancer. *Breast Cancer Res Treat.* 2021;186(3):667–676. doi: 10.1007/s10549-021-06124-8.
20. Katayama A, Miligy IM, Shiino S, et al. Predictors of pathological complete response to neoadjuvant treatment and changes to post-neoadjuvant HER2 status in HER2-positive invasive breast cancer. *Mod Pathol.* 2021;34(7):1271–1281. doi: 10.1038/s41379-021-00738-5.
21. Bae SJ, Jang JS, Kook Y, et al. Abstract P4-06-08: HER2-protein expression is a predictive marker for treatment response in patients with HER2-positive breast cancer who received neoadjuvant chemotherapy with dual HER2-blockade *Cancer Res.* 2023;83(5 Suppl):P4-06-08. doi: 10.1158/1538-7445.SABCS22-P4-06-08.
22. Chiu YN, Hsu CY, Lien PJ, et al. Impacts of HER2 immunohistochemical scores on response and outcomes of HER2-positive breast cancers after neoadjuvant therapy. *J Chin Med Assoc.* 2023;86(4):409–417. doi: 10.1097/JCMA.0000000000000883.
23. Chen HL, Chen Q, Deng YC. Pathologic complete response to neoadjuvant anti-HER2 therapy is associated with HER2 immunohistochemistry score in HER2-positive early breast cancer. *Medicine (Baltimore).* 2021;100(44): e27632. doi: 10.1097/MD.0000000000027632.
24. Sun B, Li Y, Wang J, Lu H, Li J. Predictors of pathological complete response to neoadjuvant treatment in invasive breast cancer with different human epidermal growth factor receptor 2 (HER2) subcategories. *Quant Imaging Med Surg.* 2024;14(9):6466–6478. doi: 10.21037/qims-24-397.

https://doi.org/10.5455/annalsmedres.2025.12.388

Ann Med Res

Current issue list available at Ann Med Res

Annals of Medical Research

journal page: annalsmedres.org

The role of the balance between lipid mediator resolvin D1 and interleukin-17 in the development of psoriasis

Sule Gencoglu[a], Rabia Piskin Sagir[b,*], Ahmet Karatas[c]

[a] *Turgut Ozal University, Faculty of Medicine, Department of Dermatology, Malatya, Türkiye*
[b] *İnönü University, Faculty of Medicine, Department of Rheumatology, Malatya, Türkiye*
[c] *Fırat University, Faculty of Medicine, Department of Rheumatology, Elazığ, Türkiye*
**Corresponding author: rpsagir@gmail.com (Rabia Piskin Sagir)*

MAIN POINTS

- Serum IL-17 levels were significantly higher, and Resolvin D1 (RvD1) levels were markedly lower, in patients with psoriasis than in healthy controls, demonstrating a disrupted inflammatory–proresolving balance.
- IL-17 was positively correlated with PASI and NLR, whereas RvD1 was negatively correlated with PASI and NLR, indicating that these biomarkers reflect clinical severity and systemic inflammation.
- Combined ROC analysis of IL-17 and RvD1 increased diagnostic performance (AUC: 0.814), outperforming each marker alone.
- After adjustment for confounders, high IL-17 and low RvD1 levels independently predicted psoriasis risk, suggesting their utility in diagnosis and disease monitoring.

Cite this article as: Gencoglu S, Piskin Sagir R, Karatas A. The role of the balance between lipid mediator resolvin D1 and interleukin-17 in the development of psoriasis. *Ann Med Res*. 2026;33(8):375–380. doi: 10.5455/annalsmedres.2025.11.365.

ABSTRACT

Aim: To determine serum IL-17 and resolvin D1 (RvD1) levels in patients with psoriasis and to assess their relationships with the psoriasis area severity index (PASI) and other inflammatory markers.

Materials and Methods: A total of 60 participants, 30 patients diagnosed with psoriasis vulgaris and 30 controls, were included in the study. Psoriasis was diagnosed based on the morphological appearance of the lesions. Psoriasis Area and Severity Index (PASI) scores were calculated for patients with psoriasis. Serum RvD1 and IL-7 levels were measured by ELISA. The predictive performance of IL-17 and RvD1 was assessed using Receiver Operating Characteristic (ROC) curve analysis. Optimal cut-off points were determined using the Youden index. The independent associations of IL-17 and RvD1 with psoriasis were investigated by multiple logistic regression analysis after adjusting for age, BMI, and gender.

Results: Serum IL-17 level in the psoriasis group was significantly higher than in the control group [609.32 (436.75-842.13) vs. 354.25 (260.0-659.13), p<0.001], whereas the RvD1 level was significantly lower than in the control group [7.38 (5.32-10.82) vs. 11.3 (8.7-16.1), p=0.004]. IL-17 was positively correlated with PASI and NLR, and negatively correlated with RvD1 and lymphocyte count. RvD1 was negatively correlated with PASI and NLR, and positively correlated with lymphocyte count. Although the diagnostic sensitivities of both markers were similar, their efficiency increased when combined (AUC: 0.814 (0.693-0.903)). Logistic regression analysis revealed that high IL-17 and low RvD1 were associated with psoriasis.

Conclusion: After adjusting for potential confounders, high IL-17 and low RvD1 were found to be independent risk factors for the development of psoriasis. Although the diagnostic sensitivity of both molecules was similar for psoriasis, combining the two molecules increased diagnostic yield.

Keywords: Psoriasis, IL-17, Resolvin D1, PASI, Inflammation
Received: Dec 01, 2025 **Accepted:** Feb 09, 2026 **Available Online:** Aug 25, 2026

INTRODUCTION

Inflammation is a process that involves prostaglandins, thromboxanes, and leukotrienes , which result from the enzymatic degradation of arachidonic acid and omega-3 fatty acids by cyclooxygenases and lipoxygenases. Although a physiological amount of inflammation is necessary for many cellular functions, chronicity and increased intensity of inflammation can lead to pathological inflammation and cell damage [1,2]. Psoriasis is an immune-mediated, systemic and chronic inflammatory skin disease whose exact etiology has not been clearly established [3]. With a prevalence of 2-3%, psoriasis is considered the most serious non-infectious skin pathology [4]. Sharply demarcated, erythematous, and scaly skin lesions are considered indicators of the inflammatory nature of the disease. Although physiological inflammation is a self-limiting process, resolution of inflammation in psoriasis may

be followed by relapse. Anti-inflammatory and immunomodulatory pro-soluble lipid mediators such as resolvin, protectin, and maresin play a role in the resolution of chronic inflammation associated with psoriasis [5,6].

Resolvin D1 (RvD1) is an omega-3 polyunsaturated fatty acid-derived lipid mediator involved in the resolution of inflammation [7]. RvD1 expression defects in blood and skin lesions of patients with psoriasis have been shown in isolated studies [3]. In particular, the anti-inflammatory lipid mediator RvD1 has been shown to be downregulated in active psoriasis [8]. In contrast to pro-resolvins, increased T cell stimulation triggers inflammation in psoriatic skin lesions, leading to disease progression [9]. The decreased production of anti-inflammatory cytokines such as RvD1 in psoriasis is mediated by T cells activated by interleukin 17 [9]. The remarkable increase in IL-17A and other family members in psoriasis has drawn attention to this molecule in the pathogenesis of the disease [10]. Moreover, IL-17 overexpression contributes significantly to the formation of psoriatic lesions by causing hyperproliferation and differentiation defects of epidermal keratinocytes [4].

While resolvin D1 (RvD1) exerts anti-inflammatory and pro-resolving effects that may counteract the development of psoriasis [3], overexpression of interleukin-17 (IL-17) is known to promote disease progression [9]. Although the pathogenic role of IL-17 in psoriasis has been well established for many years, circulating levels of the pro-resolving lipid mediator RvD1 have been far less extensively investigated. To date, no study has specifically examined the imbalance between a pro-inflammatory cytokine and a pro-resolving lipid mediator in psoriasis. Therefore, the primary novelty of the present study lies not only in evaluating serum RvD1 levels but also in investigating the balance between IL-17 and RvD1 and their relationship with disease severity (assessed by the Psoriasis Area and Severity Index (PASI)) and other inflammatory markers.

MATERIALS AND METHODS

Patients selection

This case-control study was approved by the Fırat University Non-Interventional Research Ethics Committee (Approval no: 29957, Date: 27.12.2024), after which patient selection and sample collection commenced. A total of 60 participants were included in the study: 30 had psoriasis vulgaris and 30 were controls. Only patients with chronic plaque-type psoriasis (psoriasis vulgaris) were included in the study. Patients with other clinical subtypes of psoriasis (guttate, pustular, and erythrodermic) and those with psoriatic arthritis were excluded to ensure a homogeneous study population. The diagnosis of psoriasis was confirmed by the presence of a symmetrical, sharply demarcated, erythematous plaque covered with silver scales. The diagnosis of psoriasis was based on characteristic clinical findings. Although histopathological confirmation was not routinely performed, this approach reflects standard clinical practice. PASI was calculated by accounting for both the body surface area affected by psoriasis and the severity of redness, swelling, and scaling. A PASI score of 10 or higher was considered to have moderate to severe psoriasis [11]. Participants were selected from patients presenting to the Malatya Gözde Hospital Dermatology Clinic. The control group consisted of age- and BMI-matched individuals without psoriasis, chronic inflammatory or autoimmune diseases, malignancy, or systemic infection. None of the controls were receiving systemic anti-inflammatory or immunomodulatory medications. Controls were recruited from among individuals attending the dermatology outpatient clinic for non-inflammatory, benign conditions. Those using anti-inflammatory drugs (including TNF alpha or IL-17 blockers), those with systemic inflammatory diseases, and those in the acute attack phase of the disease were excluded from the study. Patients receiving systemic anti-inflammatory drugs, TNF-α inhibitors, IL-17 blockers, topical corticosteroids, topical immunomodulators, phototherapy, apremilast, IL-23 inhibitors, or any systemic immunosuppressive or immunomodulatory therapy within the previous 3 months were excluded. Following an overnight fast of 8-10 hours, blood samples were collected from both groups and stored until analysis. All blood samples were collected between 08:00 and 10:00 a.m. after an overnight fast to minimize potential circadian variation in inflammatory mediators. Complete blood count (CBC) parameters (WBC, neutrophil and lymphocyte counts) were measured using the Mindray BC-6000 autohematology analyzer (Mindray Diagnostics, Shenzhen, China). The neutrophil-to-lymphocyte ratio (NLR) was calculated by dividing the neutrophil count by the lymphocyte count, both obtained from the complete blood count. The height and weight of the participants in the psoriasis and control groups were measured, and their BMI values were calculated [weight (kg)/square of height (kg/m^2)].

Measurement of serum IL-17 and RvD1 with ELISA

IL-17 and RvD1 levels in serum samples were determined by ELISA method using Human ELISA kits (Catalog no: 201-

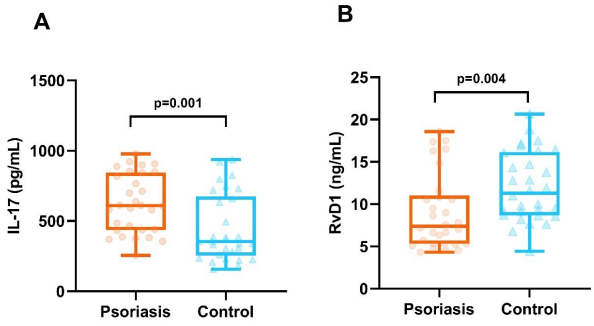

Figure 1. Graphical representation of serum values of IL-17 and RvD1 in psoriasis and control groups.

https://doi.org/10.5455/annalsmedres.2025.11.365

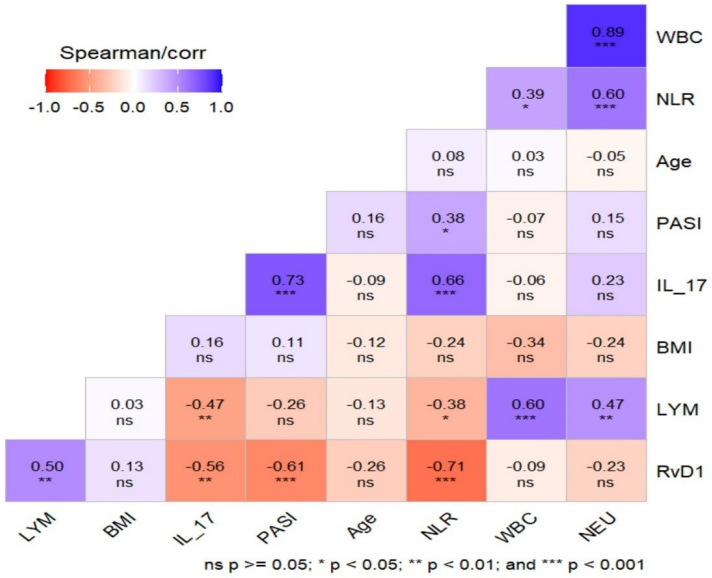

Figure 2. Graphical representation of correlation matrices of IL-17, RvD1 and other variables. Blue colors indicate positive correlations and red colors indicate negative correlations.

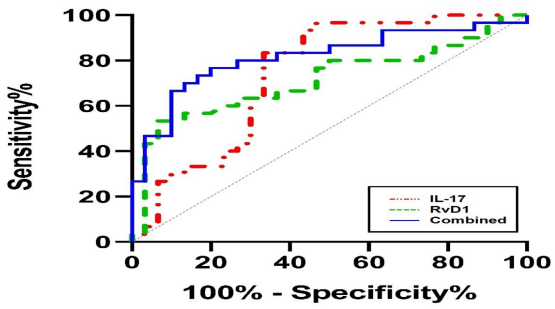

Figure 3. ROC curve analysis of IL-17, RvD1 and their combination in the diagnosis of psoriasis.

12-0143, 201-12-9313, Sunred Biotechnology Company, Shanghai, CHINA, respectively). The measurement range of the IL-17 kit was 15 pg/mL – 1000 pg/mL, and the minimum measurable level was 12.03 pg/mL. The measurement range of the RvD1 kit was 0.15–30 ng/mL, and the minimum measurable level was 0.114 ng/mL. The intra-assay CV values for both kits were <10%, while the inter-assay CV valueswere <12%. Absorbances were measured at 450 nm using a Bio-Tek ELx800 (BioTek Instruments, USA) microplate reader. Test results were reported as pg/mL for IL-17 and ng/mL for resolvin-D1, respectively.

Statistical analysis

Statistical analysis of the data was performed using SPSS v. 27 (IBM Corp., Armonk, NY). Graphpad Prism 8.3.0 (GraphPad Software, San Diego, California, USA) software was used for graphical drawing. Normality of the variables was assessed using the Kolmogorov–Smirnov test. Continuous variables were given as mean±standard deviation or median (25^{th} and 75^{th} percentile) according to the normality of the distribution. Parameters conforming to a normal distribution were compared using the independent samples t test, whereas those that did not conform were compared using the Mann-Whitney U test. Categorical variables were reported as counts and percentages, and differences between categories were assessed using the Chi-square test. The relationships between the parameters were examined using the Spearman correlation test. The relationships between the parameters were examined using the Spearman correlation test. The predictive performance of the laboratory measurements was assessed using Receiver Operating Characteristic (ROC) curve analysis. For the combined ROC analysis, predicted probabilities derived from the multivariable logistic regression model that included both IL-17 and resolvin D1 were used. Optimal cut-off points were determined by using the Youden index. The independent association between IL-17 and RvD1 with psoriasis was investigated by multiple logistic regression analysis after adjusting for age, BMI and gender. Multicollinearity was assessed using variance inflation factors (VIFs), and all variables had acceptable VIFs (<2.5). Model fit was evaluated using the Hosmer–Lemeshow goodness-of-fit test and Nagelkerke R^2. Correlation heatmap was generated via the Metan R package [12]. P<0.05 was considered statistically significant.

RESULTS

As shown in Table 1, participants in the psoriasis and control groups were similar in mean age, BMI, and gender distribution. Serum IL-17 levels in the psoriasis group were significantly higher than those in the control group [609.32(436.75-842.13) vs. 354.25 (260.0-659.13), p<0.001]. Conversely, serum RvD1 levels in the psoriasis group were significantly lower than those in the control group [7.38 (5.32-10.82) vs.

https://doi.org/10.5455/annalsmedres.2025.11.365

Table 1. Comparison of demographic characteristics of participants in the psoriasis and control groups as well as RvD1 and IL-17 levels.

Parameters	Psoriasis (n =30)	Control (n = 30)	p-value
Age (yrs)	34.87±6.85	35.97±7.89	0.567[a]
Body Mass Index (kg/m2)	24.18±1.40	24.4±2.3	0.650[a]
Gender (male/female)	19/11 (63.3%)	17/13 (56.7%)	0.792[c]
IL-17 (pg/mL)	609.32 (436.75-842.13)	354.25 (260.0-659.13)	**0.001[b]**
RvD1 (ng/mL)	7.38 (5.32-10.82)	11.3 (8.7-16.1)	**0.004[b]**
PASI	4.5 (3.0-9.1)	-	-
WBC (109/L)	8.79±1.95	6.51±1.44	**<0.001[a]**
Neutrophil count (109/L)	5.49±1.41	3.67±1.09	**<0.001[a]**
Lymphocyte count (109/L)	2.48±0.55	2.04±0.56	**0.003[a]**
NLR	2.25±0.49	1.89±0.65	**0.018[a]**

[a] Student t-test, [b] Mann-Whitney U test, [c] Chi-Square test. IL-17: Interleukin-17; RvD1: Resolvin-D1; PASI: Psoriasis Area Severity Index; WBC: white blood cell count; NLR: Neutrophil to lymphocyte ratio.

Table 2. Correlation analysis between IL-17, RvD1 and other variables in psoriasis patients.

	IL-17		RvD1	
	r	p	r	p
RvD1	**-0.559**	**0.001**	-	-
Age	-0.086	0.652	-0.259	0.168
Body Mass Index	0.155	0.413	0.129	0.496
PASI	**0.729**	**<0.001**	**-0.605**	**<0.001**
WBC	-0.058	0.761	-0.098	0.608
Neutrophil count	0.226	0.230	-0.229	0.225
Lymphocyte count	**-0.475**	**0.008**	**0.500**	**0.005**
Neutrophil/lymphocyte ratio	**0.656**	**<0.001**	**-0.706**	**<0.001**

r: Correlation coefficient.

Table 3. Cut-off value, sensitivity and specificity of IL-17 and RvD1, individually and when combined, in diagnosing psoriasis.

	Cut-off	Sensitivity	Specificity	AUC (95.0% CI)	p
IL-17	>354.8	96.7%	53.3%	0.742 (0.613 - 0.847)	**<0.001**
RvD1	≤7.56	53.3%	93.3%	0.715 (0.584- 0.824)	**0.002**
Combined	-	80.0%	76.7%	0.814 (0.693- 0.903)	**<0.001**

AUC: Area under ROC curve; CI: Confidence intervals.

Table 4. Logistic regression analysis of IL-17 and RvD1 after adjusting for age, body mass index, and gender.

	Unadjusted		Adjusted [(1)]	
	OR (95% CI)	P	OR (95% CI)	p
IL-17	1.004 (1.001 -- 1.006)	0.005	1.004 (1.001 -- 1.006)	**0.006**
RvD1	0.851 (0.749 -- 0.967)	0.013	0.829 (0.721 -- 0.953)	**0.009**

OR: Odds ratio, CI: Confidence interval, (1) Adjusted with age, body mass index, and gender.

11.3 (8.7-16.1), p=0.004]. Figure 1 shows the distributions of IL-17 and RvD1 across the groups. PASI in psoriasis patients was recorded as 4.5 (3.0-9.1). Neutrophil count, WBC, lymphocyte count, and NLR were significantly higher in psoriasis patients than in the control group (Table 1).

IL-17 was positively correlated with PASI and NLR and negatively correlated with RvD1 and lymphocyte count. RvD1 was negatively correlated with PASI and NLR and positively correlated with lymphocyte count. The correlations between IL-17, RvD1, and other parameters are detailed in both Table 2 and the correlation matrix (Figure 2).

As shown in Table 3 and Figure 3, IL-17 diagnosed psoriasis with 96.7% sensitivity and 53.3% specificity; the AUC (area under the curve) for ROC analysis was 0.742 (0.613 - 0.847) at a cut-off value of >354.8. RvD1 diagnosed psoriasis with 53.3% sensitivity and 93.3% specificity and AUC for ROC analysis was 0.715 (0.584- 0.824) at a cut-off value of ≤ 7.56. When IL-17 and RvD1 were combined, sensitivity and specificity for diagnosing psoriasis were 80% and 76.7%, respectively. When both markers were combined, the AUC reached 0.814 (0.693-0.903). This combination significantly increased diagnostic efficiency.

Multiple logistic regression analysis revealed that high IL-17 and low RvD1 were independently associated with psoria-

https://doi.org/10.5455/annalsmedres.2025.11.365

sis (Table 4). After adjusting for age, BMI, and gender, a 1-unit (1 pg/mL) increase in IL-17 levels was significantly associated with a 1.004-fold increase in the odds of having psoriasis (OR: 1.004, 95% CI: 1.001 61.006; p=0.006). After adjusting for age, BMI, and gender, the odds of psoriasis decreased by 17% with each 1-unit (1 ng/mL) increase in serum RvD1 level (OR: 0.829, 95% CI: 0.721–0.953; p=0.009). IL-17 was a risk factor for psoriasis, while RvD1 was a protective factor.

DISCUSSION

Although IL-17 and RvD1 were studied separately in psoriasis patients, the present study is clinically important because it is the first to study the balance between these two molecules in such patients and to reveal their relationship with PASI. The main finding of our study was that serum IL-17 levels were approximately two-fold higher in the psoriasis group compared to controls, whereas serum RvD1 levels were approximately 1.5-fold lower. This finding supports the concept that psoriasis is a chronic inflammatory process that disrupts the redox balance with a decrease in the expression of anti-inflammatory (RvD1) molecvules and an increase in the expression of inflammatory mediators (IL-17). The decrease in RvD1, a lipid mediator derived from docosahexaenoic acid, in psoriasis may prevent neutrophil phagocytosis and lead to the continuation of psoriasis-related inflammation [13]. Chronic inflammation that does not fully resolve in the presence of low RvD1 may prevent improvement in the clinical and laboratory findings of psoriasis. The role of this molecule in the etiology of the disease can be more clearly demonstrated by studies analyzing RvD1 levels during remission and attack periods in patients with psoriasis.

The fact that systemic indicators of inflammation such as WBC, neutrophil count, lymphocyte count, and neutrophil-to-lymphocyte ratio were increased in the psoriasis group compared to controls suggests that psoriasis activates inflammatory pathways and suppresses production of anti-inflammatory cytokines such as RvD1. The negative correlation between RvD1 and IL-17 strongly supports this idea. In addition, IL-17 has been shown to increase eightfold in psoriatic lesions and to stimulate proinflammatory cytokine production, suggesting that IL-17 is responsible for the increase in systemic inflammation indices [14]. The positive correlation between IL-17 and the neutrophil/lymphocyte ratio and the negative correlation between RvD1 and the neutrophil/lymphocyte ratio support the idea that IL-17 and RvD1 work in opposite ways to maintain the inflammatory balance in psoriasis.

The psoriasis area and severity index (PASI) is the most widely used scoring system as the primary endpoint of applied treatment efficacy [15]. The positive correlation between PASI index and IL-17, and the negative correlation between RvD1 and PASI, suggest that IL-17 increases the attacks and severity of psoriasis, while RvD1 reduces the attacks and severity. Mast cells and neutrophils that accumulate in the lesion area can be considered the main cellular sources of IL-17. However, it is not clear whether the immune and inflammatory cells accumulated in psoriatic lesions are the cause or the result of the disease [16]. The fact that IL-17A inhibitors provide almost complete resolution of skin lesions supports the positive relationship between IL-17 increase and PASI [17]. Resolvin D1 is an omega-3 polyunsaturated fatty acid–derived lipid mediator primarily produced by leukocytes, including macrophages and neutrophils. It promotes the resolution of inflammation by limiting neutrophil recruitment, enhancing macrophage-mediated clearance, and activating specific G-protein–coupled receptors such as ALX/FPR2 and GPR32 [18]. Notably, serum resolvin D1 levels were significantly reduced despite relatively low PASI scores in the psoriasis group. This finding suggests that impairment of pro-resolution pathways may occur even in patients with mild clinical disease activity. In the context of psoriasis, IL-17–driven immune activation may interfere with pro-resolving lipid mediator pathways. IL-17–activated T cells and neutrophils sustain a pro-inflammatory microenvironment that favors continued leukocyte recruitment and cytokine production, potentially suppressing the biosynthesis and bioavailability of pro-resolving mediators such as RvD1. Moreover, persistent IL-17 signaling may impair macrophage polarization toward a pro-resolving phenotype, thereby limiting effective resolution of inflammation. This imbalance between IL-17–mediated inflammation and RvD1-mediated resolution may contribute to the chronic and relapsing nature of psoriasis.

Multiple logistic regression analysis, after adjustment for age, BMI, and gender, revealed that high IL-17 and low RvD1 were independently associated with psoriasis, suggesting that these molecules could be used to diagnose psoriasis and assess its severity. The AUC obtained from ROC analysis of sensitivity and specificity for IL-17 in diagnosing psoriasis was 0.742, whereas the AUC for RvD1 was 0.715. The diagnostic sensitivities of both markers were similar. After the ROC analysis combining both markers, the AUC reached 0.814, and the diagnostic efficiency increased significantly.

Limitations

In the present study, psoriasis was diagnosed based on characteristic clinical findings rather than histopathological confirmation. Although this approach reflects routine clinical practice and is widely accepted in clinical studies, the lack of histopathological verification may have introduced a degree of diagnostic heterogeneity , and this should be considered a limitation. The relatively small sample size and the cross-sectional study design may limit the generalizability of the findings and preclude causal inferences. Although inferential statistical methods were used to evaluate predefined biological associations, the results should be interpreted as exploratory rather than confirmatory. Larger, adequately powered prospective studies are required to validate these findings.

https://doi.org/10.5455/annalsmedres.2025.11.365

CONCLUSION

This is the first study to compare serum levels of interleukin-17 (IL-17), a key driver of proinflammatory cytokine expression, and resolvin D1 (RvD1), an anti-inflammatory lipid mediator, in patients with psoriasis and to relate them to other inflammatory markers and PASI scores. Consistent with their opposing biological roles, IL-17 levels were significantly increased, whereas RvD1 levels were significantly decreased in patients with psoriasis. After adjustment for age, sex, and body mass index, elevated IL-17 and reduced RvD1 remained independently associated with psoriasis, indicating their potential contribution to disease risk in this cohort. Although diagnostic sensitivities of IL-17 and RvD1 were comparable, combined use of the two biomarkers improved overall diagnostic performance, suggesting complementary value in clinical assessment. These findings highlight IL-17 and RvD1 as promising candidates for future diagnostic and disease-monitoring strategies in psoriasis. Finally, therapeutic approaches aimed at restoring the balance between pro-inflammatory and pro-resolving pathways, including modulation of IL-17 and RvD1, may represent a promising avenue for future treatment development, warranting further investigation in larger prospective studies.

Ethics Committee Approval: Ethical approval for this study was obtained from the Fırat University Non-Interventional Research Ethics Committee, Elazığ, Turkey (Approval no: 2024/29957, Date: 27.12.2024).

Informed Consent: Written informed consent was obtained from all participants prior to their inclusion in the study.

Peer-review: Externally peer-reviewed.

Conflict of Interest: The authors declare that they have no conflict of interest.

Author Contributions: Conception: Ş.G., R.P.S, A.K., Design: Ş.G., R.P.S, A.K., Supervision: Ş.G., R.P.S, Materials: Ş.G., Data Collection and/or Processing: Ş.G., Analysis and/or Interpretation: A.K., Literature Review: Ş.G., R.P.S, A.K., Writing: Ş.G., R.P.S, Critical Review: R.P.S, A.K.

Financial Disclosure: None.

Artificial Intelligence Disclosure: The authors declare that no artificial intelligence tools were used in the preparation of this article.

REFERENCES

1. Serhan CN, Chiang N, Dalli J, Levy BD. Lipid mediators in the resolution of inflammation. *Cold Spring Harb Perspect Biol.* 2014;7(2):a016311. doi: 10.1101/cshperspect.a016311.
2. Dennis EA, Norris PC. Eicosanoid storm in infection and inflammation. *Nat Rev Immunol.* 2015;15(8):511-23. doi: 10.1038/nri3859.
3. Sorokin AV, Norris PC, English JT, et al. Identification of proresolving and inflammatory lipid mediators in human psoriasis. *J Clin Lipidol.* 2018;12(4):1047-60. doi: 10.1016/j.jacl.2018.03.091.
4. Ghoreschi K, Balato A, Enerbäck C, Sabat R. Therapeutics targeting the IL-23 and IL-17 pathway in psoriasis. *Lancet.* 2021;397(10275):754-66. doi: 10.1016/S0140-6736(21)00184-7.
5. Serhan CN. Resolution phase of inflammation: novel endogenous anti-inflammatory and proresolving lipid mediators and pathways. *Annu Rev Immunol.* 2007;25:101-37. doi: 10.1146/annurev.immunol.25.022106.141647.
6. Calder PC. n-3 polyunsaturated fatty acids, inflammation, and inflammatory diseases. *Am J Clin Nutr.* 2006;83(6 Suppl):1505s-19s. doi: 10.1093/ajcn/83.6.1505S.
7. Roohbakhsh A, Etemad L, Karimi G. Resolvin D1: A key endogenous inhibitor of neuroinflammation. *Biofactors.* 2022;48(5):1005-26. doi: 10.1002/biof.1891.
8. Coras R, Kavanaugh A, Boyd T, et al. Pro- and anti-inflammatory eicosanoids in psoriatic arthritis. *Metabolomics.* 2019;15(4):65. doi: 10.1007/s11306-019-1527-0.
9. Blauvelt A, Chiricozzi A. The Immunologic Role of IL-17 in Psoriasis and Psoriatic Arthritis Pathogenesis. *Clin Rev Allergy Immunol.* 2018;55(3):379-90. doi: 10.1007/s12016-018-8702-3.
10. Martin DA, Towne JE, Kricorian G, et al. The emerging role of IL-17 in the pathogenesis of psoriasis: preclinical and clinical findings. *J Invest Dermatol.* 2013;133(1):17-26. doi: 10.1038/jid.2012.194.
11. Maul JT, Maul LV, Didaskalu JA, et al. Correlation between Dermatology Life Quality Index and Psoriasis Area and Severity Index in Patients with Psoriasis: A Cross-sectional Global Healthcare Study on Psoriasis. *Acta Derm Venereol.* 2024;104:adv20329. doi: 10.2340/actadv.v104.20329.
12. Nardino M, Barros WS, Olivoto T, et al. Multivariate diallel analysis by factor analysis for establish mega-traits. *An Acad Bras Cienc.* 2020;92 Suppl 1:e20180874. doi: 10.1590/0001-3765202020180874.
13. Li L, Cheng SQ, Sun YQ, et al. Resolvin D1 reprograms energy metabolism to promote microglia to phagocytize neutrophils after ischemic stroke. *Cell Rep.* 2023;42(6):112617. doi: 10.1016/j.celrep.2023.112617.
14. Johansen C, Usher PA, Kjellerup RB, et al. Characterization of the interleukin-17 isoforms and receptors in lesional psoriatic skin. *Br J Dermatol.* 2009;160(2):319-24. doi: 10.1111/j.1365-2133.2008.08902.x.
15. Langley RG, Feldman SR, Nyirady J, van de Kerkhof P, Papavassilis C. The 5-point Investigator's Global Assessment (IGA) Scale: A modified tool for evaluating plaque psoriasis severity in clinical trials. *J Dermatolog Treat.* 2015;26(1):23-31. doi: 10.3109/09546634.2013.865009.
16. Lin AM, Rubin CJ, Khandpur R, et al. Mast cells and neutrophils release IL-17 through extracellular trap formation in psoriasis. *J Immunol.* 2011;187(1):490-500. doi: 10.4049/jimmunol.1100123.
17. Langley RG, Elewski BE, Lebwohl M, et al. Secukinumab in plaque psoriasis–results of two phase 3 trials. *N Engl J Med.* 2014;371(4):326-38. doi: 10.1056/NEJMoa1314258.
18. Chiurchiù V, Leuti A, Dalli J, et al. Proresolving lipid mediators resolvin D1, resolvin D2, and maresin 1 are critical in modulating T cell responses. *Sci Transl Med.* 2016;8(353):353ra111. doi: 10.1126/scitranslmed.aaf7483.

https://doi.org/10.5455/annalsmedres.2025.11.365

Ann Med Res

Current issue list available at Ann Med Res

Annals of Medical Research

journal page: annalsmedres.org

Associations of MRI-derived adrenal lipid content with hepatic and pancreatic steatosis and insulin resistance

Yunus Yasar[a], *, Sevde Nur Emir[a], Mustafa Demir[a], Servet Emir[b]

[a]University of Health Sciences, Umraniye Training and Research Hospital, Department of Radiology, Istanbul, Türkiye
[b]University of Health Sciences, Umraniye Training and Research Hospital, Department of Internal Medicine, Istanbul, Türkiye
*Corresponding author: dryunusysr@gmail.com (Yunus Yasar)

MAIN POINTS

- MRI-derived adrenal lipid indices show modest but significant associations with hepatic and pancreatic fat content.
- Higher adrenal lipid content is associated with increased ectopic fat accumulation in these organs.
- These relationships persist after adjustment for age and sex.
- No meaningful association was observed between adrenal lipid indices and the TyG index.
- These findings suggest that adrenal lipid content may reflect regional ectopic fat distribution rather than systemic insulin resistance.

Cite this article as: Yasar Y, Emir SN, Demir M, Emir S. Associations of MRI-derived adrenal lipid content with hepatic and pancreatic steatosis and insulin resistance. *Ann Med Res*. 2026;33(8):381–388. doi: 10.5455/annalsmedres.2025.10.320.

ABSTRACT

Aim: Adrenal adenomas are frequent incidental findings, and even non-functioning adrenal adenomas (NFAAs) may be linked to subtle metabolic alterations. According to the lipid overflow hypothesis, excess lipids accumulate in non-adipose organs, such as the liver, pancreas, and adrenal glands, potentially reflecting systemic metabolic stress. This study aimed to investigate the association between MRI-derived adrenal lipid indices and hepatic and pancreatic fat and to assess their correlation with the triglyceride-glucose (TyG) index as a marker of insulin resistance.

Materials and Methods: This retrospective study included 201 patients with lipid-rich adrenal adenomas [Adrenal Signal Intensity Index (ASII) $\geq$ 20%] identified on 1.5T MRI. Signal intensities were measured in adrenal lesions, liver, pancreas, and spleen using dual-echo sequences. ASII and adrenal-to-spleen chemical-shift imaging (CSI) ratios were calculated. Hepatic and pancreatic fat fractions were derived from signal intensity differences. The TyG index was computed from fasting triglyceride and glucose levels. Correlation and multivariable regression analyses were performed.

Results: Adrenal lipid indices showed significant correlations with hepatic (r = 0.32 and –0.30) and pancreatic fat fractions (r = 0.19 and –0.18) (p<0.01). These associations remained significant after adjustment for age and sex. However, no meaningful correlation was found between adrenal lipid indices and the TyG index; regression models explained only a minimal amount of the variation in TyG values (R^2 = 0.025).

Conclusion: MRI-derived adrenal lipid indices are associated with ectopic fat accumulation in the liver and pancreas but do not reflect systemic insulin resistance. These findings suggest that adrenal lipid content may serve as a marker of regional fat redistribution rather than global metabolic dysfunction.

Keywords: Adrenal adenoma, Chemical shift imaging, Ectopic fat, Hepatic steatosis, MRI, Insulin resistance

Received: Oct 19, 2025 **Accepted:** Feb 12, 2026 **Available Online:** Aug 25, 2026

INTRODUCTION

Adrenal adenomas are among the most commonly encountered incidental findings on abdominal imaging, and their detection has increased substantially with the widespread use of cross-sectional modalities such as CT and MRI [1,2]. Most of these lesions are classified as non-functioning adrenal adenomas (NFAAs), as they do not cause overt hormonal excess. However, recent studies have challenged the notion that NFAAs are metabolically inert, suggesting instead that they may be associated with subclinical metabolic alterations, including hypertension, insulin resistance, and dyslipidemia [3–5]. These associations have primarily been explored through laboratory-based assessments, while imaging-derived correlates remain largely under-investigated. This is consistent with the lipid overflow hypothesis, which suggests that ectopic fat accumulation in non-adipose organs, such as the adrenal glands, may reflect systemic metabolic burden rather than primary organ dysfunction [6]. This hypothesis posits that surplus lipids, unable to be stored in adipose tissue, accumulate in non-adipose organs such as the liver, pancreas, and

adrenal glands, potentially serving as indicators of systemic metabolic stress [6–8].

Magnetic resonance imaging (MRI), particularly chemical shift imaging (CSI), enables non-invasive, quantitative evaluation of intracellular lipid content in adrenal lesions. Quantitative metrics such as the adrenal signal intensity index (ASII) and adrenal-to-spleen CSI ratio are widely used to characterize lipid-rich adenomas in clinical practice [9–11]. These indices exploit the signal intensity differences between in-phase and opposed-phase sequences to detect microscopic intracellular lipid, a key imaging hallmark of benign adrenal cortical adenomas [10,11]. However, beyond lesion characterization, these indices may serve as potential imaging biomarkers that reflect systemic metabolic changes or ectopic fat accumulation, although this hypothesis has not been sufficiently tested.

Ectopic fat deposition in metabolically active organs, such as the liver and pancreas, plays a central role in the pathophysiology of insulin resistance and cardiometabolic risk. Hepatic steatosis—particularly in the form of non-alcoholic fatty liver disease (NAFLD)—has been well characterized and robustly linked to insulin resistance, type 2 diabetes, and cardiovascular disease [12,13]. The clinical relevance of pancreatic fat, on the other hand, remains more controversial, though emerging evidence suggests associations with beta-cell dysfunction, glucose dysregulation, and even pancreatic fibrosis [14–17].

Investigating whether adrenal lipid content, assessed by MRI, correlates with ectopic fat accumulation in these organs could provide new insights into metabolic imaging and its pathophysiology.

In addition, the extent to which adrenal lipid indices correlate with markers of systemic metabolic dysfunction remains unclear. The triglyceride-glucose (TyG) index has emerged as a simple, cost-effective, and reliable surrogate marker for insulin resistance. It has been validated against traditional methods such as the HOMA-IR and hyperinsulinemic-euglycemic clamp [18–20]. Despite its growing use in clinical and research settings, the relationship between TyG and adrenal lipid content has not been systematically examined.

This study aims to quantitatively evaluate associations of MRI-derived adrenal lipid indices with hepatic and pancreatic fat fractions and determine whether these indices correlate with systemic insulin resistance as measured by the TyG index. By addressing these questions, we seek to clarify whether adrenal lipid accumulation reflects localized metabolic alterations or broader systemic dysfunction.

MATERIALS AND METHODS

Study design and population

The Ethics Committee of the University of Health Sciences Ümraniye Training and Research Hospital approved this retrospective single-center study (Approval no: 2025/31, Date: 13.03.2025). Abdominal MRI studies performed between January 2014 and December 2023 were reviewed to identify patients with adrenal adenomas. Since this was a retrospective study and all data were anonymized, informed consent was not required. The case selection process is summarized in Figure 1.

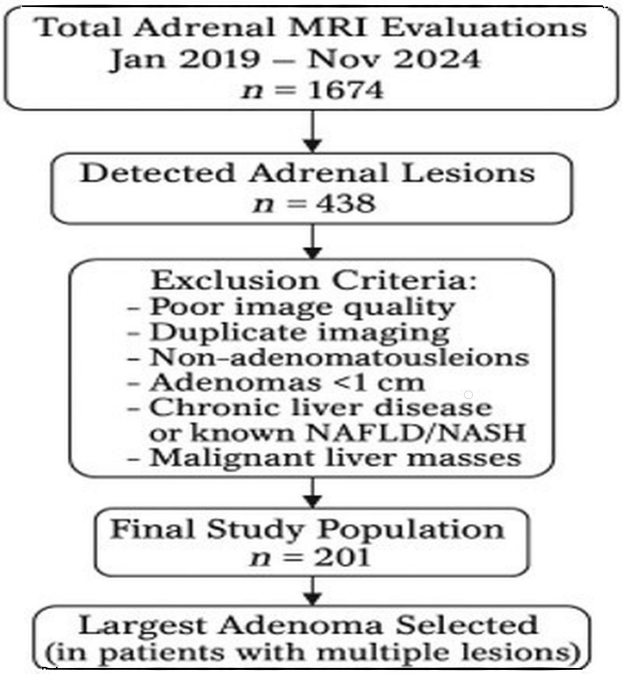

Figure 1. Flow diagram showing patient selection for the final study cohort. After exclusions, 201 patients with lipid-rich adrenal adenomas were included for analysis. In patients with multiple lesions, the largest adenoma was selected.

Inclusion criteria were: (1) radiologically confirmed adrenal adenoma based on MRI criteria, including signal drop on opposed-phase images and lesion size ≤4 cm; (2) availability of dual-echo chemical shift imaging sequences of diagnostic quality; and (3) laboratory data (fasting triglyceride and glucose levels) obtained within 7 days of MRI.

In this study, adrenal adenomas were diagnosed solely on the basis of imaging characteristics because histopathologic confirmation was not feasible, given the incidental nature of these lesions. Only lipid-rich adenomas—defined as lesions exhibiting significant intracellular fat content and an adrenal signal intensity index (ASII) greater than 20%—were included to ensure measurement reliability and biological homogeneity. This threshold was selected based on prior validation studies and reflects the sensitivity limit of chemical shift imaging for reliable fat quantification.

Lipid-poor adenomas (ASII < 20%) were excluded because they exhibit minimal signal drop on opposed-phase imaging, thereby reducing the accuracy of CSI-derived indices. Furthermore, lipid-poor lesions may exhibit distinct biological behavior, including an increased likelihood of subclinical cortisol secretion, which this study could not assess because hormonal profiling was not performed. Their inclusion would have introduced potential confounding effects and undermined the interpretability of adrenal lipid measurements.

https://doi.org/10.5455/annalsmedres.2025.10.320

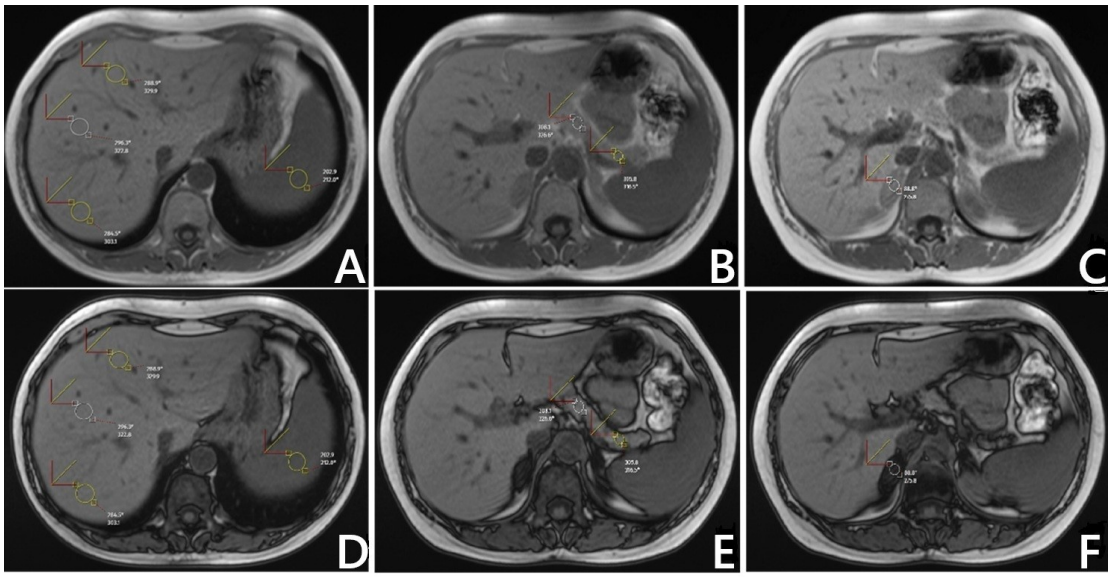

Figure 2. Axial gradient-echo T1-weighted chemical shift MRI images demonstrating ROI-based signal intensity measurements in representative cases. In-phase images are shown in panels A–C, and opposed-phase images in panels D–F. (A, D) illustrate ROI placements in the liver and spleen, (B, E) show measurements from the pancreatic head or body, and (C, F) display ROIs placed on the adrenal adenoma.

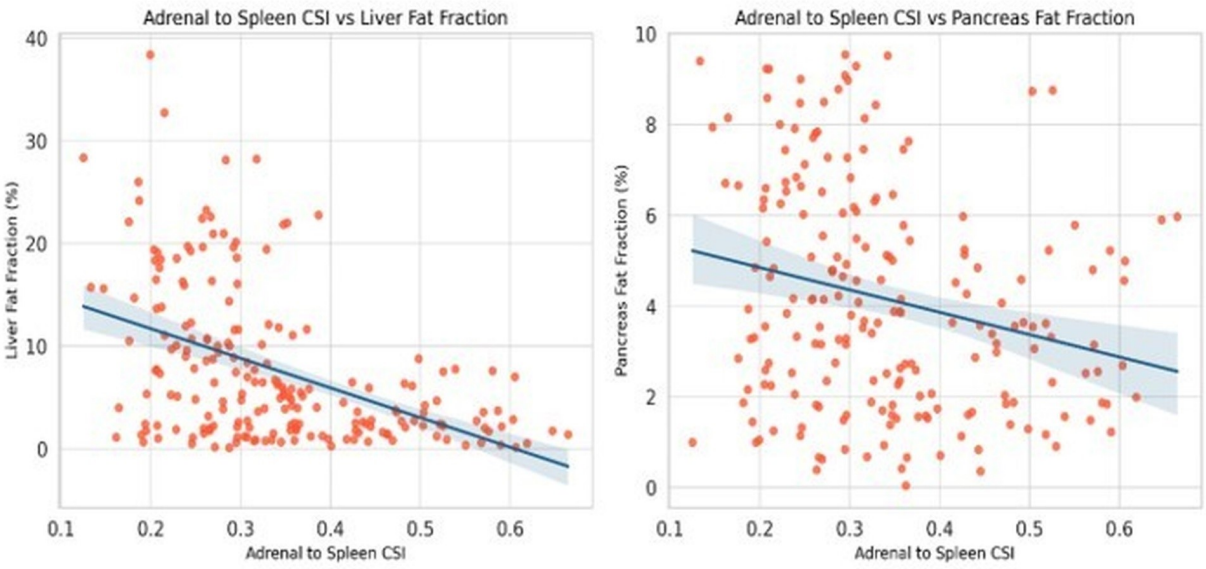

Figure 3. Correlation of adrenal to spleen CSI with liver and pancreas fat fractions.

Additional exclusion criteria were as follows: (1) known functional adrenal tumors (e.g., pheochromocytoma, cortisol-producing adenomas); (2) prior adrenal surgery or known adrenal malignancy; (3) chronic liver disease (defined as documented hepatitis, cirrhosis, or persistent liver enzyme elevation >3× upper limit of normal); (4) known NAFLD or NASH diagnosed by other modalities or by biopsy; (5) inadequate image quality; or (6) duplicate or follow-up MRI studies.

MRI acquisition and imaging analysis

All MRI examinations were performed using a 1.5T scanner (Optima MR450w, GE Healthcare). The standard abdominal MRI protocol included T2-weighted sequences, in-phase and opposed-phase dual-echo T1-weighted sequences, and diffusion-weighted imaging (DWI). Post-contrast imaging was not used for fat quantification. The dual-echo sequence parameters were as follows: TR = 165 ms; TE = 2.3/4.7 ms; slice thickness = 6 mm (Table 1).

Circular regions of interest (ROIs) with an area of 0.5–1 cm^2 were manually placed on the adrenal adenoma, liver parenchyma (segment VI), pancreatic head or body, and spleen. Care was taken to avoid visible vessels, lesions, or imaging artifacts. Three measurements were obtained for each organ and averaged for analysis (Figure 2A–F). Specifically,

https://doi.org/10.5455/annalsmedres.2025.10.320

Table 1. MRI sequence parameters used in adrenal imaging.

Sequence	TR (ms)	TE (ms)	Flip Angle (°)	Slice Thickness (mm)	Comments
Coronal & Axial T2-weighted	1000	81.3	-	6	Localization and lesion morphology
Axial T1-weighted Dual Echo (CSI)	165	TE1: 2.3 TE2: 4.7	60	6	In-phase and opposed-phase imaging
Axial T2-weighted FS (FIESTA)	4.4	1.5	70	6	Fat suppression
Diffusion-weighted Imaging (DWI)	-	-	-	6	b-values: 50, 500, 1000 s/mm²
ADC Mapping	-	-	-	6	Derived from DWI
Axial Dynamic Contrast-Enhanced (LAVA-F)	6.0	Min Full	15	5	Phases: 0, 8, 15, 30 seconds post-injection

Table 2. Quantitative MRI and laboratory formulas used in the study.

Parameter	Formula	Purpose
Fat Fraction (%)	(SIIP – SIOP) / (2 × SIIP) × 100	Quantification of hepatic and pancreatic fat
Adrenal Signal Intensity Index (ASII)	100 × [(SIIP – SIOP) / SIIP]	Measurement of adrenal lipid content
Adrenal-to-Spleen CSI Ratio	Lesion-to spleen SIIP / lesion-to-spleen SIOP	Fat sensitivity in adrenal lesions
TyG Index	Ln (2 x Triglycerides (mg/dL) × Glucose (mg/dL))	Surrogate marker of insulin resistance

(SIIP: Signal intensity in phase, SIOP: Signal intensity out-of-phase). (where SIIP and SIOP represent signal intensities in in-phase and opposed-phase images, respectively).

Table 3. Baseline characteristics of patients with adrenal adenomas.

Characteristic	Number (%)
Number of patients	201
Gender	
Female	165 (82.1%)
Male	36 (17.9%)
Mean age ± SD years	53.4 ± 9.2
Laboratory Findings	
Triglyceride (Median -- IQR)	146 - 91
Fasting Plasma Glucose (Median -- IQR)	98 - 26
TYG Index (Mean ± SD)	4.82 ± 0.39
Volume of adenoma (cm3)	
Mean ± SD	6.3 ± 5.3
Median -- IQR	4.46 - 6.05
Range	0.6 -- 25.8
Localisation of adenoma	
Right	99 (49.3%)
Left	102 (50.7%)

ROIs for the liver and spleen were placed as shown in Figures 2A and 2D; ROIs for the pancreatic head or body were placed as shown in Figures 2B and 2E; and ROIs for adrenal adenomas were placed as shown in Figures 2C and 2F. All measurements were performed jointly by two radiologists (with 5 and 10 years' experience in abdominal MRI) and recorded by consensus.

Quantitative indices, including the adrenal signal intensity index (ASII), adrenal-to-spleen chemical shift ratio (CSI ratio), liver and pancreas fat fractions, and TyG index, were calculated using standardized formulas summarized in Table 2.

Statistical analysis

All statistical analyses were performed using SPSS v24. Scatter plots were generated for visualization purposes using external software based on SPSS-derived outputs. Continuous variables were reported as mean ± standard deviation or median (interquartile range), as appropriate. The Kolmogorov–Smirnov test was used to assess the normality of the data. Univariable associations between adrenal lipid indices (CSI ratio, ASII) and hepatic and pancreatic fat content or the TyG index were evaluated using Spearman's rank correlation.

To account for potential confounding factors, separate multivariable linear regression models were constructed for each dependent variable (hepatic fat fraction, pancreatic fat fraction, and TyG index). In these models, the independent variables were the adrenal-to-spleen CSI ratio (the representative imaging-derived adrenal lipid parameter), age, and sex. The ASII was excluded from the multivariable models because it is derived from the same signal-intensity measurements as the CSI ratio; including both would violate the assumption of independence among predictors.

https://doi.org/10.5455/annalsmedres.2025.10.320

A two-tailed p-value < 0.05 was considered statistically significant. As this was a retrospective observational study, no a priori sample size or power calculation was performed; instead, the study population consisted of all eligible patients who met the predefined inclusion criteria during the study period.

RESULTS

The final analysis included 201 patients with lipid-rich adrenal adenomas (ASII ≥ 20%). The mean age was 53.4 ± 9.2 years (range: 30–75), and 82.1% were female (n = 165), while 17.9% were male (n = 36). Laboratory parameters showed median triglyceride and fasting plasma glucose levels of 146 mg/dL (IQR: 91) and 98 mg/dL (IQR: 26), respectively. The mean TyG index was 4.82 ± 0.39. The mean volume of adrenal adenomas was 6.3 ± 5.3 cm^3, with a median volume of 4.46 cm^3 (IQR: 6.05) and a range of 0.6 to 25.8 cm^3. Lesions were evenly distributed between the right (n = 99, 49.3%) and left (n = 102, 50.7%) adrenal glands (Table 3).

The median adrenal signal intensity index (ASII) was 68.9% (IQR: 16.5), and the adrenal-to-spleen CSI ratio was 0.316 (IQR: 0.167). The median hepatic fat fraction was 5.11% (IQR: 8.68), and the median pancreatic fat fraction was 3.67% (IQR: 3.94) (Table 4).

Descriptive and correlation analysis

Hepatic fat demonstrated wide interindividual variability, with 34.8% of patients exhibiting moderate to severe steatosis (fat fraction ≥ 5%). Pancreatic fat was more narrowly distributed, with 22.4% of individuals exceeding a 6% fat fraction.

Spearman correlation analysis revealed significant and directionally consistent associations between the adrenal-to-spleen CSI ratio and both hepatic and pancreatic fat fractions. Specifically, the CSI ratio was inversely correlated with hepatic fat ($r = -0.458$, $p<0.001$) and pancreatic fat ($r = -0.245$, $p<0.001$), indicating that lower adrenal CSI values (i.e., higher lipid content) were associated with increased ectopic fat accumulation in both organs (Figure 3). The TyG index did not correlate significantly with the CSI ratio ($r = -0.080$, $p = 0.258$) (Table 5).

Multivariable regression analysis

In multivariable linear regression analyses adjusting for age and sex, the adrenal-to-spleen CSI ratio demonstrated a statistically significant inverse association with both hepatic and pancreatic fat fractions. Specifically, lower CSI ratios, indicative of higher adrenal lipid content, were independently associated with increased hepatic fat accumulation ($\beta = -27.36$, $p<0.001$). The model explained approximately 25.3% of the variance in hepatic fat ($R^2 = 0.253$, $p<0.001$). A similar pattern was observed for pancreatic fat, where the CSI ratio again showed a strong inverse association ($\beta = -5.64$, $p<0.001$), with age emerging as a significant positive predictor ($\beta = 0.051$, $p=0.006$); this model accounted for 16.2% of the variance in pancreatic fat content ($R^2 = 0.162$, $p<0.001$).

When predictors of the TyG index were evaluated, the CSI ratio showed a small, marginally significant inverse association ($\beta = -1.97$, $p=0.043$). However, the overall model explained only a minimal proportion of the variance in the TyG index ($R^2 = 0.025$, $p=0.285$), indicating the limited explanatory value of adrenal lipid indices and demographic covariates (age and sex) for systemic insulin resistance (Table 6).

DISCUSSION

This study demonstrates that MRI-based adrenal lipid indices—specifically, the adrenal signal intensity index (ASII) and the adrenal-to-spleen chemical shift imaging (CSI) ratio—are independently associated with ectopic fat accumulation in the liver and pancreas, but not with systemic insulin resistance, as assessed by the triglyceride-glucose (TyG) index. These findings support the concept that adrenal lipid content may serve as an imaging correlate of localized ectopic fat redistribution rather than a marker of global metabolic dysfunction, particularly insulin resistance.

Several studies have reported that non-functioning adrenal adenomas (NFAAs), though traditionally considered hormonally silent, are associated with metabolic syndrome components such as hypertension, visceral adiposity, and impaired glucose metabolism [3–5,21]. While subclinical hypercortisolism was previously thought to drive this association, recent data suggest that metabolic alterations may occur independently of hormonal secretion [22,23]. Our findings align with this paradigm shift, suggesting that adrenal lipid accumulation may reflect systemic metabolic stress, rather than direct endocrine involvement.

The significant association between adrenal lipid content and hepatic steatosis observed in our study reinforces the "lipid overflow" hypothesis, which posits that excess lipids not stored in adipose tissue are deposited in non-adipose organs such as the liver, pancreas, and adrenal glands [6–8]. This ectopic fat redistribution is a hallmark of metabolic stress and has been strongly linked to insulin resistance, particularly in the liver [12,13]. Previous imaging studies, including a recent chemical shift MRI analysis, have reported a positive correlation between adrenal and hepatic fat content [24]. Our study adds to this evidence by confirming the relationship using multivariable regression models adjusted for age and sex, thereby strengthening the generalizability of this association.

MRI-based fat quantification using CSI offers advantages over CT attenuation in detecting intracellular lipid content [9–11, 25–27]. While CT has limited sensitivity for detecting microscopic fat, CSI enables non-invasive and reproducible quantification of fat in adrenal lesions. Our study employed established indices, such as the ASII and the adrenal-to-spleen CSI ratio, to ensure methodological reliability. Notably, lipid-poor adenomas (ASII < 20%) were excluded to avoid biolog-

https://doi.org/10.5455/annalsmedres.2025.10.320

Table 4. Quantitative measurements of liver, pancreas, spleen, and adrenal lesions.

	In Phase (Median–IQR)	Out-of-Phase (Median–IQR)	Fat Fraction (Median -- IQR)	
Liver Measurement	292.65-115.72	250.49-116.24	5.11-8.68	
Pancreas Measurement	323.79-156.44	297.88-141.74	3.67-3.94	
Spleen Measurement	191.79-61.87	186.21-57.13		
			ASII (Median-IQR)	Adrenal/Spleen CSI Ratio (Median -- IQR)
Adrenal Lesion Measurement	273.48-84.76	89.65-53.52	68.9-16.5	0.316-0.167

Table 5. Correlation of Adrenal/Spleen CSI ratio, ASII, and TyG index with liver fat fraction, pancreatic fat fraction, and inter-parameter relationships.

		Adrenal/Spleen CSI ratio	ASII
Liver Fat Fraction	Spearman correlation coefficient	**-0.439**	**0.452**
	p-value	**p<0.01**	**p<0.01**
Pancreatic Fat Fraction	Spearman correlation coefficient	**-0.245**	**0.220**
	p-value	**p=0.01**	**p=0.02**
Tyg Index	Spearman correlation coefficient	-0.079	0.078
	p-value	p=0.265	P=0.273

Table 6. Multivariable linear regression analysis of CSI ratio, age, and sex with liver fat fraction, pancreatic fat fraction, and TyG index.

		Intercept	Adrenal/Spleen CSI ratio	Age	Sex
Liver Fat Fraction	β	19.17	**-27.36**	-0.037	-2.25
	SE	3.05	**4.02**	0.053	1.27
	95% CI	13.14 to 25.19	**-34.43 to -18.55**	-0.13 to 0.07	-5.04 to 0.02
	p-value	<0.001	**<0.001**	0.479	0.076
Pancreatic Fat Fraction	β	2.98	**-5.64**	**0.051**	1.04
	SE	1.03	**1.36**	**0.018**	0.431
	95% CI	0.94 to 5.02	**-7.74 to -2.38**	**0.02 to 0.09**	0.93 to 1.78
	p-value	0.004	**<0.001**	**0.006**	0.141
Tyg Index	β	4.81	-1.97	-0.001	-0.135
	SE	0.21	0.28	0.004	0.091
	95% CI	4.38 to 5.24	-2.23 to 0.12	-0.007 to 0.009	-0.27 to 0.08
	p-value	<0.001	0.043	0.973	0.863

ical heterogeneity and minimize the inclusion of potentially functional tumors [22,23].

The observed inverse relationship between adrenal lipid indices and pancreatic fat is notable. Although pancreatic fat is less well understood than hepatic steatosis, several studies have linked it to impaired insulin secretion, beta-cell dysfunction, and glucose dysregulation [12,13,15–17]. Our results suggest that adrenal lipid accumulation may parallel pancreatic fat deposition, implying a broader role for ectopic lipid redistribution across metabolically active organs. Whether this association reflects a shared pathogenic mechanism or is merely coincidental remains to be studied further.

In contrast to hepatic and pancreatic fat, adrenal lipid indices were not meaningfully associated with the TyG index. Although a marginally significant beta coefficient was observed in the regression analysis, the model demonstrated very low explanatory power (R^2 = 0.025), indicating limited clinical relevance. The temporal mismatch between static imaging-derived measures and dynamic metabolic indices may partly explain this discrepancy. While the TyG index is a validated surrogate marker of insulin resistance [18–20], it primarily reflects short-term metabolic fluctuations. It may not correspond to the slower, cumulative process of ectopic lipid deposition within tissues. Similar discrepancies between structural imaging biomarkers and functional metabolic markers have been reported previously [28].

Our findings underscore the need to interpret adrenal lipid content not as a marker of systemic insulin resistance, but rather as a regional indicator of ectopic fat burden, particularly in the liver and pancreas. The adrenal gland, due to its vascularity and lipid-handling capacity, may act as a passive depot for circulating lipids in individuals with excess visceral fat, in line with the lipid overflow hypothesis [6].

Limitations

This study has several limitations. The retrospective design limited access to comprehensive endocrine and anthropometric data, such as cortisol, insulin levels, BMI, and waist circumference. Consequently, the metabolic status of patients

https://doi.org/10.5455/annalsmedres.2025.10.320

could not be fully characterized. Although we excluded individuals with known NAFLD or NASH to reduce confounding, this may have inadvertently introduced selection bias by excluding those with advanced hepatic fat accumulation. Furthermore, while the TyG index is practical and widely used, it does not accurately reflect organ-specific insulin sensitivity and may underestimate the complexity of metabolic relationships. Finally, although CSI-based fat quantification is reliable, can be affected by T2* decay or iron deposition. Newer techniques, such as proton density fat fraction (PDFF), may offer improved accuracy and cross-platform reproducibility, especially in longitudinal or multi-center studies [25,28].

CONCLUSION

In conclusion, MRI-derived adrenal lipid indices, particularly the adrenal-to-spleen CSI ratio and ASII, are associated with hepatic and pancreatic fat content but not with systemic insulin resistance as measured by the TyG index. These results suggest that adrenal lipid accumulation may reflect localized ectopic fat redistribution rather than generalized metabolic dysfunction. Future studies using advanced fat quantification methods and comprehensive metabolic profiling are warranted to clarify the potential role of adrenal fat content as an imaging biomarker of metabolic health.

Ethics Committee Approval: This study received approval from the Institutional Review Board of the University of Health Sciences, Ümraniye Training and Research Hospital (Approval no: 2025/31, Date: 13.03.2025).

Informed Consent: Informed consent was not obtained because of the study's retrospective design.

Peer-review: Externally peer-reviewed.

Conflict of Interest: The authors declare that they have no competing interests.

Author Contributions: Concept: Y.Y., S.N.E.; Design: Y.Y., S.N.E.; Supervision: Y.Y.; Materials: Y.Y., S.N.E., M.D., S.E.; Data Collection or Processing: Y.Y., S.N.E., M.D., S.E.; Analysis or Interpretation: Y.Y., M.D.; Literature Search: Y.Y., S.N.E., M.D., S.E.; Writing: Y.Y., S.N.E.; Critical Review: S.N.E., M.D., S.E.

Financial Disclosure: No financial support was obtained for this study.

Artificial Intelligence Disclosure: The authors declare that an artificial intelligence–based tool (ChatGPT, GPT-4o, OpenAI) was used solely for language editing and improving the clarity and readability of the manuscript. The AI tool did not contribute to the study design, data analysis, interpretation of results, or scientific conclusions. All content was critically reviewed and approved by the authors, who take full responsibility for the manuscript.

REFERENCES

1. Barzon L, Sonino N, Fallo F, Palu G, Boscaro M. Prevalence and natural history of adrenal incidentalomas. *Eur J Endocrinol.* 2003;149(4):273-85. doi: 10.1530/eje.0.1490273.
2. Sherlock M, Scarsbrook A, Abbas A, et al. Adrenal Incidentaloma. *Endocr Rev.* 2020;41(6):775–820. doi: 10.1210/endrev/bnaa008.
3. Tuna MM, Imga NN, Doğan BA, et al. Non-functioning adrenal incidentalomas are associated with higher hypertension prevalence and higher risk of atherosclerosis. *J Endocrinol Invest.* 2014;37(8):765-768. doi: 10.1007/s40618-014-0106-5.
4. Midorikawa S, Sanada H, Hashimoto S, Suzuki T, Watanabe T. The improvement of insulin resistance in patients with adrenal incidentaloma by surgical resection. *Clin Endocrinol (Oxf).* 2001;54(6):797-804. doi: 10.1046/j.1365-2265.2001.01274.x.
5. Terzolo M, Pia A, Alì A, et al. Adrenal incidentaloma: a new cause of the metabolic syndrome? *J Clin Endocrinol Metab.* 2002;87(3):998-1003. doi: 10.1210/jcem.87.3.8277.
6. Janssen JAMJL. The Causal Role of Ectopic Fat Deposition in the Pathogenesis of Metabolic Syndrome. *Int J Mol Sci.* 2024;25(24):13238. doi: 10.3390/ijms252413238.
7. Guebre-Egziabher F, Alix PM, Koppe L, et al. Ectopic lipid accumulation: A potential cause for metabolic disturbances and a contributor to the alteration of kidney function. *Biochimie.* 2013;95(11):1971-9. doi: 10.1016/j.biochi.2013.07.017.
8. Trouwborst I, Bowser SM, Goossens GH, Blaak EE. Ectopic Fat Accumulation in Distinct Insulin Resistant Phenotypes; Targets for Personalized Nutritional Interventions. *Front Nutr.* 2018;5:77. doi: 10.3389/fnut.2018.00077.
9. d'Amuri FV, Maestroni U, Pagnini F, et al. Magnetic resonance imaging of adrenal gland: state of the art. *Gland Surg.* 2019;8(Suppl 3):S223-S232. doi: 10.21037/gs.2019.06.02.
10. Blake MA, Cronin CG, Boland GW. Adrenal imaging. *AJR Am J Roentgenol.* 2010;194(6):1450-60. doi: 10.2214/AJR.10.4547.
11. Elbanan MG, Javadi S, Ganeshan D, et al. Adrenal cortical adenoma: current update, imaging features, atypical findings, and mimics. *Abdom Radiol (NY).* 2020;45(4):905-916. doi: 10.1007/s00261-019-02215-9.
12. Taylor SA, Carucci LR. The role of imaging in obesity special feature. *Br J Radiol.* 2018;91(1089):20189002. doi: 10.1259/bjr.20189002.
13. Bi Y, Wang JL, Li ML, Zhou J, Sun XL. The association between pancreas steatosis and metabolic syndrome: A systematic review and meta-analysis. *Diabetes Metab Res Rev.* 2019;35(5):e3142. doi: 10.1002/dmrr.3142.
14. Wong VW, Wong GL, Yeung DK, et al. Fatty pancreas, insulin resistance, and β-cell function: a population study using fat-water magnetic resonance imaging. *Am J Gastroenterol.* 2014;109(4):589-97. doi: 10.1038/ajg.2014.1.
15. Patel NS, Peterson MR, Brenner DA, Heba E, Sirlin C, Loomba R. Association between novel MRI-estimated pancreatic fat and liver histology-determined steatosis and fibrosis in non-alcoholic fatty liver disease. *Aliment Pharmacol Ther.* 2013;37(6):630-9. doi: 10.1111/apt.12237.
16. Koyuncu Sokmen B, Sahin T, Oral A, Kocak E, Inan N. The comparison of pancreatic and hepatic steatosis in healthy liver donor candidates. *Sci Rep.* 2021;11(1):4507. doi: 10.1038/s41598-021-83871-0.
17. Tushuizen ME, Bunck MC, Pouwels PJ, et al. Pancreatic fat content and beta-cell function in men with and without type 2 diabetes. *Diabetes Care.* 2007;30(11):2916-21. doi: 10.2337/dc07-0326.
18. Sánchez-García A, Rodríguez-Gutiérrez R, Mancillas-Adame L, et al. Diagnostic Accuracy of the Triglyceride and Glucose Index for Insulin Resistance: A Systematic Review. *Int J Endocrinol.* 2020;2020:4678526. doi: 10.1155/2020/4678526.
19. Minh HV, Tien HA, Sinh CT, et al. Assessment of preferred methods to measure insulin resistance in Asian patients with hypertension. *J Clin Hypertens (Greenwich).* 2021;23(3):529-537. doi: 10.1111/jch.14155.
20. Tian X, Zuo Y, Chen S, et al. Triglyceride-glucose index is associated with the risk of myocardial infarction: an 11-year prospective study in the Kailuan cohort. *Cardiovasc Diabetol.* 2021;20(1):19. doi: 10.1186/s12933-020-01210-5.

21. Ivović M, Vujović S, Penezić Z, Zarković M, Drezgić M. Insulin sensitivity in patients with adrenal incidentaloma. *Srp Arh Celok Lek.* 2006;134(7-8):315-9. doi: 10.2298/sarh0608315i.
22. Higgs JA, Quinn AP, Seely KD, et al. Pathophysiological Link between Insulin Resistance and Adrenal Incidentalomas. *Int J Mol Sci.* 2022;23(8):4340. doi: 10.3390/ijms23084340.
23. Olsen H, Olofsson L, Mjöman M. Cortisol secretion from adrenal adenomas discovered as incidentalomas is responsive to ACTH. *Clin Endocrinol (Oxf).* 2014;80(3):335-41. doi: 10.1111/cen.12295.
24. Buz Yaşar A, Ayhan ZY. Radiologic correlation with fatty liver and adrenal adenoma using dual echo chemical shift magnetic resonance imaging. *Abdom Radiol (NY).* 2025;50(4):1868-1875. doi: 10.1007/s00261-024-04622-z.
25. Guglielmo FF, Barr RG, Yokoo T, et al. Liver Fibrosis, Fat, and Iron Evaluation with MRI and Fibrosis and Fat Evaluation with US: A Practical Guide for Radiologists. *Radiographics.* 2023;43(6):e220181. doi: 10.1148/rg.220181.
26. Yamada T, Ishibashi T, Saito H,et al. Adrenal adenomas: relationship between histologic lipid-rich cells and CT attenuation number. *Eur J Radiol.* 2003;48(2):198-202. doi: 10.1016/S0720-048X(02)00217-6.
27. Nishie A, Asayama Y, Ishigami K, et al. Impact of body mass index on CT attenuation of adrenal adenoma. *Eur. J. Radiol.* 2018;108:184-188. doi: 10.1016/j.ejrad.2018.09.033.
28. Idilman IS, Aniktar H, Idilman R, et al. Hepatic steatosis: quantification by proton density fat fraction with MR imaging versus liver biopsy. *Radiology.* 2013;267(3):767-75. doi: 10.1148/radiol.13121360.

https://doi.org/10.5455/annalsmedres.2025.10.320

Ann Med Res

Current issue list available at Ann Med Res

Annals of Medical Research

journal page: annalsmedres.org

Vascular pathology prevalence and presentation patterns in patients presenting with leg pain to a tertiary vascular surgery clinic: A cross-sectional observational study

Kubra Gozacik Karakoc[a], *, Tamer Cebe[a], Anil Akbas[a], Bekir Yildiz[a], Gokhan Karakoc[b]

[a]Batman Training and Research Hospital, Department of Cardiovascular Surgery, Batman, Türkiye
[b]Model Statistics CRO and Clinical Trials Center, Biostatistics and Medical Informatics, Kayseri, Türkiye
*Corresponding author: drgozacikkubra@gmail.com (Kubra Gozacik Karakoc)

MAIN POINTS

- Nearly half (46.1%) of patients presenting with leg pain at a tertiary vascular surgery clinic had no vascular disease.
- The vast majority of patients (92.8%) bypassed primary care referral systems and presented directly to the tertiary clinic.
- CVI was the predominant vascular disease (46.7%), while peripheral artery disease was less common (7.9%).
- Simple physical examination findings (pulse loss, cold extremities, edema) were highly discriminatory in identifying vascular disease (all p<0.05).
- In this clinic-based cohort from a region with limited specialist availability, the high rate of direct presentations without referral suggests opportunities for improved primary care screening.

Cite this article as: Gozacik Karakoc K, Cebe T, Akbas A, Yildiz B, Karakoc G. Vascular pathology prevalence and presentation patterns in patients presenting with leg pain to a tertiary vascular surgery clinic: A cross-sectional observational study. *Ann Med Res*. 2026;33(8):389–397. doi: 10.5455/annalsmedres.2025.11.354.

ABSTRACT

Aim: Lower extremity pain is a common complaint with diverse etiologies. This study aimed to determine the prevalence of vascular pathology among patients presenting with leg pain to a tertiary vascular surgery clinic and to evaluate patterns of presentation in a resource-limited region.

Materials and Methods: This cross-sectional observational study included 152 consecutive patients aged ≥18 years who presented with primary complaint of leg pain to the Cardiovascular Surgery outpatient clinic. All patients underwent bilateral arterial and venous Doppler ultrasonography. Vascular pathology was defined as the presence of peripheral artery disease (PAD) and/or chronic venous insufficiency (CVI). Referral status, clinical characteristics, and physical examination findings were recorded.

Results: Vascular pathology was identified in 82 patients (53.9%; 95% CI: 46.0-61.7), with CVI predominant (46.7%; 95% CI: 39.0-54.6) and peripheral artery disease less common (7.9%; 95% CI: 4.6-13.3). Notably, 70 patients (46.1%) had no vascular disease. The majority of patients (92.8%) presented directly without referral from primary care. Patients with vascular pathology were significantly older (45.3±15.0 vs. 36.7±13.9 years, p<0.001), had higher body mass index (27.5±4.5 vs. 25.8±4.0 kg/m², p=0.008), and exhibited higher rates of diabetes mellitus (20.7% vs. 7.1%, p=0.032) and hypertension (20.7% vs. 5.7%, p=0.015). Physical examination findings, including pulse loss, cold extremity, and edema, were significantly more common in patients with vascular pathology (all p<0.05). Multivariable analysis revealed that none of the cardiovascular risk factors remained independently associated with vascular pathology after adjustment.

Conclusion: Nearly half of patients presenting with leg pain at a tertiary vascular surgery clinic lack vascular pathology, and the vast majority bypass primary care referral systems. These findings highlight that a substantial proportion of tertiary vascular surgery consultations may be manageable at the primary care level, suggesting a potential benefit from strengthening primary care screening capacity and developing clinical pathways to guide appropriate referrals.

Keywords: Leg pain, Peripheral artery disease, Chronic venous insufficiency, Referral and consultation, Ultrasonography, Doppler

Received: Nov 25, 2025 **Accepted:** Feb 19, 2026 **Available Online:** Aug 25, 2026

INTRODUCTION

Lower extremity pain is a common presenting complaint that significantly impairs quality of life and places a substantial burden on healthcare systems. Vascular diseases such as peripheral artery disease (PAD) and chronic venous insufficiency (CVI) represent major etiologic factors, while musculoskeletal disorders and neurologic conditions constitute other important causes. Current epidemiologic data indicate that more than 200 million people worldwide are affected by PAD [1]. However, the clinical presentation is highly variable;

only 10-30% of patients exhibit classic intermittent claudication, while 30-60% report no exercise-related leg symptoms [2]. This heterogeneous clinical picture complicates differential diagnosis and can lead to inappropriate patient referrals.

The increasing number of patients presenting directly to tertiary vascular surgery clinics without referral from primary care has substantially increased the clinical workload. A large-scale study from Brazil found that 43% of referrals to a quaternary vascular surgery center were inappropriate, with a significant proportion consisting of venous diseases that could be managed at the primary care level [3]. Although structured referral forms and educational interventions have been shown to improve referral appropriateness, the success of these strategies is context-specific [4].

CVI affects 53% to 84% of the general population, with a substantial portion presenting at early stages (CEAP C0-C1) that can be effectively managed with conservative treatment in primary care settings [5,6].

Regional disparities are an important factor in healthcare delivery. In resource-limited regions such as southeastern Anatolia, imbalances in specialist distribution directly impact patient access to appropriate care and increase the workload of available specialists. Given the importance of early diagnosis and risk factor modification in PAD, strengthening primary care services and establishing effective referral systems has become essential [7].

This study aimed to determine the prevalence of vascular pathology and to characterize presentation patterns among patients with leg pain at a tertiary vascular surgery clinic in a resource-limited region, with the goal of informing strategies for healthcare optimization.

MATERIALS AND METHODS

Study design and population

This cross-sectional observational study was designed to evaluate patients presenting with leg pain at the Cardiovascular Surgery outpatient clinic of Batman Training and Research Hospital. The study was conducted between December 1, 2024, and March 1, 2025 and enrolled patients aged 18 years and older who met the inclusion criteria.

The study was conducted in accordance with the latest version of the Declaration of Helsinki (2013), the International Conference on Harmonisation Good Clinical Practice (ICH-GCP) guidelines, and current national regulations. All participants received detailed information regarding the study objectives, methods, expected benefits, and potential risks and provided written informed consent. The study protocol was approved by the Clinical Research Ethics Committee of Batman Training and Research Hospital (Decision no: 394, Date: 18.12.2024).

Study universe and sample selection

The study population consisted of all adult patients presenting with leg pain to the Cardiovascular Surgery outpatient clinic at Batman Training and Research Hospital. Patients who met the inclusion criteria and did not meet any exclusion criteria were enrolled using consecutive sampling. The sample size was estimated based on the pragmatic assumption that approximately one-third of patients presenting to a tertiary vascular surgery clinic with lower-extremity pain would have detectable vascular pathology. The minimum sample size was calculated to be 350 patients, using a 95% confidence level and a 5% margin of error. This parameter was adopted at the design stage to support the planning of descriptive analyses rather than to provide a definitive estimate of prevalence.

During the study period, 152 patients who met the inclusion criteria were enrolled by consecutive sampling. The target sample size of 350 patients was not achieved, primarily because the study duration was limited to three months and patient presentations were reduced during the winter months owing to regional characteristics. Although this constitutes a methodological limitation, we employed Wilson score confidence intervals to provide reliable prevalence estimates given the available sample. The observed vascular disease prevalence was 53.9% (Wilson 95% CI: 46.0-61.7%), with a margin of error of ±7.9%. This approach is considered more appropriate than post-hoc power analysis for prevalence studies, as it directly quantifies the precision of our estimates rather than retrospectively justifying sample size [8].

Inclusion and exclusion criteria

Patients aged 18 years and older who presented to the Cardiovascular Surgery outpatient clinic with leg pain as their primary complaint and who signed the informed consent form were included in the study. Only individuals making their first presentation during the study period were enrolled.

Conversely, patients younger than 18 years, those with trauma-related leg pain, those with a history of lower extremity surgery within the past 6 months, and those under follow-up for peripheral artery disease (PAD) were excluded. Additionally, patients referred from the emergency department with suspected acute vascular disease, those who could not be evaluated due to cognitive impairment, and individuals who declined participation were excluded from the study.

Data source, collection, and management

Study data were obtained through primary data collection using standardized data forms. The research team collected data through face-to-face interviews and physical examinations. All data were initially recorded on printed forms and subsequently transferred to an electronic database using double data entry. Patient data were stored electronically using only codes, with personal identifying information removed.

Variables and measurement methods

Demographic data included age, sex, body mass index (BMI), occupation, education level, and residential area (city center/district/rural). BMI was calculated from height (m) and

https://doi.org/10.5455/annalsmedres.2025.11.354

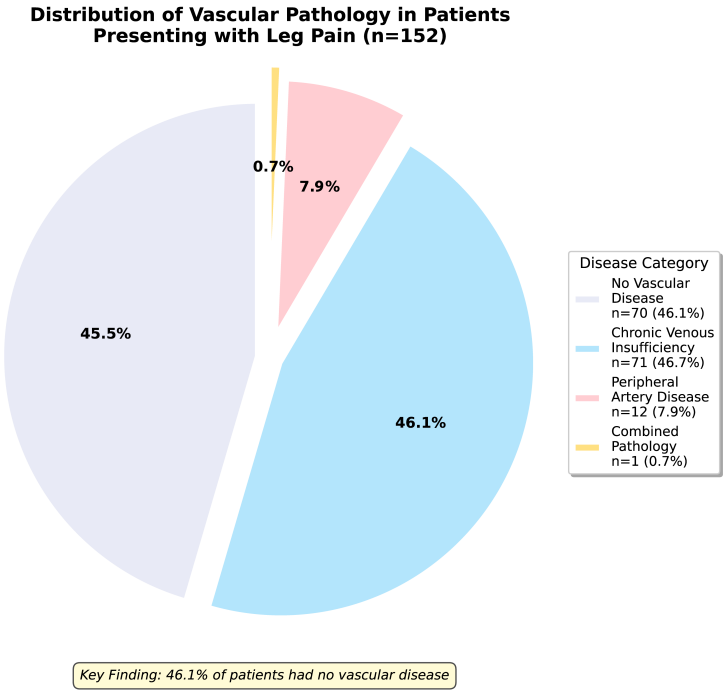

Figure 1. Distribution of vascular pathology detected by Doppler ultrasonography in patients presenting with leg pain (n=152). Chronic venous insufficiency and no vascular disease each affected approximately half of patients, while peripheral artery disease was considerably less common.

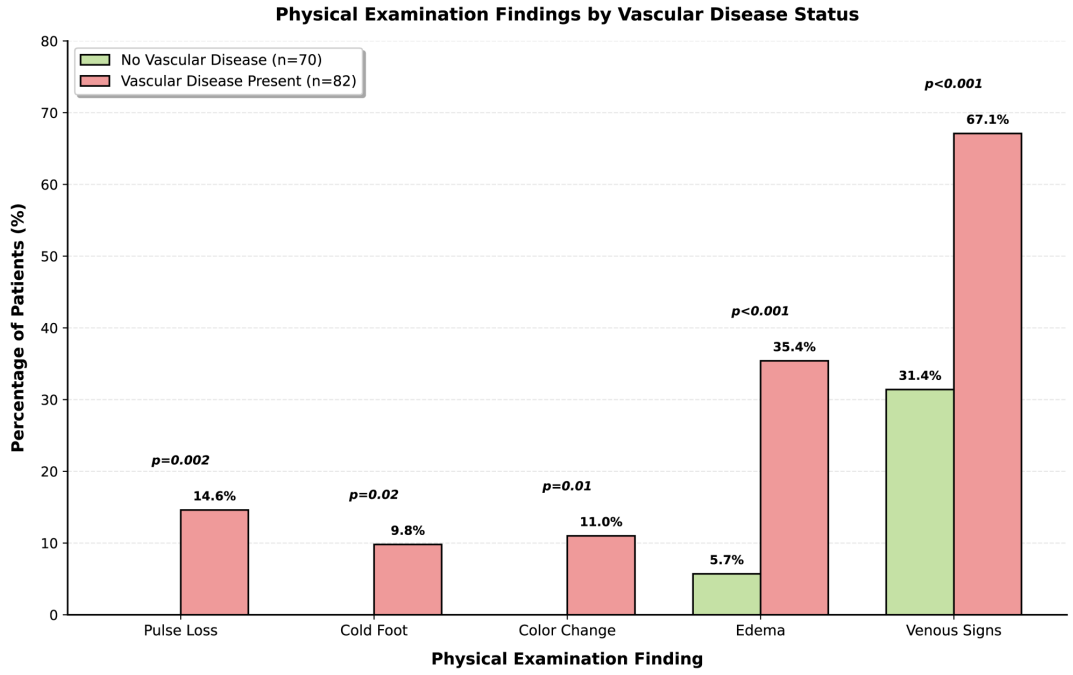

Figure 2. Comparison of physical examination findings between patients with and without vascular disease. Pulse loss, cold foot, and color change were absent in patients without vascular disease. Edema and venous signs showed significant differences between groups (all p<0.05).

weight (kg) measurements obtained using calibrated scales and a stadiometer.

Patient presentation mode (direct presentation or referral from primary care or other clinics) was recorded through patient statement and query of the hospital registration system. Direct presentation was defined as a patient presenting to the clinic of their own accord without a referral document from any healthcare facility. A referred presentation was recorded when patients arrived with official referral documents from family medicine units, other outpatient clinics, or healthcare facilities.

Risk factors assessed included smoking (never smoked, for-

https://doi.org/10.5455/annalsmedres.2025.11.354

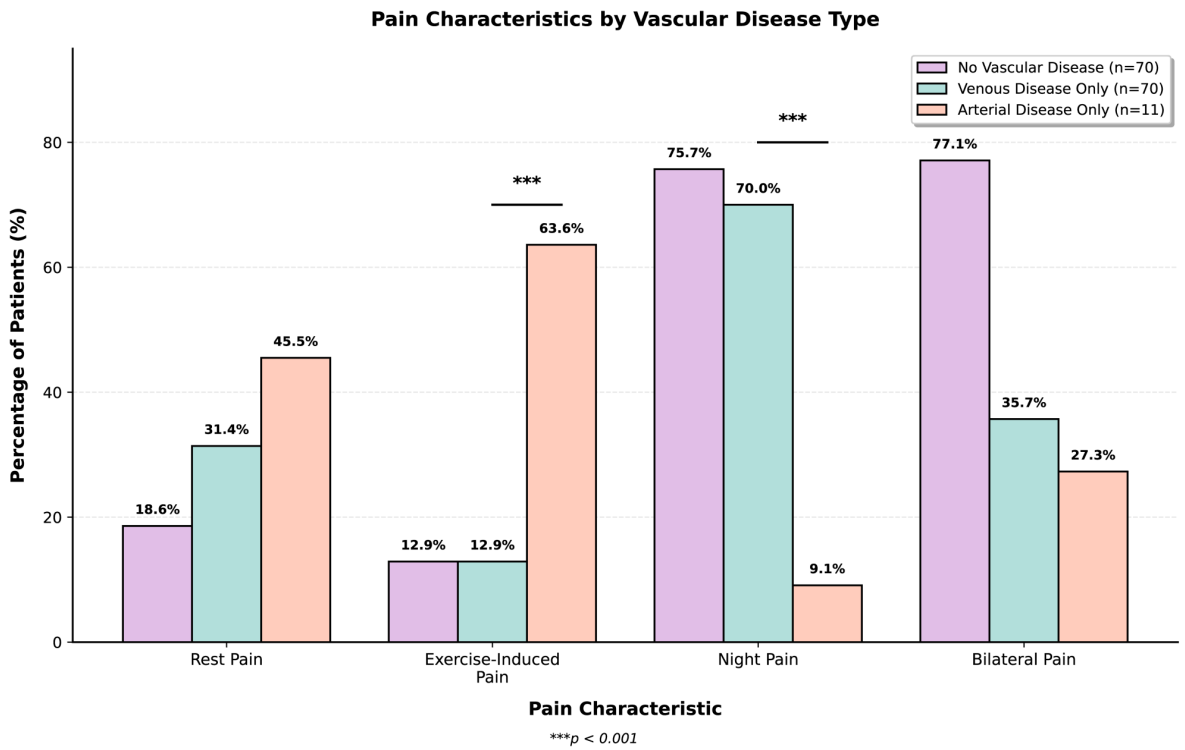

Figure 3. Pain characteristics stratified by vascular disease type. Exercise-induced pain was significantly more common in arterial disease (p<0.001), while night pain predominated in venous disease (p<0.001). Bilateral pain was more prevalent in patients without vascular disease (p<0.001). ***p<0.001.

mer smoker, active smoker, and pack-years), diabetes mellitus (fasting blood glucose ≥126 mg/dL, HbA1c ≥6.5%, or antidiabetic medication use), hypertension (systolic blood pressure ≥140 mmHg, diastolic blood pressure ≥90 mmHg, or antihypertensive medication use), coronary artery disease (previous diagnosis or revascularization history), and history of thrombosis.

Clinical evaluation included the medical history, including the duration of complaint (months), pain character (rest/exercise/night), claudication distance (meters), associated symptoms, and previous treatments.

Physical examination assessed peripheral pulses (0: not palpable, 1: weak, 2: normal, 3: strong), skin changes (temperature, color, trophic changes), presence of edema (0: absent, 1: mild, 2: moderate, 3: severe), presence of varicose veins, neurologic findings, and musculoskeletal findings.

Diagnostic protocols

All patients underwent bilateral lower extremity arterial and venous Doppler ultrasonography as a standard procedure. Doppler ultrasonography examinations were performed by radiology specialists with at least 5 years' experience, using high-resolution color Doppler ultrasonography equipment.

Arterial Doppler ultrasonography evaluated flow patterns in the femoral, popliteal, tibialis anterior, tibialis posterior, and dorsalis pedis arteries. Peripheral artery disease was diagnosed in the presence of arterial stenosis (≥50% stenosis), occlusion, or abnormal flow pattern (monophasic or absent).

Venous Doppler ultrasonography evaluated the great saphenous vein, small saphenous vein, deep venous system (femoral, popliteal, and tibial veins), and perforating veins for diameter, compressibility, flow direction, and presence of reflux. CVI was diagnosed in the presence of any of the following: venous reflux >0.5 seconds, valvular insufficiency, varicose veins, venous dilation, or sequelae of deep vein thrombosis.

Presence of vascular disease was defined as the detection of PAD on arterial Doppler ultrasonography and/or CVI on venous Doppler ultrasonography. Patients with normal findings on both examinations were classified in the "no vascular disease" group.

Statistical analysis

All statistical analyses were performed using Jamovi (Version 2.6.44, The Jamovi Project, 2023, https://www.jamovi.org) and JASP (Version 0.19.3, Jeffreys' Amazing Statistics Program, 2024, https://jasp-stats.org). Statistical significance was set at $p \leq 0.05$. Continuous variables were assessed for normality using the Kolmogorov-Smirnov test. Variables with normal distribution were expressed as mean ± standard deviation, while non-normally distributed variables were expressed as median [Minimum-Maximum]. Categorical variables were reported as frequencies (percentages). The prevalence of vascular disease and its subtypes was calculated with 95% confidence intervals using the Wilson score method. Comparisons between patients with and without vascular dis-

https://doi.org/10.5455/annalsmedres.2025.11.354

ease were performed using Student's t-test for normally distributed continuous variables and the Mann-Whitney U test for non-normally distributed continuous variables. Categorical variables were compared using Pearson's chi-square test; Fisher's exact test was used when more than 20% of expected cell frequencies were less than 5. Relationships between pain characteristics and the presence of vascular disease, and comparisons of pain patterns between arterial and venous disease, were examined using chi-square or Fisher's exact tests, depending on expected cell frequencies.

Univariable binary logistic regression was performed for each potential risk factor to identify independent predictors of vascular pathology. Variables with $p<0.20$ in univariable analysis were entered into a multivariable logistic regression model using the enter method. Multicollinearity was assessed using the variance inflation factor (VIF), with VIF > 5 indicating problematic collinearity. Model fit was evaluated using the Hosmer-Lemeshow goodness-of-fit test, with $p>0.05$ indicating an adequate fit. Discriminative ability was assessed by the area under the receiver operating characteristic curve (AUC). Results were expressed as odds ratios (ORs) with 95% confidence intervals (CIs).

RESULTS

Baseline characteristics and study population

The study cohort comprised 152 patients presenting with leg pain (Table 1). Mean age was 41.3 ± 15.1 years, with a female predominance (67.8%). Most patients (80.3%) resided in urban areas , and education levels were distributed across all categories. Among cardiovascular risk factors, smoking was the most prevalent (37.5%), followed by diabetes mellitus (14.5%) and hypertension (13.8%). The median duration of complaints was 6 months (range, 0–120). Night pain was the most frequently reported symptom (68.4%), while rest pain and exercise-induced pain affected 26.3% and 16.4% of patients, respectively. More than half (54.6%) experienced bilateral lower extremity pain, and the vast majority (92.8%) presented directly without referral.

Table 1. Baseline demographic and clinical characteristics of patients presenting with lower extremity pain.

Variables	Total Cohort (n=152)
Age (years)	41.3 ± 15.1
Gender	
Male	49 (32.2%)
Female	103 (67.8%)
Height (cm)	168.6 ± 9.3
Weight (kg)	75.8 ± 12.5
Body Mass Index (kg/m²)	26.7 ± 4.3
Education Level	
Illiterate/Primary school	26 (17.1%)
Middle school	45 (29.6%)
High school	16 (10.5%)
Vocational school	43 (28.3%)
University	22 (14.5%)
Residential Area	
City center	122 (80.3%)
District	20 (13.2%)
Rural	10 (6.6%)
Risk Factors	
Smoking, present	57 (37.5%)
Diabetes mellitus, present	22 (14.5%)
Hypertension, present	21 (13.8%)
Coronary artery disease, present	13 (8.6%)
History of thrombosis, present	10 (6.6%)
Duration of Complaint (months)	6 [0-120]
Pain Characteristics	
Rest pain, present	40 (26.3%)
Exercise-induced pain, present	25 (16.4%)
Night pain, present	104 (68.4%)
Pain Location	
Right lower extremity	32 (21.1%)
Left lower extremity	37 (24.3%)
Bilateral	83 (54.6%)
Referral Status	
Direct admission	141 (92.8%)
Referred	11 (7.2%)

Continuous variables are presented as mean ± SD or median [Minimum- Maximum]. Categorical variables are presented as n (%). Vocational school includes vocational high schools and two-year post-secondary vocational colleges in the Turkish educational system. Abbreviations: SD, standard deviation.

Vascular disease prevalence

Doppler ultrasonography detected vascular disease in 82 patients (53.9%; 95% CI: 46.0-61.7) (Table 2, Figure 1). CVI was the predominant finding, affecting 71 patients (46.7%; 95% CI: 39.0-54.6). Peripheral artery disease was considerably less common; it was identified in 12 patients (7.9%; 95% CI: 4.6-13.3). Combined arterial and venous disease was present in only one patient (0.7%). Both Doppler examinations were normal in 70 patients (46.1%), indicating a substantial proportion of non-vascular etiologies (Figure 1).

Comparison according to vascular disease presence

Patients with vascular disease were significantly older than those without (45.3 ± 15.0 vs. 36.7 ± 13.9 years; $p<0.001$) and had higher body mass index (27.5 ± 4.5 vs. 25.8 ± 4.0 kg/m²; $p = 0.008$) (Table 3). Sex distribution and residential area showed no significant associations ($p = 0.47$ and $p>0.99$, respectively). Diabetes mellitus (20.7% vs. 7.1%; $p = 0.03$), hypertension (20.7% vs. 5.7%; $p = 0.015$), and history of thrombosis (11.0% vs. 1.4%; $p = 0.04$) were significantly more prevalent in patients with vascular disease. There were no significant differences in smoking and coronary artery disease ($p = 0.93$ and $p = 0.15$, respectively).

None of the pain characteristics reached statistical significance between groups, although rest pain showed a trend toward a higher prevalence in patients with vascular disease (32.9% vs. 18.6%; $p = 0.069$) (Figure 2). Physical examination findings were highly discriminative. Notably, pulse loss, cold foot, and color change were absent in patients without vascular disease, were present in 14.6% ($p = 0.002$), 9.8% ($p =$

https://doi.org/10.5455/annalsmedres.2025.11.354

Table 2. Distribution of vascular pathology detected by doppler ultrasonography.

Diagnostic Category	n	%	95% CI
Arterial Pathology			
Peripheral artery disease	12	7.9	4.6-13.3
Venous Pathology			
Chronic venous insufficiency (CVI)	71	46.7	39.0-54.6
Combined Pathology			
Both arterial and venous	1	0.7	0.1-3.6
No Vascular Pathology			
Both Doppler studies normal	70	46.1	38.3-54.0
Total Vascular Pathology			
At least one Doppler positive	82	53.9	46.0-61.7

Abbreviations: CI, confidence interval.

0.02), and 11.0% (p = 0.01) of those with vascular disease, respectively. Edema (35.4% vs. 5.7%; p<0.001) and venous signs (67.1% vs. 31.4%; p<0.001) were substantially more common in the vascular disease group (Figure 2).

Pain characteristics and vascular disease type

Pain characteristics differed across disease types (Table 4, Figure 3). Bilateral pain was significantly more prevalent in patients without vascular disease (77.1% vs. 35.4%; p<0.001). Comparison of arterial and venous disease revealed striking differences: exercise-induced pain was markedly more common in arterial disease (63.6% vs. 12.9%; p<0.001), whereas night pain was significantly more prevalent in venous disease (70.0% vs. 9.1%; p<0.001) (Figure 3). Rest pain, bilateral pain distribution, and chronic pain duration showed no significant differences between disease types.

Predictors of vascular pathology

Univariable logistic regression analysis identified age (OR: 1.04; 95% CI: 1.02–1.07; p < 0.001), BMI (OR: 1.11; 95% CI: 1.02–1.20; p = 0.013), diabetes mellitus (OR: 3.40; 95% CI: 1.18–9.76; p = 0.023), hypertension (OR: 4.32; 95% CI: 1.38–13.52; p = 0.012), and history of thrombosis (OR: 8.51; 95% CI: 1.05–68.92; p = 0.045) as significant predictors of vascular pathology (Table 5). Coronary artery disease showed a trend toward statistical significance (OR: 3.10; 95% CI: 0.82–11.76; p = 0.096). In multivariable analysis adjusting for age, BMI, diabetes mellitus, hypertension, and coronary artery disease, none of the cardiovascular risk factors remained independently associated with vascular pathology. The multivariable model demonstrated acceptable discrimination (AUC = 0.697) and adequate calibration (Hosmer-Lemeshow p = 0.675).

DISCUSSION

In our study, nearly half (46.1%) of patients presenting to our tertiary vascular surgery outpatient clinic with primary complaints of leg pain had no vascular disease. Moreover, the vast majority of patients (92.8%) presented directly to our clinic without any referral from primary care services. These findings suggest that, in our region, patients frequently bypass the referral system, where specialist availability is limited, potentially increasing specialists' workload with cases that might be managed at the primary care level.

Our results , consistent with the literature, reveal the complexity of the differential diagnosis of leg pain and the prevalence of vascular diseases in this clinic-based population. McDermott's comprehensive review emphasized that 30% to 60% of patients with peripheral artery disease in primary care settings exhibit no exercise-related leg symptoms, and 45% to 50% report atypical complaints that do not meet classic intermittent claudication criteria [2]. This demonstrates that even vascular diseases can present with heterogeneous clinical presentations; therefore, not every patient with leg pain has a vascular etiology.

CVI was present in 46.7% patients with detected vascular disease in our study. The prevalence of CVI ranges from 53% to 84% in European studies, although a substantial portion consists of mild forms and telangiectasias [5,9]. In Turkey, a study of patients presenting with lumbar spinal disease reported CVI prevalence of 53.1%, with early-stage disease (78.6% C0-1) being predominant [10]. In our cohort, the rate of symptomatic venous insufficiency was higher than reported in the literature, which can be explained by patients actively presenting with symptoms. However, most cases of venous insufficiency can be managed at the primary care level with conservative treatment and compression. In our study, body mass index was significantly higher in patients with vascular disease (27.5±4.5 vs. 25.8±4.0 kg/m^2, p=0.008). Popplewell et al.'s study in obese patients in the United Kingdom found that while 25% of patients attending weight management services had a diagnosis of lower extremity venous disease, 82% had symptoms related to venous disease [11]. Notably, 69% of patients were unaware of the association between obesity and venous disease [11]. This may explain the high rate of direct presentation (92.8%) and the burden of undiagnosed disease in our study.

Our prevalence of peripheral artery disease (7.9%) is consistent with global estimates reported in the literature. Song and colleagues' 2019 systematic review reported that PAD affects 238 million people worldwide and that prevalence increases with age [12]. In our cohort, diabetes mellitus (20.7% vs. 7.1%, p=0.032) and hypertension (20.7% vs. 5.7%, p=0.015) were significantly more common in patients with detected PAD, consistent with established risk factors. However, strikingly even among patients with PAD, only 63.6% reported exercise-related pain; this observation should be interpreted cautiously given the small subgroup size (n=12). Nevertheless, this finding is consistent with studies showing that classic intermittent claudication is not the most frequent presentation of PAD [2,7].

International studies evaluating the effectiveness of referral

https://doi.org/10.5455/annalsmedres.2025.11.354

Table 3. Clinical and physical examination findings according to vascular pathology status.

Variables	No Vascular Pathology (n=70)	Vascular Pathology Present (n=82)	p value
Demographic Characteristics			
Age (years)	36.7 ± 13.9	45.3 ± 15.0	**<0.001**
Gender (Female)	50 (71.4%)	53 (64.6%)	0.472
Body Mass Index (kg/m²)	25.8 ± 4.0	27.5 ± 4.5	**0.008**
Education (Illiterate/Primary school)	7 (10.0%)	19 (23.2%)	0.053
Residential Area (City center)	56 (80.0%)	66 (80.5%)	0.999
Risk Factors			
Smoking, present	27 (38.6%)	30 (36.6%)	0.933
Diabetes mellitus, present	5 (7.1%)	17 (20.7%)	**0.032**
Hypertension, present	4 (5.7%)	17 (20.7%)	**0.015**
Coronary artery disease, present	3 (4.3%)	10 (12.2%)	0.148
History of thrombosis, present	1 (1.4%)	9 (11.0%)	**0.042**
Clinical Characteristics			
Duration of complaint (months)	6 [0-60]	7 [1-120]	0.161
Pain Characteristics			
Rest pain, present	13 (18.6%)	27 (32.9%)	0.069
Exercise-induced pain, present	9 (12.9%)	16 (19.5%)	0.377
Night pain, present	53 (75.7%)	51 (62.2%)	0.107
Physical Examination Findings			
Any pulse loss, present	0 (0.0%)	12 (14.6%)	**0.002**
Cold foot, present	0 (0.0%)	8 (9.8%)	**0.020**
Color change, present	0 (0.0%)	9 (11.0%)	**0.012**
Edema, present	4 (5.7%)	29 (35.4%)	**<0.001**
Venous signs, present	22 (31.4%)	55 (67.1%)	**<0.001**

Bold p-values indicate statistical significance ($p \leq 0.05$). Student t-test or Mann-Whitney U test for continuous variables; Chi-square or Fisher's exact test for categorical variables. Abbreviations: SD, standard deviation.

Table 4. Pain characteristics stratified by pathology type: arterial versus venous disease.

Pain Characteristics	No Pathology (n=70)	Vascular Pathology Present (n=82)	p value†	Arterial Only (n=11)	Venous Only (n=70)	p value‡
Rest pain, present	13 (18.6%)	27 (32.9%)	0.069	5 (45.5%)	22 (31.4%)	0.566
Exercise-induced pain, present	9 (12.9%)	16 (19.5%)	0.377	7 (63.6%)	9 (12.9%)	<0.001
Night pain, present	53 (75.7%)	51 (62.2%)	0.107	1 (9.1%)	49 (70.0%)	<0.001
Bilateral pain, present	54 (77.1%)	29 (35.4%)	<0.001	3 (27.3%)	25 (35.7%)	0.837
Chronic pain (≥12 months), present	28 (40.0%)	39 (47.6%)	0.440	4 (36.4%)	34 (48.6%)	0.668

Bold p-values indicate statistical significance ($p \leq 0.05$). † Comparison between vascular pathology present vs absent (Chi-square or Fisher's exact test). ‡ Comparison between arterial only vs venous only pathology (Chi-square or Fisher's exact test).

Table 5. Univariable and multivariable logistic regression analysis for predictors of vascular pathology in patients presenting with leg pain.

Independent Variables	Univariable OR [95% CI]	p	Multivariable OR [95% CI]	p
Age, per 1-year increase	1.04 [1.02–1.07]	**<0.001**	1.03 [1.00–1.06]	0.072
BMI, per 1 kg/m² increase	1.11 [1.02–1.20]	**0.013**	1.03 [0.93–1.13]	0.604
Diabetes mellitus, present vs absent	3.40 [1.18–9.76]	**0.023**	1.49 [0.44–5.02]	0.521
Hypertension, present vs absent	4.32 [1.38–13.52]	**0.012**	1.88 [0.51–6.96]	0.341
Coronary artery disease, present vs absent	3.10 [0.82–11.76]	0.096	1.09 [0.23–5.10]	0.916

Model summary: −2 Log Likelihood = 193.85; Nagelkerke $R^2 = 0.133$; AUC = 0.697 (95% CI: 0.614–0.780); Hosmer-Lemeshow $\chi^2 = 5.75$, p = 0.675. Bold p-values indicate statistical significance ($p \leq 0.05$). Multivariable analysis included all variables with $p<0.20$ in univariable analysis using the enter method. The dependent variable was vascular pathology presence (peripheral artery disease and/or chronic venous insufficiency) confirmed by Doppler ultrasonography. Abbreviations: OR, odds ratio; CI, confidence interval; BMI, body mass index; AUC, area under the receiver operating characteristic curve.

systems support our findings. In Brazil, Portela and colleagues evaluated 1,203 referrals to a quaternary vascular surgery center and found 43% of referrals to be inappropriate [3]. While venous disease was the most common referral indication (53%), only 39.92% of patients underwent surgical treatment. The authors suggested that these inappropriate referrals lead to underutilization of high-complexity services and that telemedicine could reduce this rate. A sys-

https://doi.org/10.5455/annalsmedres.2025.11.354

tematic review from the United Kingdom demonstrated that structured referral forms, peer feedback, and educational interventions involving specialists improved referral appropriateness [4]. However, the success of such interventions is context-specific, and information regarding implementation challenges remains limited.

In our study, 54.6% of patients without vascular disease had bilateral leg pain. Bilateral pain was significantly less frequent in venous disease (35.7%) and in arterial disease (27.3%) ($p<0.001$). These findings suggest that bilateral leg pain is more likely to be associated with musculoskeletal, neurologic, or systemic causes than with a vascular etiology. In Mendoza's review addressing differential diagnosis of leg pain in phlebology practice, it was emphasized that leg pain often does not originate from varicose veins or venous disease, and that incidental varicose veins are found in 90% of the population [13]. This suggests that a significant proportion of our patients may have been referred for vascular surgery due to misperception.

In the context of our region's healthcare system, these clinic-based findings carry practical implications for local service planning. In the Southeastern Anatolia Region, the number of specialists, particularly in critical specialties such as vascular surgery, is lower than the national average. According to data from the Ministry of Health, the number of vascular surgery specialists per 100,000 population in our region is approximately 40% lower than the national average. In our clinical experience, a substantial proportion of specialist consultations involved patients who could be managed at the primary care level. Particularly, 46.1% of patients without detected vascular disease could be managed at the family medicine level through appropriate examination and evaluation.

In our study, we found that physical examination findings (pulse loss, cold foot, color change, edema, and venous signs) were significantly more common in patients with vascular disease (all $p<0.05$). These findings demonstrate that even a simple physical examination can be quite effective in predicting the presence of vascular disease. Multivariable analysis revealed that traditional cardiovascular risk factors lost their predictive significance after mutual adjustment, suggesting substantial shared variance among these correlated variables. This finding indicates that risk factor inquiry alone cannot reliably identify vascular pathology in patients presenting with leg pain. Rather, clinical examination findings—particularly pulse assessment, skin changes, and edema—should guide referral decisions at the primary care level. These observations suggest that future efforts to strengthen basic vascular examination skills among primary care physicians and to develop standardized evaluation protocols warrant investigation as potential strategies to optimize referral patterns.

Strengthening family medicine services and improving care coordination may help optimize patient flow to appropriate levels of care, although the specific barriers to primary care utilization in our population require further investigation. Health literacy initiatives informing patients that not every leg pain requires specialist evaluation may be beneficial, though the effectiveness of such interventions in our setting remains to be determined. Future studies should evaluate whether targeted educational programs for family physicians that focus on the clinical differentiation of vascular and non-vascular leg pain could improve the appropriateness of referrals. Our findings may contribute to improving resource utilization in regions with imbalanced specialist distribution and may support the development of evidence-based referral algorithms.

Our study has several limitations. First, the target sample size of 350 patients was not achieved; only 152 patients (43% of the target) were enrolled due to the predefined three-month study duration and reduced patient presentations during the winter months. This represents a significant methodological limitation, resulting in a margin of error of ±7.9% rather than the planned ±5% for our prevalence estimates, which reduces precision and limits statistical power for subgroup analyses. However, we employed Wilson score confidence intervals to quantify the uncertainty of our estimates appropriately, rather than conducting post-hoc power analysis. Second, our cross-sectional design captures associations at a single time point; causal relationships cannot be inferred, and we cannot evaluate factors influencing patient referral decisions over time. Third, the generalizability of our findings is limited because the study was conducted at a single center and included patients from the Southeastern Anatolia region; however, this limitation also provides value by revealing regional healthcare patterns. Fourth, and critically, we did not systematically assess why patients chose to present directly to the tertiary clinic rather than seeking primary care evaluation first. This represents a missed opportunity, as understanding patient motivations is essential for designing effective interventions to optimize referral pathways. Potential factors—including transportation difficulties, perceived access barriers, trust in the family medicine system, appointment availability, health literacy, and symptom severity concerns—remain speculative without a formal qualitative assessment. Future studies should evaluate these factors using structured questionnaires and include primary care physicians to ascertain reasons for referral. Finally, a significant limitation is that we did not systematically record subsequent diagnoses for the 70 patients (46.1%) without vascular pathology; consequently, data on actual etiologies (e.g., musculoskeletal, neurological) and clinical outcomes were not collected. Additionally, CEAP clinical severity classification was not recorded for patients with CVI, precluding determination of the proportion of patients with early-stage (C0–C2) versus advanced (C3–C6) disease.

Acknowledgements: We would like to thank Model Statistics CRO and Clinical Trials Center (www.modelistatistik.com) for their support and expertise in statistical analysis throughout this research project.

Ethics Committee Approval: This study was approved by the

https://doi.org/10.5455/annalsmedres.2025.11.354

Clinical Research Ethics Committee of Batman Training and Research Hospital (Decision no: 394, Date: 18.12.2024).

Informed Consent: All participants received detailed information regarding the study objectives, methods, expected benefits, and potential risks and provided written informed consent.

Peer-review: Externally peer-reviewed.

Conflict of Interest: The authors declare no conflicts of interest regarding this study.

Author Contributions: Conceptualization: K.G.K.; Methodology: K.G.K.; Data curation: T.C., A.A., B.Y.; Formal analysis: G.K.; Investigation: T.C.; Writing – original draft: K.G.K.; Writing – review & editing: K.G.K., T.C.; Supervision: K.G.K.; Project administration: K.G.K.

Financial Disclosure: The authors received no financial support for the research, authorship, or publication of this article.

Artificial Intelligence Disclosure: During the preparation of this manuscript, the authors used Claude (Anthropic, Claude Opus 4.6) to assist with language editing, improving clarity and readability, and text organization. The AI tool was not used for study design, data collection, statistical analysis, interpretation of findings, or the formulation of scientific conclusions; these were performed solely by the authors. All AI-assisted content was critically reviewed, verified for accuracy, and revised by the authors, who take full responsibility for the integrity, originality, and scholarly content of the manuscript.

REFERENCES

1. Kou T, Qian X, Liu Y, et al. Global, regional, and national burden of peripheral artery disease: a systematic analysis of prevalence, incidence, deaths, and DALYs with projections for the next 15 years. *Nutr Metab Cardiovasc Dis.* 2025;35(12):104226. doi: 10.1016/j.numecd.2025.104226.
2. McDermott MM. Lower extremity manifestations of peripheral artery disease: the pathophysiologic and functional implications of leg ischemia. *Circ Res.* 2015;116(9):1540-50. doi: 10.1161/CIRCRESAHA.114.303517.
3. Portela FSO, Rossetti CA, Souza TF, et al. Retrospective analysis of 1,203 cases of referral to a quaternary vascular surgery outpatient clinic within the Unified Health System, São Paulo, Brazil. *Einstein (Sao Paulo).* 2024;22:eAO0676. doi: 10.31744/einstein_journal/2024AO0676. PMID: 38808797.
4. Bolton Saghdaoui L, Lampridou S, Tavares S, et al. Interventions to improve referrals from primary care to outpatient specialist services for chronic conditions: a systematic review and framework synthesis update. *Syst Rev.* 2025;14(1):103. doi: 10.1186/s13643-025-02841-z.
5. Vuylsteke ME, Thomis S, Guillaume G, et al. Epidemiological study on chronic venous disease in Belgium and Luxembourg: prevalence, risk factors, and symptomatology. *Eur J Vasc Endovasc Surg.* 2015;49(4):432-9. doi: 10.1016/j.ejvs.2014.12.031.
6. Yang DH, Kim M, Yang JW, et al. Early-stage chronic venous disorder as a cause of leg pain overlooked for lumbar spinal disease. *Sci Rep.* 2023;13(1):18303. doi: 10.1038/s41598-023-45623-0.
7. Polonsky TS, McDermott MM. Lower Extremity Peripheral Artery Disease Without Chronic Limb-Threatening Ischemia: A Review. *JAMA.* 2021;325(21):2188-2198. doi: 10.1001/jama.2021.2126.
8. Brown LD, Cai TT, DasGupta A. Interval estimation for a binomial proportion. *Stat Sci.* 2001;16(2):101-133. doi: 10.1214/ss/1009213286.
9. Sinikumpu SP, Keränen MH, Jokelainen J, Keinänen-Kiukaanniemi S, Huilaja L. The association between chronic venous disease and measures of physical performance in older people: a population-based study. *BMC Geriatr.* 2021;21(1):556. doi: 10.1186/s12877-021-02528-9.
10. Chang MC. Chronic venous insufficiency, could it be one of the missing pieces in the puzzle of treating pain? *World J Clin Cases.* 2024;12(1):232-235. doi: 10.12998/wjcc.v12.i1.232.
11. Popplewell MA, Mahesh S, Nandra S, et al. The obese population's views on the symptoms and risks of chronic venous insufficiency - 2 (OBVIOUS-2) cross-sectional survey. *Phlebology.* 2025;40(3):161-166. doi: 10.1177/02683555241284179.
12. Song P, Rudan D, Zhu Y, et al. Global, regional, and national prevalence and risk factors for peripheral artery disease in 2015: an updated systematic review and analysis. *Lancet Glob Health.* 2019;7(8):e1020-e1030. doi: 10.1016/S2214-109X(19)30255-4.
13. Mendoza E. Differentialdiagnose von Beinschmerzen in der Phlebologie. *Phlebologie.* 2019;48(6):366-372. doi: 10.1055/a-1013-6358.

Ann Med Res

Current issue list available at Ann Med Res

Annals of Medical Research

journal page: annalsmedres.org

Serum progranulin as an early diagnostic biomarker in acute stroke

Merve Sena Odabasi[a,*], Hasan Ferhat Kurs[b], Guven Ozkaya[c], Zeynep Mine Yalcinkaya Kara[a], Ertugrul Altinbilek[b], Erdinc Serin[a]

[a]Sisli Hamidiye Etfal Research and Training Hospital, Department of Biochemistry, Istanbul, Türkiye
[b]Sisli Hamidiye Etfal Research and Training Hospital, Department of Emergency, Istanbul, Türkiye
[c]Bursa Uludag University, Faculty of Medicine, Department of Biostatistics, Bursa, Türkiye
*Corresponding author: msdur88@gmail.com (Merve Sena Odabasi)

MAIN POINTS

- PGRN shows diagnostic value within six hours of onset.
- First study comparing PGRN in ischemic vs hemorrhagic stroke.
- PGRN differentiates stroke patients from controls.
- No prognostic association was found for mortality or severity.

Cite this article as: Odabasi MS, Kurs HF, Ozkaya G, Yalcinkaya Kara ZM, Altinbilek E, Serin E. Serum progranulin as an early diagnostic biomarker in acute stroke. *Ann Med Res*. 2026;33(8):398–402. doi: 10.5455/annalsmedres.2026.01.028.

ABSTRACT

Aim: Rapid differentiation between ischemic stroke (IS) and intracerebral hemorrhage (ICH) is crucial for early management. Progranulin, a multifunctional glycoprotein with neuroprotective and anti-inflammatory effects, is involved in neuronal survival and the control of inflammation. Although animal studies suggest a protective role, its diagnostic and prognostic value in acute human stroke remains uncertain. This study aimed to evaluate the diagnostic and prognostic significance of serum progranulin in acute IS and ICH within six hours of onset.

Materials and Methods: Forty-two acute stroke patients and forty-four healthy controls were enrolled. Inclusion criteria were an acute focal neurological deficit, a presentation within six hours, and imaging confirmation of the subtype. Exclusion criteria included prior stroke, trauma, tumors, systemic failure, or major comorbidities. Serum progranulin was measured by ELISA. Statistical analyses included t-tests, Mann–Whitney U tests, ANOVA, chi-square tests, and ROC analyses.

Results: Serum progranulin was significantly higher in stroke patients than in controls (69.6±15.4 pg/mL vs 52.2±18.9 pg/mL; p<0.001). ROC analysis yielded a cut-off value of 53 pg/mL (sensitivity, 64%; specificity, 84%; AUC, 0.778; 95% CI, 0.676–0.861). Progranulin levels did not differ between IS and ICH, nor by severity. No correlations were observed with mortality, ICU admission, or hospital stay; only the Glasgow Coma Scale correlated with clinical outcomes.

Conclusion: An elevated level of progranulin early in stroke supports its potential as a diagnostic biomarker, but it does not distinguish stroke type or predict prognosis. Larger longitudinal studies are needed to clarify its clinical utility.

Keywords: Stroke, Ischemic, Hemorrhagic, Progranulin, Diagnostic

Received: Jan 22, 2026 **Accepted:** Feb 23, 2026 **Available Online:** Aug 25, 2026

INTRODUCTION

Cerebrovascular diseases are a group of clinical conditions characterized by sudden onset and potentially life-threatening ischemic or hemorrhagic damage [1]. Cerebrovascular diseases are among the three leading causes of death worldwide. Ischemic stroke (IS) accounts for around 85% of all stroke cases and is associated with serious consequences such as permanent disability, dependency, loss of employment, and social isolation [2]. IS is more common, while intracerebral hemorrhage (ICH) is more severe, with in-hospital mortality rates of 20–30%, and up to 80% of survivors require long-term care [3]. In developed countries, the incidence of stroke is increasing with aging populations, posing a significant economic burden on healthcare systems [4].

While computed tomography (CT) can accurately detect intracerebral hemorrhage, it is relatively to acute, small ISs. However, expensive magnetic resonance imaging (MRI) scanners (especially diffusion-weighted imaging (DWI)) are unsuitable for unstable patients or for those with contraindications, and are available only in specialist hospitals staffed by experienced neuroradiologists. Yet, they have improved stroke detection to approximately 95%. Some may not appear at all [5,6]. Therefore, rapid and accurate diagnosis of patients with suspected stroke, reliable distinction between IS and ICH, the selection of the appropriate patient population for thrombolytic therapy, and the improvement of patient outcomes

are of critical importance [7]. In addition, accurate prognostic evaluation following cerebrovascular events plays a pivotal role across a broad spectrum, from acute treatment decisions and long-term rehabilitation planning to patient and family counseling and the formulation of healthcare policies [8].

Progranulin (PGRN) is a multifunctional glycoprotein that plays an important role in stroke pathogenesis [9]. Thanks to its anti-inflammatory and neurotrophic properties, PGRN supports nerve cell survival and regulates physiological processes, including cell proliferation, wound healing, and nervous system development [10–12]. Primarily expressed by microglia and pyramidal neurons in brain tissue, PGRN exerts a neuroprotective effect by limiting post-stroke inflammation, cell death, and blood–brain barrier damage [13,14]. PGRN promotes the proliferation of neural stem/progenitor cells via PI3K/AKT and MAPK/ERK signaling pathways and supports post-ischaemic recovery by increasing neurogenesis in the subventricular zone [14–16]. Furthermore, it reduces impairments to cognitive function, such as learning and memory disorders, by increasing neuronal differentiation [17]. The suppression of the NF-κB pathway by PGRN and the reduction of oxidative stress and necroptosis play central roles in limiting stroke-induced damage [18]. Given these properties, PGRN stands out as both a biomarker and a potential therapeutic target.

Despite its biological relevance, the clinical significance of PGRN in acute stroke remains incompletely understood. This study aimed to determine the diagnostic and prognostic value of serum PGRN levels measured within the first 6 hours in patients with IS and ICH. This is the first study to compare PGRN levels across subtypes and evaluate PGRN levels in ICH in relation to mortality and prognosis.

MATERIALS AND METHODS

This case-control study included 42 patients with acute stroke who were admitted to the Emergency Department of a tertiary training and research hospital, as well as 44 healthy volunteers. Patients were included if they met the following criteria: sudden-onset focal neurological deficit due to ICH or IS; admission within 6 hours of symptom onset; neurological symptoms during admission; and adequate access to patient information. Patients with a history of stroke, traumatic brain injury, brain tumor, infection, degenerative brain disease, liver failure, kidney failure, chronic heart disease, and acute myocardial infarction were excluded from the study. The Glasgow Coma Scale (GCS) was used to assess neurological status at admission. CT or MRI confirmed the stroke subtype. Up to 2 cc of blood was collected and placed in serum-separating tubes. The tubes were incubated at room temperature for 20 minutes and then centrifuged at 3000 rpm for 15 minutes. The obtained serum was then divided into Eppendorf aliquots of at least 0.3 cc. Eppendorf tubes were labeled and stored at -80°C until analyzed. This study was conducted in accordance with the principles outlined in the Declaration of Helsinki. Approval was granted by the Clinical Research Ethics Committee of the University of Health Sciences, Sisli Hamidiye Etfal Research and Training Hospital (Approval no: 4825, Date: 08.04.2025). Written informed consent was obtained from all participants.

Sample analysis

Serum PRGN levels were measured using a Human Progranulin ELISA Kit (Elabscience Biotechnology, China). Different standard concentrations were prepared by diluting the lyophilized standard provided with the kit. Following the kit procedure, the absorbance of the examined samples was measured at 450 nm with an EBLX-800 microplate reader (BioTek Instruments, Inc., USA). Concentrations corresponding to absorbance values were calculated using the formula obtained from the standard curve (sensitivity: 37.5 pg/mL, assay range: 62.5-4000 pg/mL, intra-assay CV< 10%).

Statistical analysis

Data distribution was evaluated using the Shapiro–Wilk normality test. Continuous variables are reported as mean ± standard deviation or median with minimum and maximum values, while categorical variables are expressed as counts and percentages. For comparisons between groups, parametric methods(independent-samples t-test or one-way analysis of variance)were applied when distributional assumptions were met; otherwise, nonparametric alternatives (Mann–Whitney U or Kruskal–Wallis tests) were used. Post-hoc analyses were adjusted using the Bonferroni method where appropriate. Associations between categorical variables were examined using the chi-square test or Fisher's exact test, depending on the expected cell counts. A two-sided p-value < 0.05 was considered statistically significant. Statistical analyses were conducted using IBM SPSS Statistics for Windows (version 29.0.2.0; IBM Corp., Armonk, NY, USA).

The discriminative ability of PGRN for patient status was assessed by receiver operating characteristic (ROC) curve analysis, with the area under the curve (AUC) serving as the primary measure of diagnostic performance. ROC analyses were performed using MedCalc Statistical Software (version 23.2.1).

RESULTS

Descriptive statistics for patient demographic and clinical variables are presented in Table 1. The study groups showed similar baseline demographic characteristics. The median age was comparable between the control and patient groups [59 (28-90) vs 62.5 (13-92) years, p=0.069], indicating no significant age difference. The gender distribution was also similar across groups, with no statistically significant difference (p=0.117).

PGRN levels differed significantly between the groups. The control group had significantly lower mean PGRN levels (52.2±18.9 pg/mL) than the patient group (69.6±15.4

https://doi.org/10.5455/annalsmedres.2026.01.028

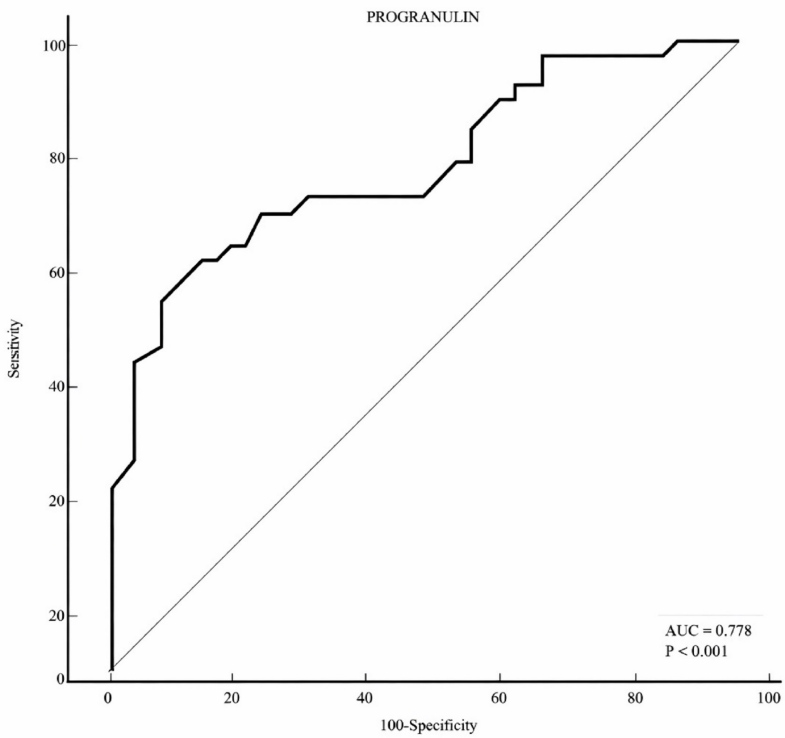

Figure 1. ROC curve analysis demonstrating the diagnostic value of serum progranulin in acute stroke.

Table 1. Demographic data of patients.

Characteristic	n (%)
Gender	
Male	28 (67)
Female	14 (33)
Glasgow Coma Scale	
Mild (<11)	34 (81)
Severe (≥12)	8 (19)
Hypertension	
Yes	12 (29)
No	30 (71)
Diabetes Mellitus	
Yes	6 (14)
No	36 (86)
Atrial Fibrillation	
Yes	4 (10)
No	38 (90)

Table 2. Demographic and biomarker comparison between groups.

	Control (n=44)	Patient (n=42)	p value
Age median (min-max)	59 (28-90)	62.5 (13-92)	0.069
Sex (male/female)	22/22	28/14	0.117
PGRN (pg/mL) mean±SD	52.2±18.9	69.6±15.4	<0.001

PGRN: Progranulin.

pg/mL; p<0.001) (Table 2). For disease detection, PGRN had a cutoff of 53 pg/mL, yielding 64% sensitivity and 84% specificity [AUC = 0.778; 95% CI (0.676 to 0.861)] (Figure 1). There was no correlation between PGRN levels and hospital stay length (42±27 days) or ICU use (12±29 days). Only the GCS score was correlated with length of hospital stay (p=0.019; r=-0.395) and with ICU use (p=0.022; r=-0.385). When we grouped patients as severe or mild (GCS < 11 as severe; GCS ≥ 12 as mild), there was no significant difference in PGRN levels. No significant difference in PGRN levels between IS and ICH was observed (Table 3).

Table 3. Comparison of PGRN according to GCS, mortality, ischemic, and hemorrhagic subtypes.

	PGRN pg/mL
GCS<11 (mild) (n=34)	49.5 (26-110)
GCS≥12 (severe) (n=8)	46 (15-75)
p-value	0.814
Ex (n=8)	43 (26-90)
Survivor (n=34)	56 (15-110)
p-value	0.192
IS (n=22)	47 (31-110)
ICH (n=20)	50 (15-90)
p-value	0.801

PGRN: Progranulin; GCS: Glasgow Coma Scale; IS: Ischemic stroke; ICH: Intracerebral hemorrhage.

DISCUSSION

In this study, we investigated the diagnostic and prognostic significance of serum PGRN levels in patients with acute ischemic or hemorrhagic stroke within the first six hours of symptom onset. Our findings indicate that serum PGRN

https://doi.org/10.5455/annalsmedres.2026.01.028

concentrations are significantly higher in stroke patients than in healthy controls, suggesting that PGRN may be an early biomarker of cerebrovascular events. However, PGRN levels did not show a significant association with stroke subtype (ischemic vs. hemorrhagic) or clinical severity and outcome indicators such as mortality, intensive care unit admission, or length of hospital stay. These findings imply that while PGRN reflects an acute response to stroke, its role in prognosis requires further clarification.

Previous studies have reported heterogeneous results regarding the prognostic value of PGRN. Lasek-Bal et al. similarly found elevated serum PGRN levels in the early phase of ischemic stroke, without a significant relationship to patient outcomes [19]. In contrast, Xie et al. demonstrated that increased serum PGRN was independently associated with all-cause mortality in acute ischemic stroke, suggesting a possible prognostic utility [20]. Zhou et al. demonstrated decreased PGRN levels in patients with ICH and in experimental rat models The decrease in PGRN paralleled neutrophil activation and increased proinflammatory cytokines (IL-1β, TNF-α), suggesting that inflammation contributes to early brain injury [12]. This discrepancy may be attributable to differences in study design, sample size, timing of blood sampling, and patient selection criteria. Our study, by including both ischemic and hemorrhagic stroke patients, contributes novel insights into the broader spectrum of cerebrovascular disease. Stroke and traumatic brain injury (TBI) share converging pathophysiological pathways, including acute neuronal injury, neuroinflammation, and microglial activation, suggesting that common inflammatory mediators may be involved across these conditions. In TBI, elevated serum and urine progranulin (PGRN) levels in the early phase have been associated with cortical microglial activation, reflecting an acute neuroinflammatory response [21]. These findings support the biological plausibility that PGRN may also serve as a marker of injury-related inflammatory processes in acute stroke.

Experimental data have consistently shown the neuroprotective and anti-inflammatory roles of PGRN. Animal studies indicate that reduced PGRN levels are associated with increased neutrophil infiltration, blood–brain barrier disruption, and neuronal apoptosis, whereas recombinant PGRN administration mitigates these effects and improves neurological outcomes. These mechanistic findings support the hypothesis that PGRN elevation in human stroke may reflect a compensatory neuroprotective response. However, whether this response is sufficient to influence clinical prognosis remains uncertain [12]. Emerging evidence highlights progranulin as a key regulator of lysosomal function and proteostatic stress, processes that are critically involved in neuronal vulnerability and neuroinflammatory responses across neurological diseases. This mechanistic framework supports the view that altered serum progranulin levels observed in acute stroke reflect injury-related lysosomal and inflammatory pathways [22]. In another study, PGRN was shown to be a multifunctional mediator in ischemic stroke, exerting neuroprotective and anti-inflammatory effects by modulating microglial activation, oxidative stress, apoptosis, and blood–brain barrier integrity [23]. These mechanisms provide a biological rationale for the altered serum levels of progranulin observed in our cohort and support its relevance as a potential biomarker in acute stroke. Interestingly, we did not observe a significant relationship between PGRN levels and either stroke severity (as measured by the GCS) or patient mortality. This lack of association may reflect the complexity of stroke pathophysiology, where multiple inflammatory, vascular, and neurodegenerative pathways interact.

The present study has several strengths, including its prospective design, early sampling within 6 hours of stroke onset, and inclusion of both ischemic and hemorrhagic subtypes. Nonetheless, some limitations must be acknowledged. The relatively small sample size may have limited the power to detect subtle prognostic associations. Moreover, we measured PGRN levels only at a single time point; serial measurements could provide more dynamic insights into temporal changes in this biomarker. Additionally, long-term functional outcomes, such as disability scores and quality of life, were not assessed; their inclusion may have provided a more comprehensive understanding of PGRN's prognostic role.

Limitations

This study has several limitations. First, the relatively small sample size may have limited the statistical power to detect subtle differences, particularly regarding prognostic outcomes. Second, serum progranulin levels were measured at a single time point within the first six hours of symptom onset; therefore, changes over time could not be evaluated. Third, long-term functional outcomes and disability scores were not assessed. Finally, as this was a single-center study, the generalizability of the results may be limited.

CONCLUSION

This study is the first to compare PGRN between IS and ICH and to evaluate its relationship with ICH-related mortality. Elevated serum progranulin levels in the early phase of acute stroke suggest a potential role as a diagnostic biomarker. However, no difference in levels between IS and ICH was observed, and neither was associated with severity or short-term outcomes, indicating limited prognostic value. Further research is required to confirm its clinical utility.

Ethics Committee Approval: Approval was granted by the Ethics Committee of the University of Health Sciences, Sisli Hamidiye Etfal Research and Training Hospital Clinical Research (Approval no: 4825, Date: 08.04.2025).

Informed Consent: Written informed consent was obtained from all participants.

Peer-review: Externally peer-reviewed.

https://doi.org/10.5455/annalsmedres.2026.01.028

Conflict of Interest: The authors declare no potential conflicts of interest regarding the research, authorship, or publication of this article.

Author Contributions: MSO: Conceptualization, Methodology, Writing - original draft; HFK: Conceptualization, Resources, Writing - review & editing; GO: Data curation, Formal analysis, Visualization, Writing - review & editing, Supervision; ZMYK: Visualization, Writing - review & editing, Supervision; EA: Visualization, Writing - review & editing, Supervision; ES: Visualization, Writing - review & editing, Supervision.

Financial Disclosure: The authors received no financial support for the research, authorship, or publication of this article.

Data availability statement: The datasets used in this study are available from the corresponding author upon reasonable request.

Artificial Intelligence Disclosure: An artificial intelligence–based tool (ChatGPT, OpenAI, version 4.1) was used solely for language editing and readability improvement, including minor text organization and grammatical refinement. The AI tool was not used for study design, data analysis, data interpretation, or the generation of scientific conclusions. All content in the manuscript, including the study design, statistical analyses, results, and interpretations, was developed entirely by the authors. The manuscript was critically reviewed, revised, and approved by all authors to ensure accuracy, originality, and scientific integrity. We confirm that all authors take full responsibility for the content of the manuscript and that the use of AI complies with the journal's ethical guidelines. No AI tool has been listed as an author.

REFERENCES

1. Feigin VL, Lawes CM, Bennett DA, Barker-Collo SL, Parag V. Worldwide stroke incidence and early case fatality reported in 56 population-based studies: a systematic review. *Lancet Neurol.* 2009;8(4):355–369. doi: 10.1016/S1474-4422(09)70025-0.
2. Zhou F, Yu T, Du R, et al. Clinical course and risk factors for mortality of adult inpatients with COVID-19 in Wuhan, China: a retrospective cohort study. *Lancet.* 2020;395(10229):1054–1062. doi: 10.1016/S0140-6736(20)30566-3.
3. Feigin VL, Stark BA, Johnson CO, et al. Global, regional, and national burden of stroke and its risk factors, 1990-2019: A systematic analysis for the Global Burden of Disease Study 2019. *Lancet Neurol.* 2021;20(10):795-820. doi: 10.1016/S1474-4422(21)00252-0.
4. Rajsic S, Gothe H, Borba HH, et al. Economic burden of stroke: a systematic review on post-stroke care. *Eur J Health Econ.* 2019;20(1):107–134. doi: 10.1007/S10198-018-0984-0.
5. Jauch EC, Saver JL, Adams HP, Bruno A, et al. Guidelines for the early management of patients with acute ischemic stroke: A guideline for healthcare professionals from the American Heart Association/American Stroke Association. *Stroke.* 2013;44(3):870–947. doi: 10.1161/STR.0B013E318284056A.
6. Chalela JA, Kidwell CS, Nentwich LM, et al. Magnetic resonance imaging and computed tomography in emergency assessment of patients with suspected acute stroke: a prospective comparison. *Lancet.* 2007;369(9558):293–298. doi: 10.1016/S0140-6736(07)60151-2.
7. Johnson KB, Wei WQ, Weeraratne D, et al. Precision Medicine, AI, and the Future of Personalized Health Care. *Clin Transl Sci.* 2021;14(1):86–93. doi: 10.1111/CTS.12884.
8. Joundi RA, Adekanye J, Leung AA, et al. Health State Utility Values in People With Stroke: A Systematic Review and Meta-Analysis. *J Am Heart Assoc.* 2022;11(13). doi: 10.1161/JAHA.121.024296.
9. Anakwe OO, Gerton GL. Acrosome Biogenesis Begins during Meiosis: Evidence from the Synthesis and Distribution of an Acrosomal Glycoprotein, Acrogranin, during Guinea Pig Spermatogenesis. *Biol Reprod.* 1990;42(2):317–328. doi: 10.1095/BIOLREPROD42.2.317.
10. Lui H, Zhang J, Makinson SR, et al. Progranulin Deficiency Promotes Circuit-Specific Synaptic Pruning by Microglia via Complement Activation. *Cell.* 2016;165(4):921–935. doi: 10.1016/j.cell.2016.04.001.
11. Tanaka Y, Matsuwaki T, Yamanouchi K, Nishihara M. Exacerbated inflammatory responses related to activated microglia after traumatic brain injury in progranulin-deficient mice. *Neuroscience.* 2013;231:49–60. doi: 10.1016/j.neuroscience.2012.11.032.
12. Zhou C, Xie G, Wang C, et al. Decreased progranulin levels in patients and rats with subarachnoid hemorrhage: A potential role in inhibiting inflammation by suppressing neutrophil recruitment. *J Neuroinflammation.* 2015;12:200. doi: 10.1186/S12974-015-0415-4.
13. Wang C, Zhang L, Ndong JDLC, et al. Progranulin deficiency exacerbates spinal cord injury by promoting neuroinflammation and cell apoptosis in mice. *J Neuroinflammation.* 2019;16(1):238. doi: 10.1186/S12974-019-1630-1.
14. Tao J, Ji F, Wang F, Liu B, Zhu Y. Neuroprotective effects of progranulin in ischemic mice. *Brain Res.* 2012;1436: 130–136. doi: 10.1016/j.brainres.2011.11.063.
15. Wang L, Zhang ZG, Zhang RL, Chopp M. Activation of the PI3-K/Akt pathway mediates cGMP enhanced-neurogenesis in the adult progenitor cells derived from the subventricular zone. *J Cereb Blood Flow Metab.* 2005;25(9):1150–1158. doi: 10.1038/SJ.JCBFM.9600112.
16. Shioda N, Han F, Fukunaga K. Chapter 26 Role of Akt and Erk Signaling in the Neurogenesis Following Brain Ischemia. *Int Rev Neurobiol.* 2009;85:375-87. doi: 10.1016/S0074-7742(09)85026-5.
17. Zhang K, Li YJ, Feng D, et al. Imbalance between TNFα and progranulin contributes to memory impairment and anxiety in sleep-deprived mice. *Sci Rep.* 2017;7:43594. doi: 10.1038/srep43594.
18. Egashira Y, Suzuki Y, Azuma Y, et al. The growth factor progranulin attenuates neuronal injury induced by cerebral ischemia-reperfusion through the suppression of neutrophil recruitment. *J Neuroinflammation.* 2013;10:105. doi: 10.1186/1742-2094-10-105.
19. Lasek-Bal A, Jedrzejowska-Szypulka H, Student S, et al. The importance of selected markers of inflammation and blood-brain barrier damage for short-term ischemic stroke prognosis. *J Physiol Pharmacol.* 2019;70(2). doi: 10.26402/jpp.2019.2.04.
20. Xie S, Lu L, Liu L, Bi G, Zheng L. Progranulin and short-term outcome in patients with acute ischaemic stroke. *Eur J Neurol.* 2016;23(3):648-55. doi: 10.1111/ene.12920.
21. Olczak M, Poniatowski LA, Siwinska A, et al. Elevated serum and urine levels of progranulin (PGRN) as a predictorof microglia activation in the early phase of traumatic brain injury:a further link with the development of neurodegenerative diseases. *Folia Neuropathol.* 2021;59(1):81–90. doi: 10.5114/FN.2021.105137.
22. Lane-Donovan C, Paredes M, Kao AW. The lysosome and proteostatic stress at the intersection of pediatric neurological disorders and adult neurodegenerative diseases. *Prog Neurobiol.* 2025;255:102854. doi: 10.1016/j.pneurobio.2025.102854.
23. Purrahman D, Shojaeian A, Poniatowski ŁA, Piechowski-Jóźwiak B, Mahmoudian-Sani MR. The Role of Progranulin (PGRN) in the Pathogenesis of Ischemic Stroke. *Cell Mol Neurobiol.* 2023;43(7):3435-47. doi: 10.1007/S10571-023-01396-8.

Ann Med Res

Current issue list available at Ann Med Res

Annals of Medical Research

journal page: annalsmedres.org

Four-year evaluation of tuberculosis diagnostics and drug resistance patterns: A retrospective analysis of smear microscopy, MTB/RIF PCR, and culture-confirmed *Mycobacterium tuberculosis* isolates

Baris Can[a], *, Gizem Nigdelioglu[a], Elvan Sayin[a], Arzu Ilki[a]

[a]*Marmara University, Faculty of Medicine, Department of Medical Microbiology, Istanbul, Türkiye*

**Corresponding author: can.baris@marmara.edu.tr (Baris Can)*

MAIN POINTS

- MTB/RIF PCR demonstrated markedly higher sensitivity than direct smear microscopy in diagnosing culture-confirmed tuberculosis.
- Direct smear microscopy showed excellent specificity but limited sensitivity, particularly in smear-negative tuberculosis cases.
- Tuberculosis positivity rates declined over the four-year study period; however, resistance to isoniazid remained the most frequently detected first-line drug resistance.
- Despite low multidrug-resistant tuberculosis rates, routine molecular diagnostics and drug susceptibility testing remain essential for effective tuberculosis management.

Cite this article as: Can B, Nigdelioglu G, Sayin E, Ilki A. Four-year evaluation of tuberculosis diagnostics and drug resistance patterns: A retrospective analysis of smear microscopy, MTB/RIF PCR, and culture-confirmed *Mycobacterium tuberculosis* isolates. *Ann Med Res*. 2026;33(8):403–408. doi: 10.5455/annalsmedres.2026.01.026.

ABSTRACT

Aim: Accurate and timely diagnosis of tuberculosis remains a major clinical challenge. This study aimed to evaluate the diagnostic performance of direct smear microscopy and MTB/RIF PCR compared with culture, and to assess first-line drug resistance patterns among *Mycobacterium tuberculosis* complex (MTBC) isolates.

Materials and Methods: This retrospective study analyzed non-duplicate mycobacterial culture records obtained between 2020 and 2023 at a tertiary care center. Culture-confirmed MTBC cases served as the reference standard. The diagnostic performance of direct smear microscopy and MTB/RIF PCR was evaluated in patients who underwent both the index test and the culture. Drug susceptibility testing was performed for first-line antituberculosis agents, including isoniazid, rifampicin, ethambutol, and streptomycin. The study was reported in accordance with the STROBE and STARD guidelines.

Results: A total of 8,863 mycobacterial cultures were evaluated, yielding 165 MTBC-positive isolates. MTB positivity rates decreased from 2.18% in 2020 to 1.31% in 2023. When data from all years were combined, direct smear microscopy demonstrated a sensitivity of 34.5% and a specificity of 99.8%, whereas MTB/RIF PCR showed a sensitivity of 91.5% and a specificity of 98.5%, all for culture-confirmed tuberculosis. Drug susceptibility testing was available for 160 isolates. Resistance to isoniazid, rifampicin, ethambutol, and streptomycin was detected in 14.4%, 1.9%, 6.3%, and 8.8% of isolates, respectively. Multidrug-resistant tuberculosis was identified in 1.25% of cases.

Conclusion: Direct smear microscopy exhibited limited sensitivity despite high specificity, whereas MTB/RIF PCR demonstrated excellent diagnostic performance and a high negative predictive value. Although overall drug resistance rates were relatively low, the presence of isoniazid resistance underscores the importance of routine susceptibility testing in the management of tuberculosis.

Keywords: *Mycobacterium tuberculosis* complex, Smear microscopy, MTB/RIF PCR, Drug resistance, Diagnostic performance

Received: Jan 14, 2026 **Accepted:** Apr 28, 2026 **Available Online:** Aug 25, 2026

INTRODUCTION

Tuberculosis (TB) remains one of the leading infectious causes of morbidity and mortality worldwide, despite major advances in diagnostic technologies and treatment strategies [1]. Rapid and accurate identification of *Mycobacterium tuberculosis* complex (MTBC) is essential to initiate timely, appropriate therapy, prevent transmission, and limit the emergence of drug-resistant strains. Although mycobacterial culture is considered the reference standard for TB diagnosis, its prolonged turnaround time limits its usefulness in urgent clinical decision-making.

Direct smear microscopy has traditionally served as a cornerstone of TB diagnosis, particularly in resource-limited settings, due to its simplicity, low cost, and high specificity. However, its sensitivity is highly variable and depends on factors such as bacillary load, specimen quality, and laboratory expertise [2,3]. In recent years, molecular diagnostic assays, including MTB/RIF PCR, have substantially improved TB

diagnostics by enabling rapid detection of MTBC and rifampicin resistance, thereby facilitating earlier initiation of targeted treatment [4,5]. Nevertheless, the diagnostic performance of these molecular methods may vary in real-world settings depending on patient populations, laboratory workflows, and specimen characteristics [6–9].

In addition to diagnostic challenges, drug-resistant TB continues to represent a major global public health concern. Resistance to first-line antituberculosis agents, particularly isoniazid and rifampicin, is associated with unfavorable treatment outcomes, prolonged infectiousness, and increased healthcare costs [10–13]. Continuous local surveillance of resistance patterns is therefore essential to guide empirical treatment strategies and identify emerging trends in multidrug-resistant tuberculosis.

The present study aimed to conduct a comprehensive four-year evaluation of TB diagnostics at a tertiary care center by comparing the diagnostic performance of direct smear microscopy and MTB/RIF PCR, with culture-confirmed MTBC as the reference standard. Additionally, the study sought to assess the prevalence and patterns of resistance to first-line antituberculosis drugs in MTBC isolates, thus providing clinically relevant data for laboratory specialists and treating clinicians.

MATERIALS AND METHODS

Study design and isolates

This retrospective observational study included non-duplicate clinical specimens submitted to the Microbiology Laboratory of Marmara University Pendik Training and Research Hospital, Istanbul, Turkey, for mycobacterial investigation between January 2020 and December 2023. To avoid repeated sampling, follow-up or repeat specimens/records from the same patient were excluded, and only the first eligible specimen per patient was included in the analysis. The study was conducted following approval by the Marmara University Faculty of Medicine Ethics Committee and in accordance with the principles of the Declaration of Helsinki (Protocol No: 09.2025.25-0982, Date: 10.12.2025), and it was reported in accordance with the STROBE and STARD guidelines for observational and diagnostic accuracy studies. Culture-confirmed *Mycobacterium tuberculosis* complex (MTBC) isolates were included in the analysis.

Direct smear microscopy and mycobacterial culture

Clinical specimens were processed using standard decontamination and concentration procedures. Direct smear microscopy was performed using Ziehl–Neelsen staining. Mycobacterial cultures were incubated on Löwenstein–Jensen medium and in an automated liquid culture system (BACTEC MGIT 960; Becton Dickinson, Sparks, MD, USA). Culture results were reported as positive when mycobacterial growth was detected and as negative when no growth was observed after the recommended incubation period.

Identification of Mycobacterium tuberculosis complex

Isolates were identified as MTBC by routine laboratory identification algorithms. Only culture-confirmed MTBC isolates were accepted as the reference standard for diagnostic performance analysis.

MTB/RIF PCR assay

Molecular detection of MTBC was performed using the Xpert MTB/RIF assay (Cepheid, Sunnyvale, CA, USA) in accordance with the manufacturer's instructions. Results were reported as positive or negative for MTBC. When TRACE/very-low results were reported by the platform, these were interpreted cautiously in routine practice and evaluated together with smear microscopy, culture results, and clinical information; repeat testing and/or a follow-up specimen were recommended when clinically indicated.

Drug susceptibility testing

Drug susceptibility testing was performed for first-line antituberculosis agents, including isoniazid (INH), rifampicin (RIF), ethambutol (EMB), and streptomycin (SM), using the BACTEC MGIT 960 system, according to the manufacturer's instructions and the standard critical concentrations (INH 0.1 μg/mL, RIF 1.0 μg/mL, EMB 5.0 μg/mL, SM 1.0 μg/mL). Of the 165 culture-confirmed MTBC isolates, susceptibility results were available for 160. Five isolates were excluded from resistance analysis because of insufficient growth or technical limitations.

Statistical analysis

Culture-confirmed MTBC was accepted as the reference standard. The diagnostic performance of direct smear microscopy and MTB/RIF PCR was evaluated separately by comparing each test with culture results in patients who had both the index test and culture performed. Sensitivity, specificity, positive predictive value (PPV), and negative predictive value (NPV) were calculated using standard formulas, and 95% confidence intervals (CIs) were calculated using the exact (Clopper–Pearson) method. Comparisons of sensitivity and specificity between smear microscopy and MTB/RIF

Table 1. Annual distribution of culture-confirmed *Mycobacterium tuberculosis* complex isolates (2020--2023).

Year	Total cultures (n)	MTBC positive (n)	MTBC positivity (%)
2020	1,847	40	2.18
2021	1,996	56	2.81
2022	2,187	32	1.46
2023	2,833	37	1.31
Total	8,863	165	1.86

MTBC: *Mycobacterium tuberculosis* complex.

https://doi.org/10.5455/annalsmedres.2026.01.026

Table 2. Diagnostic performance of direct smear microscopy and MTB/RIF PCR compared with culture (2020--2023).

Test	n	TP	FP	FN	TN	Sensitivity (%)	Specificity (%)	PPV (%)	NPV (%)
Smear microscopy	8,858	57	16	108	8,677	34.5 (27.3--42.3)	99.8 (99.7--99.9)	78.1 (66.9--86.9)	98.8 (98.5--99.0)
MTB/RIF PCR	4,096	107	61	10	3,918	91.5 (84.8--95.8)	98.5 (98.0--98.8)	63.7 (55.9--71.0)	99.7 (99.5--99.9)

TP: true positive; FP: false positive; FN: false negative; TN: true negative; PPV: positive predictive value; NPV: negative predictive value. Culture-confirmed *Mycobacterium tuberculosis* complex was used as the reference standard. Diagnostic performance estimates are presented as percentage with 95% confidence intervals calculated using the exact (Clopper–Pearson) method.

Table 3. Sensitivity and specificity of smear microscopy and MTB/RIF PCR according to specimen group.

Specimen group	Test	n	Sensitivity (%)	Specificity (%)
Pulmonary	Smear microscopy	4,430	50.5	99.9
	MTB/RIF PCR	2,591	97.6	98.4
Extrapulmonary	Smear microscopy	4,428	9.4	99.8
	MTB/RIF PCR	1,505	77.1	98.5

MTB/RIF PCR, Xpert MTB/RIF assay.

Table 4. Drug susceptibility patterns of *Mycobacterium tuberculosis* complex isolates (n = 160)

Test result	Antibiotics	n	%
Susceptible to four drugs	INH, RIF, EMB, SM	125	78.1
Single-drug resistance	INH	10	6.2
	RIF	1	0.6
	EMB	6	3.8
	SM	5	3.1
Resistance to two drugs	INH + RIF	1	0.6
	INH + SM	7	4.4
	INH + EMB	3	1.9
Resistance to three drugs	INH + RIF + SM	1	0.6
	INH + EMB + SM	1	0.6

INH: isoniazid; RIF: rifampicin; EMB: ethambutol; SM: streptomycin.

Table 5. Culture outcomes of TRACE-positive MTB/RIF PCR results among smear-negative patients.

Culture outcome	MTBC n (%)	NTM n (%)	No growth n (%)	Total n (%)
TRACE-positive cases	8 (27.6)	2 (6.9)	19 (65.5)	29 (100)

TRACE: very low-level positivity reported by the Xpert MTB/RIF assay; MTBC: *Mycobacterium tuberculosis* complex; NTM: non-tuberculous mycobacteria.

PCR were performed using two-proportion z-tests (equivalent to chi-square tests) on available tested subsets; p values <0.05 were considered statistically significant. Because not all patients underwent both tests simultaneously, comparisons were performed on the available subsets and did not represent fully paired analyses. Statistical analyses were performed using descriptive and inferential methods as appropriate.

RESULTS

Study population and culture results

Between January 2020 and December 2023, a total of 8,863 non-duplicate mycobacterial cultures were evaluated. Among these, 165 cultures (1.86%) were positive for *Mycobacterium tuberculosis* complex (MTBC). The annual MTBC positivity rate declined from 2.18% in 2020 to 1.31% in 2023 (Table 1).

In addition to MTBC, 21 non-tuberculous mycobacterial (NTM) isolates were identified during the study period. These isolates were excluded from subsequent analyses of diagnostic performance and drug resistance.

Diagnostic performance of direct smear microscopy and MTB/RIF PCR

Among patients who underwent both direct smear microscopy and culture (n = 8,858), smear microscopy demonstrated a sensitivity of 34.5% (95% CI: 27.3–42.3) and a specificity of 99.8% (95% CI: 99.7–99.9). The positive predictive value (PPV) was 78.1% (95% CI: 66.9–86.9), and the negative predictive value (NPV) was 98.8% (95% CI: 98.5–99.0).

Among patients with both MTB/RIF PCR and culture results available (n = 4,096), MTB/RIF PCR showed a substantially higher sensitivity of 91.5% (95% CI: 84.8–95.8) and a specificity of 98.5% (95% CI: 98.0–98.8), with a PPV of 63.7% (95% CI: 55.9–71.0) and an NPV of 99.7% (95% CI: 99.5–99.9) (Table 2). In subgroup-based comparisons,

https://doi.org/10.5455/annalsmedres.2026.01.026

MTB/RIF PCR demonstrated significantly higher sensitivity than smear microscopy (p<0.001). Although the absolute difference in specificity was small, it also reached statistical significance (p<0.001).

When data were stratified by specimen type, smear microscopy exhibited markedly higher sensitivity for pulmonary samples (50.5%) than for extrapulmonary samples (9.4%). MTB/RIF PCR maintained high sensitivity in both specimen groups; however, diagnostic performance was higher in pulmonary specimens (97.6%) than in extrapulmonary specimens (77.1%) (Table 3).

Drug susceptibility patterns of MTBC isolates

Drug susceptibility testing was successfully performed for 160 of the 165 MTBC isolates. Resistance to at least one first-line antituberculosis drug was detected in 35 isolates (21.9%), whereas 125 isolates (78.1%) were fully susceptible to all tested agents.

The most frequently observed resistance was to isoniazid (14.4%), followed by resistance to streptomycin (8.8%), ethambutol (6.3%), and rifampicin (1.9%). Multidrug-resistant tuberculosis, defined as combined resistance to both isoniazid and rifampicin, was identified in two isolates (1.25%) (Table 4).

Regarding the extent of resistance, 22 isolates (13.8%) exhibited resistance to a single drug, 11 isolates (6.9%) to two drugs, and 2 isolates (1.25%) to three drugs. No isolate demonstrated resistance to all four first-line antituberculosis agents.

TRACE-positive MTB/RIF PCR results

In the cohort of 8,863 patients, TRACE-level MTB/RIF PCR positivity was observed in 29 cases. Culture confirmed MTBC in 8 of these TRACE-positive cases (27.6%), while non-tuberculous mycobacteria were identified in 2 cases (6.9%). No mycobacterial growth was detected in the remaining 19 cases (65.5%) (Table 5).

DISCUSSION

In this four-year retrospective study, we evaluated the diagnostic performance of direct smear microscopy and MTB/RIF PCR, compared with culture-confirmed *Mycobacterium tuberculosis* complex (MTBC), and analyzed first-line drug resistance patterns in a tertiary care setting. Our findings demonstrate a declining trend in culture-confirmed tuberculosis over the study period, together with the markedly superior sensitivity of MTB/RIF PCR compared with smear microscopy, consistent with previous reports [1,4].

The overall sensitivity of direct smear microscopy in our cohort was 34.5%, in line with earlier studies reporting substantial variability depending on specimen quality, bacillary burden, and laboratory expertise [6,9,14]. Despite its limited sensitivity, smear microscopy maintained excellent specificity (99.8%), supporting its continued role as a rapid and inexpensive method for identifying highly infectious cases. However, the low sensitivity underscores the considerable risk of missed diagnoses when smear microscopy is used as a standalone diagnostic tool.

In contrast, MTB/RIF PCR demonstrated high sensitivity (91.5%), high specificity (98.5%), and a very high negative predictive value (99.7%). These findings highlight the clinical value of molecular testing as a reliable rule-out method, particularly in patients with smear-negative tuberculosis [15]. The relatively lower positive predictive value of MTB/RIF PCR likely reflects the low prevalence of culture-confirmed tuberculosis in our study population, as well as the detection of non-viable bacilli or residual mycobacterial DNA in previously treated patients [16].

In addition to MTBC isolates, a subset of culture-positive isolates were identified as non-tuberculous mycobacteria (NTM). Although these isolates were excluded from diagnostic performance and resistance analyses, their identification remains clinically relevant. NTM are increasingly recognized as opportunistic pathogens, particularly in individuals with chronic lung disease, immunosuppression, or structural airway abnormalities [17,18]. Importantly, NTM infections may yield smear-positive but MTB/RIF PCR–negative results, which can be misinterpreted as false-negative molecular testing [15,19,20]. These findings emphasize the continued importance of culture-based methods to accurately differentiate MTBC from NTM in routine clinical practice.

The low rate of culture confirmation among TRACE-positive, smear-negative cases (27.6%) further supports the need for cautious interpretation of TRACE results. Such findings may represent residual DNA from non-viable organisms, early infection, or cross-reactivity with NTM rather than active tuberculosis, particularly in low-prevalence settings [15,17–20].

Analysis of drug susceptibility patterns revealed that 21.9% of MTBC isolates were resistant to at least one first-line antituberculosis drug. Isoniazid resistance was the most frequently observed resistance pattern (14.4%), whereas rifampicin resistance was relatively low (1.9%). The multidrug-resistant tuberculosis (MDR-TB) rate of 1.25% observed in our cohort is lower than that reported in many national and international studies, suggesting that MDR-TB is currently uncommon in our region; nevertheless, continued surveillance remains essential [11,12].

The observed decline in MTBC positivity between 2020 and 2023 may reflect improvements in public health interventions, enhanced case detection strategies, or changes in healthcare utilization during the COVID-19 pandemic. However, the persistence of isoniazid resistance highlights the ongoing need for routine drug susceptibility testing, even in settings with declining tuberculosis incidence.

Limitations

This study has several limitations. First, the retrospective design limited access to complete clinical data and precluded re-

https://doi.org/10.5455/annalsmedres.2026.01.026

analysis of archived specimens. Second, drug susceptibility testing could not be performed for all culture-positive isolates because of technical constraints. Finally, the single-center design may limit the generalizability of the findings.

Although overall drug resistance rates were relatively low, the persistence of isoniazid resistance underscores the importance of ongoing resistance monitoring. The integration of rapid molecular diagnostics with conventional methods remains essential for effective tuberculosis management.

CONCLUSION

In this four-year retrospective analysis, MTB/RIF PCR demonstrated substantially higher sensitivity and an excellent negative predictive value compared with direct smear microscopy for the diagnosis of culture-confirmed tuberculosis. Although smear microscopy retains high specificity, its limited sensitivity underscores the risk of missed diagnoses when used as a standalone test. Despite relatively low overall drug resistance rates, the persistence of isoniazid resistance highlights the importance of routine drug susceptibility testing. These findings support the integration of rapid molecular diagnostics with conventional culture-based methods to improve the accuracy and timeliness of tuberculosis diagnosis and management.

Ethics Committee Approval: Ethical approval was obtained from the Marmara University Faculty of Medicine Ethics Committee (Protocol No: 09.2025.25-0982, Date: 10.12.2025).

Informed Consent: Due to the retrospective nature of the study, informed consent was waived.

Peer-review: Externally peer-reviewed.

Conflict of Interest: The authors declare that they have no conflict of interest.

Author Contributions: Concept: BC, GN, ES, AI; Design: BC, GN, ES, AI; Supervision: AI; Materials: BC, GN, ES, AI; Data Collection and/or Processing: BC, GN, ES; Analysis and Interpretation: BC, ES, AI; Literature Review: BC, GN; Writing Manuscript: BC; Critical Review: GN, ES, AI.

Financial Disclosure: This study did not receive any specific grant from funding agencies in the public, commercial, or not-for-profit sectors.

Artificial Intelligence Disclosure: The AI tool used only for limited language editing and readability improvement was ChatGPT (OpenAI, GPT-4). It was not used for study design, data analysis, data interpretation, or scientific conclusions. All content was reviewed and approved by the authors, who retain full responsibility for the manuscript.

REFERENCES

1. Kaswala C, Schmiedel Y, Kundu D, et al. Accuracy of Xpert MTB/RIF Ultra for the diagnosis of tuberculosis in adult patients: a retrospective cohort study. *Int J Infect Dis.* 2022;122:566–568. doi: 10.1016/j.ijid.2022.07.016.
2. Hueda-Zavaleta M, Gomez-de-la-Torre J, Barletta-Carrillo C, et al. Diagnostic accu-racy of Xpert MTB/RIF and Xpert Ultra tests in pulmonary and extrapulmonary tuber-culosis compared with Löwenstein–Jensen culture. *Clin Epidemiol Glob Health.* 2024;29:101730. doi: 10.1016/j.cegh.2024.101730.
3. Gupta-Wright A, Ha H, Abdulgadar S, et al. Evaluation of the Xpert MTB Host Response assay for the triage of patients with presumed pulmonary tuberculosis: a prospective diagnostic accuracy study in Viet Nam, India, the Philippines, Uganda, and South Africa. *Lancet Glob Health.* 2024;12(2):e226–e234. doi: 10.1016/S2214-109X(23)00541-7.
4. Dorman SE, Schumacher SG, Alland D, et al. Xpert MTB/RIF Ultra for detection of Mycobacterium tuberculosis and rifampicin resistance: a prospective multicentre diag-nostic accuracy study. *Lancet Infect Dis.* 2018;18(1):76–84. doi: 10.1016/S1473-3099(17)30691-6.
5. Park M, Kon OM. Use of Xpert MTB/RIF and Xpert Ultra in extrapulmonary tuberculosis. *Expert Rev Anti Infect Ther.* 2021;19(1):65–77. doi: 10.1080/14787210.2020.1810565.
6. Kohli M, Inbaraj LR, Salomon A, et al. Low-complexity automated nucleic acid amplification tests for extrapulmonary tuberculosis and rifampicin resistance in adults and adolescents. *Cochrane Database Syst Rev.* 2025;8:CD012768. doi: 10.1002/14651858.CD012768.pub4.
7. López-Roa P, Martin-Higuera C, Ruiz-Serrano MJ, et al. Performance of Xpert MTB/RIF Ultra assay on respiratory and extra-respiratory samples in a high-resource setting with a low tuberculosis prevalence. *Diagn Microbiol Infect Dis.* 2021;99(2):115235. doi: 10.1016/j.diagmicrobio.2020.115235.
8. Minnies S, Reeve BWP, Rockman L, et al. Xpert MTB/RIF Ultra Is Highly Sensitive for the Diagnosis of Tuberculosis Lymphadenitis in a High-HIV Setting. *J Clin Microbiol.* 2021;59(12):e01316-21. doi: 10.1128/JCM.01316-21.
9. Kabir S, Parash MTH, Emran NA, et al. Diagnostic challenges and Gene-Xpert utility in detecting Mycobacterium tuberculosis among suspected cases of Pulmonary tuberculosis. *PLoS One.* 2021;16(5):e0251858. doi: 10.1371/journal.pone.0251858.
10. Velen K, Podewils LJ, Shah NS, et al. Performance of GeneXpert MTB/RIF for Diagnosing Tuberculosis Among Symptomatic Household Contacts of Index Patients in South Africa. *Open Forum Infect Dis.* 2021;8(4):ofab025. doi: 10.1093/ofid/ofab025.
11. Tomaz APDO, Raboni SM, Kussen GMB, et al. The Xpert® MTB/RIF diagnostic test for pulmonary and extrapulmonary tuberculosis in immunocompetent and immunocompromised patients: Benefits and experiences over 2 years in different clinical contexts. *PLoS One.* 2021;16(3):e0247185. doi: 10.1371/journal.pone.0247185.
12. Zhang H, Li H, Tan M, et al. GeneXpert MTB/RIF combined with conventional methods for tuberculosis in Shanghai Regional Medical Center: a retrospective diagnostic study. *Ann Transl Med.* 2022;10(10):575. doi: 10.21037/atm-22-1374.
13. Kay AW, Ness T, Verkuijl SE, et al. Xpert MTB/RIF and Xpert MTB/RIF Ultra assays for active tuberculosis and rifampicin resistance in children. *Cochrane Database Syst Rev*. 2022;(9):CD013359. doi: 10.1002/14651858.CD013359.pub2.
14. Gupta J, Joshi P, Gupta R, et al. Comparative Evaluation of GeneXpert With Ziehl-Neelsen (ZN) Stain in Samples of Suspected Tuberculosis Cases at a Tertiary Care Teaching Hospital in Central India. *Cureus.* 2024;16(10):e71402. doi: 10.7759/cureus.71402.
15. Kusumaningrum D, Mertaniasih NM, Soedarsono S, et al. Implication of Negative GeneXpert Mycobacterium tuberculosis/Rifampicin Results in Suspected Tuberculosis Patients: A Research Study. *Int J Mycobacteriol.* 2024;13(2):152–157. doi: 10.4103/ijmy.ijmy_100_24.
16. Horne DJ, Zifodya JS, Shapiro AE, et al. Xpert MTB/RIF and Xpert MTB/RIF Ultra for pulmonary tuberculosis and rifampicin resistance in adults. *Cochrane Database Syst Rev.* 2025;(7):CD009593. doi: 10.1002/14651858.CD009593.pub4.

https://doi.org/10.5455/annalsmedres.2026.01.026

17. Cissé AB, Dean AS, Van Deun A, et al. Prevalence of non-tuberculous mycobacteria among people with acid-fast positive presumptive tuberculosis in Mali. *PLoS One.* 2024;19(12):e0301731. doi: 10.1371/journal.pone.0301731.
18. Li X, Sun D, Liang C, Gu W. Characterization of non-tuberculous mycobacterial pulmonary disease and pulmonary tuberculosis in patients with AFB smear-positive sputum: A retrospective comparative study. *Heliyon.* 2024;10(17):e37434. doi: 10.1016/j.heliyon.2024.e37434.
19. Liang Q, Jiang X, Jia J, et al. An early and trustable indicator suggestive of non-tuberculosis mycobacteria isolation in a high tuberculosis burden setting. *J Infect.* 2024;88(5):106149. doi: 10.1016/j.jinf.2024.106149.
20. Alemu A, Diriba G, Seid G, et al. Probe amplifications in the Xpert MTB/RIF Ultra assay for non-tuberculous mycobacteria identified from diabetes mellitus and chronic kidney disease patients in Ethiopia. *Sci Rep.* 2025;15:18465. *Sci Rep.* 2025;15(1):18465. doi: 10.1038/s41598-025-03716-y.

https://doi.org/10.5455/annalsmedres.2026.01.026

Ann Med Res

Current issue list available at Ann Med Res

Annals of Medical Research

journal page: annalsmedres.org

Serum ADAM8, ADAM10, and ADAM17 levels in attack-free familial Mediterranean fever patients: A cross-sectional case-control study

Ertugrul Yigit[a], *, Osman Cure[b], Huseyin Cinar Zihni[c], Mehtap Atak[d], Merve Huner Yigit[d]

[a]Karadeniz Technical University, Faculty of Medicine, Department of Medical Biochemistry, Trabzon, Türkiye
[b]Recep Tayyip Erdogan University, Faculty of Medicine, Department of Rheumatology, Rize, Türkiye
[c]Karadeniz Technical University, Graduate School of Health Sciences, Department of Medical Biochemistry, Trabzon, Türkiye
[d]Recep Tayyip Erdogan University, Faculty of Medicine, Department of Medical Biochemistry, Rize, Türkiye
*Corresponding author: ertugrulyigit@ktu.edu.tr (Ertugrul Yigit)

MAIN POINTS

- Serum ADAM8 and ADAM10 levels were significantly higher in clinically attack-free FMF patients than those in healthy controls, and both remained independently associated with FMF after adjustment for age, sex, body mass index, and smoking status.
- ADAM17 levels did not differ between FMF patients and controls, suggesting a distinct regulatory profile among ADAM family members.
- ADAM10 showed weak-to-moderate associations with classical inflammatory markers, whereas ADAM8 and ADAM17 showed limited correlations.
- ROC analyses indicated that ADAM8 and ADAM10 had moderate discriminatory performance; however, these findings are exploratory and not intended for clinical diagnostic use.

Cite this article as: Yigit E, Cure O, Zihni HC, Atak M, Huner Yigit M. Serum ADAM8, ADAM10, and ADAM17 levels in attack-free familial Mediterranean fever patients: A cross-sectional case-control study. *Ann Med Res*. 2026;33(8):409–417. doi: 10.5455/annalsmedres.2026.01.019.

ABSTRACT

Aim: Familial Mediterranean Fever (FMF) is a monogenic autoinflammatory disease characterized by recurrent inflammatory attacks and persistent subclinical inflammation. The role of the ADAM (a disintegrin and metalloproteinase) family of metalloproteinases in FMF pathogenesis remains unclear. This study aimed to compare serum levels of ADAM8, ADAM10, and ADAM17 between FMF patients during attack-free periods and healthy controls and evaluate their associations with inflammatory markers.

Materials and Methods: This single-center, cross-sectional, case--control study included 36 FMF patients and 36 age and sex-matched healthy controls. All patients received regular colchicine therapy, and blood samples were collected during attack-free periods. Serum levels of ADAM8, ADAM10, and ADAM17 were measured by ELISA. Acute-phase reactants [C-reactive protein (CRP), serum amyloid A (SAA), and fibrinogen] were analyzed using routine laboratory methods. Between-group comparisons, correlation analyses, multivariable binary logistic regression analyses, and receiver operating characteristic (ROC) analyses were performed.

Results: Serum ADAM8 and ADAM10 levels were significantly higher in FMF patients than in controls ($p<0.001$), whereas ADAM17 levels did not differ between groups. ADAM10 showed weak-to-moderate positive correlations with CRP and fibrinogen, while ADAM8 and ADAM17 exhibited limited associations with inflammatory markers. ROC analysis demonstrated moderate discriminatory performance for ADAM8 and ADAM10; however, these findings should be interpreted as exploratory due to the cross-sectional design and potential confounding factors.

Conclusion: Serum ADAM8 and ADAM10 levels were higher in clinically attack-free FMF patients than in healthy controls. In multivariable analyses adjusted for age, sex, body mass index, and smoking status, ADAM8 and ADAM10 remained independently associated with FMF, whereas ADAM17 did not. These findings should be interpreted cautiously and may reflect the chronic/subclinical inflammatory burden of FMF rather than disease-specific pathogenic mechanisms. Furthermore, larger longitudinal studies are needed.

Keywords: Familial Mediterranean fever, ADAM8, ADAM10, ADAM17, Autoinflammatory diseases, Inflammation

Received: Jan 14, 2026 **Accepted:** Apr 28, 2026 **Available Online:** Aug 25, 2026

INTRODUCTION

Familial Mediterranean Fever (FMF) is the most common monogenic autoinflammatory disease, caused by pathogenic variants in the *MEFV* gene and characterized by recurrent attacks of fever and serositis [1,2]. In the pathogenesis of the disease, dysregulation of inflammasome control due to mutant pyrin protein leads to caspase-1 activation and excessive release of proinflammatory cytokines, particularly interleukin-1 beta (IL-1β) [2-4]. This process results in intense neutrophil-mediated inflammatory attacks occurring in the absence of an infectious trigger [5].

Inflammatory responses driven by the IL-1β and IL-6 axes

have been shown to play a central role in FMF, both in terms of clinical manifestations and therapeutic response [6,7]. The efficacy of colchicine and IL-1 inhibitors further supports the pivotal role of these cytokine pathways in disease pathogenesis [8]. However, inflammation is shaped not only by cytokine production but also by proteolytic mechanisms that regulate cytokine shedding and bioavailability [9].

In this context, the ADAM (a disintegrin and metalloproteinase) family, which is responsible for the proteolytic cleavage of cell surface cytokines and receptors, plays an important regulatory role in the modulation of inflammatory responses [9,10]. In particular, ADAM8, ADAM10, and ADAM17 have been associated with several inflammatory processes relevant to FMF pathogenesis, including neutrophil activation, IL-6 trans-signaling, and tumor necrosis factor-alpha (TNF-α) release [11,12]. The ability of ADAM17 to activate IL-6 trans-signaling through cleavage of the IL-6 receptor, as well as the association of ADAM8 with neutrophil migration, supports the biological plausibility of a role for these proteases in FMF pathogenesis [11-13]. Given the attack-based, neutrophil-dominant, and IL-1β/IL-6-driven inflammatory nature of FMF, ADAM proteases capable of regulating these pathways may be associated with disease pathogenesis.

Nevertheless, clinical data regarding ADAM8, ADAM10, and ADAM17 levels in FMF patients are limited in the literature, and no study has evaluated these molecules collectively. Accordingly, it has been hypothesized that ADAM levels may be increased in FMF patients, and that this increase may be associated with disease activity. The present study aimed to compare serum ADAM8, ADAM10, and ADAM17 levels between clinically attack-free FMF patients and healthy controls, and to investigate their relationships with conventional inflammatory markers.

MATERIALS AND METHODS

Study design and participants

This study was conducted using a single-center, cross-sectional case–control design comparing patients with FMF (n=36) and healthy controls (n=36). In all FMF cases, sampling was performed during the clinically attack-free period; individuals who were asymptomatic at presentation and had not experienced an acute attack within at least the preceding two weeks were included [14]. Among FMF patients, the time elapsed since the last documented attack ranged from 20 days to 11 months at the time of blood sampling. We acknowledge that this criterion reflects clinical remission but does not necessarily indicate complete biological remission because low-grade inflammatory activity may persist between attacks. The primary rationale for excluding patients during overt attack periods was that acute inflammatory responses may be associated with transient elevations in inflammation-related biomarkers, which could hinder the assessment of persistent low-grade inflammatory activity. Accordingly, inclusion of clinically attack-free patients was methodologically preferable for evaluating whether circulating levels of ADAM8, ADAM10, and ADAM17 are associated with the chronic or subclinical inflammatory component of FMF. All FMF patients were receiving regular colchicine therapy, with doses ranging from 1 to 2 mg/day. The healthy control group was selected from volunteers who were matched to the patient group for age and sex. Based on a sensitivity analysis performed using G*Power (v3.1), the available sample size (total n=72; FMF=36, control=36) was calculated to be sufficient to detect at least moderate-to-large differences between the means of two independent groups (Cohen's d≈0.70) with 80% power at a two-sided α level of 0.05.

The study protocol was approved by the Non-Interventional Clinical Research Ethics Committee of Recep Tayyip Erdoğan University (Approval No: 2025/476, Date: 24.11.2025). Written informed consent was obtained from all participants prior to enrollment in the study.

Inclusion and exclusion criteria

The inclusion criteria for the study were a confirmed diagnosis of FMF according to the Tel Hashomer criteria (defined by the presence of either one major criterion or two minor criteria), including major clinical manifestations (recurrent febrile attacks, peritonitis, pleuritis, and arthritis) and minor features (incomplete attacks, exertional leg pain, and response to colchicine therapy), and the exclusion of other autoinflammatory diseases. In addition, participants were required to be aged between 18 and 65 years and to be in an attack-free period at the time of sampling. The exclusion criteria included the presence of active or chronic infection, malignancy, advanced hepatic or renal failure, and diabetes mellitus; pregnancy; and the use of systemic corticosteroids, immunosuppressive agents, or biological therapies—other than colchicine—that could affect biomarker levels [15,16].

Clinical data collection

Demographic data (age, sex), smoking and alcohol use, body mass index (BMI), symptoms (fever, abdominal–chest pain, arthritis), and colchicine dose (as recorded in the clinical files) were extracted from medical records using a standardized data collection form.

Blood sampling and pre-analytical procedures

Biochemical analyses were performed on an AU5800 automated analyzer (Beckman Coulter, Brea, CA, USA) in accordance with the manufacturer's procedures and the laboratory's routine internal quality control protocols. Acute-phase reactants C-reactive protein (CRP), serum amyloid A (SAA), and fibrinogen were measured using immunoturbidimetric methods. Following measurement, serum samples were stored at −80 °C until the day of analysis.

https://doi.org/10.5455/annalsmedres.2026.01.019

Measurement of serum ADAM8, ADAM10, and ADAM17

Serum levels of ADAM8 (E-EL-H0264), ADAM10 (E-EL-H0263), and ADAM17 (E-EL-H2305) were measured using commercially available ELISA kits according to the manufacturer's instructions (Elabscience, Houston, TX, USA). A standard curve based on polynomial regression was generated from the absorbance values of the standards, and sample concentrations were calculated from it.

Statistical analysis

All statistical analyses were performed using OriginPro 2025 (OriginLab Corp., Northampton, MA, USA). Data were tabulated and archived in Microsoft Excel (Microsoft Corp., Redmond, WA, USA). Normality of continuous variables was assessed using the Shapiro–Wilk test. Continuous data are presented as median (Q1–Q3) for non-normally distributed variables and as mean ± standard deviation for normally distributed variables, whereas categorical variables are summarized as frequency (percentage). Between-group comparisons (FMF vs healthy controls) were performed using the Mann–Whitney U test for non-normally distributed variables and the independent two-sample t-test for normally distributed variables. Categorical variables (sex, smoking, alcohol use, and genetic mutations) were compared using the Chi-square test. Associations between circulating ADAM8, ADAM10, and ADAM17 levels and clinical and laboratory parameters were evaluated using Spearman's rank correlation coefficient (ρ); correlation heatmaps were generated in OriginPro. To address potential confounding, multivariable binary logistic regression analyses were additionally performed, with FMF status as the dependent variable and each ADAM protein was entered into a separate model adjusted for age, sex, BMI, and smoking status. The diagnostic performance of ADAM proteins in discriminating FMF patients from healthy controls was assessed using receiver operating characteristic (ROC) curve analysis. The area under the curve (AUC) with 95% confidence intervals and p-values was reported, and optimal cut-off values were used to estimate sensitivity and specificity. All tests were two-tailed, and $p < .05$ was considered statistically significant. Given that three ADAM proteins were evaluated simultaneously, the potential for type I error from multiple comparisons is acknowledged. No formal correction was applied, and, accordingly, all findings should be interpreted as exploratory and hypothesis-generating rather than confirmatory.

RESULTS

Demographic and anthropometric characteristics of the study population and MEFV genotype distribution in FMF patients

Comparison of demographic characteristics between the FMF patient group (n=36) and the healthy control group (n=36) showed no statistically significant differences in age distribution ($p = .97$) or sex distribution ($p = .13$). Similarly, the groups were comparable with respect to smoking status ($p = .20$) and alcohol consumption ($p = 1.00$). Evaluation of anthropometric measurements revealed no significant differences between the groups in either height or body weight ($p > .05$). However, BMI analysis showed that the median BMI in the control group (27.58 kg/m^2) was significantly higher than that in the FMF group (24.86 kg/m^2) ($p = .03$). Detailed demographic and anthropometric data for the groups are presented in Table 1. Assessment of mutation distribution within the FMF group demonstrated that 66.7% of patients (n=24) carried a single heterozygous mutation, 30.6% (n=11) had a homozygous mutation, and 2.8% (n=1) had a compound heterozygous mutation. The detailed distribution of the genetic analysis results is also shown in Table 1.

Comparison of acute-phase reactants between study groups

Comparison of acute-phase reactant levels between the study groups revealed CRP, SAA, and fibrinogen levels ($p < .05$ for all). In the FMF patient group, median levels of CRP (9.89 mg/dL), SAA (17.3 mg/L), and fibrinogen (313 mg/dL) were significantly higher than those in the healthy control group (1.69 mg/dL, 9.48 mg/L, and 270 mg/dL, respectively) ($p < .001$, $p = .004$, and $p = .006$). A detailed comparison of acute-phase reactants is presented in Table 2.

Comparison of circulating ADAM8, ADAM10, and ADAM17 levels between FMF and control groups

In the FMF patient group, circulating ADAM8 and ADAM10 levels were significantly higher than in the healthy control group, whereas no significant difference in ADAM17 levels was observed between the groups. For ADAM8, the median (Q1–Q3) level was 2567.18 (2064.26–3214.93) pg/mL in the FMF group and 1938.10 (1598.63–2470.46) pg/mL in the control group; this difference was statistically significant (Mann–Whitney U test, $p < .001$).

Because the Shapiro–Wilk test for ADAM10 did not indicate a significant deviation from normality, an independent two-sample t-test was used. Mean ± standard deviation values were 6291.37 ± 3828.30 pg/mL in the FMF group and 3312.68 ± 1950.23 pg/mL in the control group, and the between-group difference was statistically significant ($p < 0.001$). To further summarize the distribution of this parameter, median (Q1–Q3) values were calculated 3114.54 (1732.85–4527.07) pg/mL in the control group and 6115.46 (3495.34–8663.67) pg/mL in the FMF group.

In contrast, for ADAM17, the median (Q1–Q3) level was 278.05 (232.81–364.31) pg/mL in the FMF group and 270.07 (239.53–322.24) pg/mL in the control group, and this difference was not statistically significant (Mann–Whitney U test, $p = .74$) (Figure 1).

Multivariable binary logistic regression analyses

To further evaluate whether the associations of serum ADAM8, ADAM10, and ADAM17 with FMF were inde-

https://doi.org/10.5455/annalsmedres.2026.01.019

Table 1. Demographic and anthropometric characteristics of the study population and *MEFV* mutation distribution in the FMF group.

Parameters	Control (n=36) Median (Q1-Q3)	FMF (n=36) Median (Q1-Q3)	p *Chi-Square †Mann-Whitney U
Age (years)	31.5 (25.5-37.75)	32 (25.5-43.75)	†p > .05
Sex [female (n) / male (n)]	28/8	22/14	*p > .05
Smoking [yes (n) / no (n)]	23/13	28/8	*p > .05
Alcohol consumption [yes (n) / no (n)]	2/34	3/33	*p > .05
Weight (kg)	77.5 (71.25-84)	71.5 (55.75-84.5)	†p > .05
Height (cm)	163.5 (160.25-169.75)	167.5 (160.25-170.75)	†p > .05
BMI (kg/m²)	27.5 (25.7-30.4)	24.6 (20.5-30.09)	†p = .03
Genetic Mutations (MEFV)			
Single heterozygous mutation		24 (66.7 %)	
Homozygous mutation		11 (30.6 %)	
Compound heterozygous mutation		1 (2.8 %)	

BMI: body mass index. *MEFV:* Mediterranean fever (pyrin) gene.

Table 2. Comparison of acute-phase reactants between familial Mediterranean fever patients and healthy controls.

Parameters	Control (n=36) Median (Q1-Q3)	FMF (n=36) Median (Q1-Q3)	p †Mann-Whitney U
CRP (mg/dL)	1.68 (0.86-4.15)	9.88 (2.1-13.9)	†p < .001
Fibrinogen (mg/dL)	270 (230.25-320.75)	313 (263.5-362.25)	†p = .006
SAA (mg/L)	9.4 (5.9-12.6)	17.3 (8.52-27.5)	†p = .004

CRP: C-reactive protein; SAA: serum amyloid A.

Table 3. Multivariable binary logistic regression analyses assessing the association of serum ADAM8, ADAM10, and ADAM17 levels with FMF status.

	ADAM8 aOR (95% CI)	p value	ADAM10 aOR (95% CI)	p value	ADAM17 aOR (95% CI)	p value
ADAM biomarker	1.16 (1.05--1.28)	0.003	1.05 (1.02--1.08)	<0.001	1.05 (0.89--1.24)	.561
Age	1.08 (1.00--1.16)	0.065	1.05 (0.96--1.14)	0.323	1.05 (0.98--1.13)	.150
Male sex	3.39 (0.81--14.12)	0.093	8.27 (1.58--43.43)	0.013	3.81 (0.98--14.78)	.053
Body mass index	0.88 (0.76--1.01)	0.064	0.80 (0.66--0.95)	0.013	0.88 (0.76--1.00)	.053
Smoking	0.44 (0.11--1.79)	0.249	0.16 (0.03--0.83)	0.029	0.26 (0.07--1.00)	.049

FMF status was entered as the dependent variable (control = 0, FMF = 1). Model 1 included ADAM8, age, sex, body mass index, and smoking status; Model 2 included ADAM10, age, sex, body mass index, and smoking status; and Model 3 included ADAM17, age, sex, body mass index, and smoking status. Sex was coded as female = 0 and male = 1, and smoking status as absent = 0 and present = 1. For interpretability, odds ratios for ADAM8, ADAM10, and ADAM17 are presented per 100 pg/mL increase. aOR, adjusted odds ratio; CI, confidence interval.

pendent of potential confounding factors, multivariable binary logistic regression analyses were performed, with FMF status as the dependent variable and age, sex, BMI, and smoking status included as covariates. As presented in Table 3, higher serum ADAM8 and ADAM10 levels remained independently associated with FMF, whereas ADAM17 did not. When expressed per 100 pg/mL increase, the adjusted odds ratios were 1.16 (95% CI 1.05–1.28; p = .003) for ADAM8, 1.05 (95% CI 1.02–1.08; p< .001) for ADAM10, and 1.05 (95% CI 0.89–1.24; p = .561) for ADAM17. The complete model results for each covariate are shown in Supplementary Table S1.

Spearman correlation analyses: Whole-cohort and FMF-restricted results

When Spearman's rank correlation analysis (two-tailed) was performed across all participants (n=72), significant positive correlations were identified between age and BMI (ρ = 0.415, p< .001), CRP (ρ = 0.387, p< .001), and fibrinogen levels (ρ = 0.265, p= .024). In contrast, no significant correlations were observed between age and levels of SAA, ADAM8, ADAM10, or ADAM17 (p> .05 for all). Regarding interrelationships among inflammatory parameters, CRP levels showed positive correlations with SAA (ρ = 0.374) and fibrinogen (ρ = 0.311), and a weak-to-moderate positive correlation with ADAM10 (ρ = 0.240) (p< .05; Figure 2). Fibrinogen levels were positively correlated with SAA (ρ = 0.264) and showed significant positive correlations with ADAM10 (ρ = 0.344) and ADAM17 (ρ = 0.265) among the ADAM proteins (p< .05; Figure 2). Regarding ADAM proteins, ADAM10 levels were positively correlated with ADAM8 levels (ρ = 0.286; p < .05), whereas ADAM17 correlated significantly only with fibrinogen. ADAM8 levels did not show significant associations with other clinical or laboratory parameters, with the exception of ADAM10 (Figure 2).

When the correlation analysis was restricted to the FMF

https://doi.org/10.5455/annalsmedres.2026.01.019

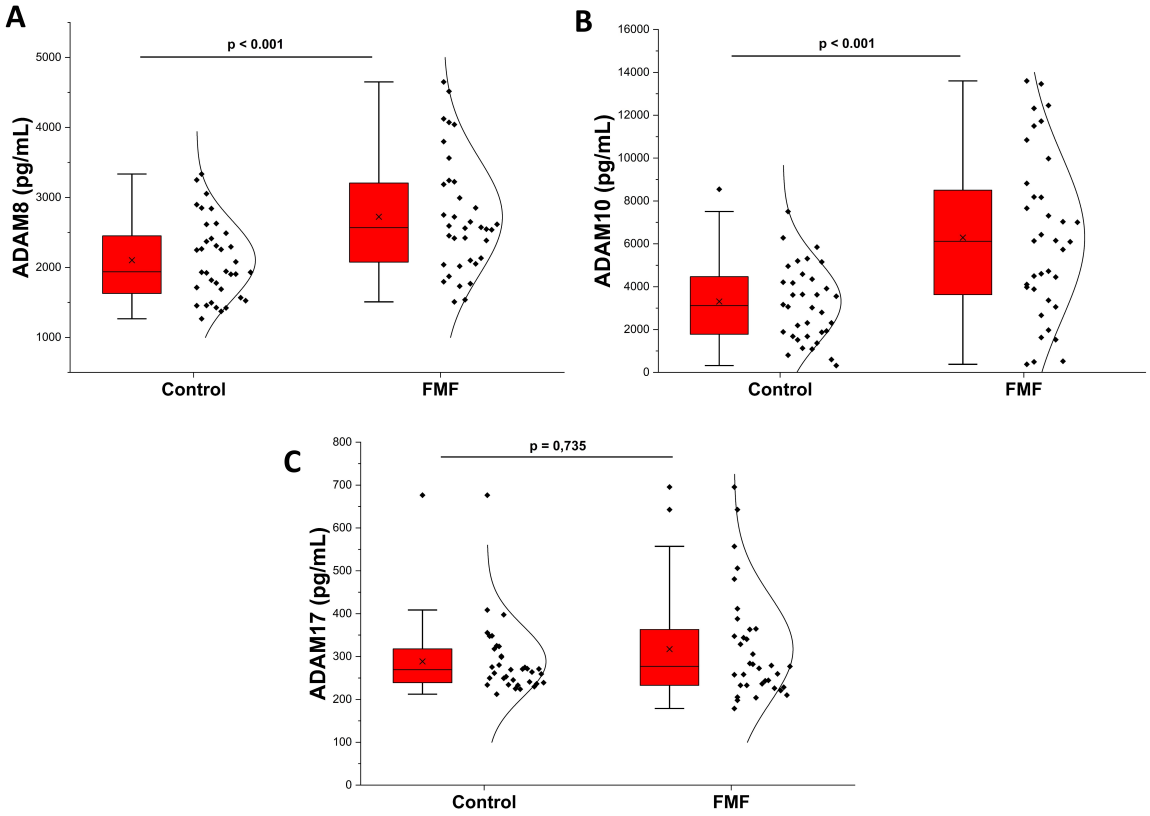

Figure 1. Circulating ADAM8, ADAM10, and ADAM17 levels in FMF patients versus healthy controls. (A) ADAM8, (B) ADAM10, and (C) ADAM17 concentrations (pg/mL) are shown for the FMF group (n=36) and the healthy control group (n=36). Data are presented as violin plots overlaid with box-and-whisker plots and individual data points. The box denotes the interquartile range (Q1--Q3), the horizontal line inside the box indicates the median, and the "×" symbol represents the mean; whiskers indicate the data spread (min--max). Between-group comparisons were performed using two-sided tests according to distributional assumptions: the Mann--Whitney U test for ADAM8 and ADAM17, and the independent two-sample t-test for ADAM10, for which Shapiro--Wilk testing did not indicate a significant deviation from normality. P values are displayed above each panel (A and B: p<0.001; C: p=0.74). Statistical significance was set at p<0.05. FMF: Familial Mediterranean Fever; ADAM: a disintegrin and metalloprotease.

group alone (n=36), the pattern of associations differed notably from that observed across the entire cohort. Age remained positively correlated with BMI (ρ = 0.606, p< .001), whereas its previously significant associations with CRP and fibrinogen were no longer statistically significant (p> .05 for both). Within the FMF group, no significant intercorrelations were identified among CRP, SAA, and fibrinogen (p> .05 for all). None of the ADAM proteins demonstrated significant associations with CRP or SAA. The only statistically significant ADAM-related association within the FMF group was between ADAM17 and fibrinogen (ρ = 0.383, p = .021). Notably, the previously observed correlations of ADAM10 with CRP, fibrinogen, and ADAM8 across the full cohort were not replicated in this subgroup analysis. Additionally, BMI showed a significant positive correlation with ADAM10 within the FMF group (ρ = 0.394, p = .018), which was not observed in the full-cohort analysis. The FMF-group correlation heatmap is presented in Supplementary Figure S1. These subgroup findings should be interpreted with caution, given the reduced statistical power (n=36) and the exploratory nature of the analysis.

Diagnostic performance of ADAMs in distinguishing FMF and controls

The diagnostic performance of circulating ADAM proteins in discriminating between FMF patients and healthy controls was evaluated using ROC curve analysis. For ADAM8, the AUC was 0.728 (standard error = 0.059; 95% confidence interval: 0.613–0.844), indicating statistically significant discriminatory performance (p< .001). Similarly, for ADAM10, the AUC was 0.738 (standard error = 0.060; 95% confidence interval: 0.620–0.857), and this performance was statistically significant (p< .001). In contrast, the discriminatory ability of ADAM17 was not statistically significant (AUC 0.524; 95% confidence interval: 0.386–0.661; p = .73).

Based on the optimal cut-off values derived from this dataset, thresholds of 2415.28 pg/mL for ADAM8 and 5524.09 pg/mL for ADAM10 yielded sensitivities of 66.7% and 55.6% and specificities of 75.0% and 88.9%, respectively (Figure 3). These cut-offs were determined within the present sample and should be considered exploratory; they are not intended for direct clinical implementation without independent replication and validation in larger, BMI-matched cohorts (Figure 3).

https://doi.org/10.5455/annalsmedres.2026.01.019

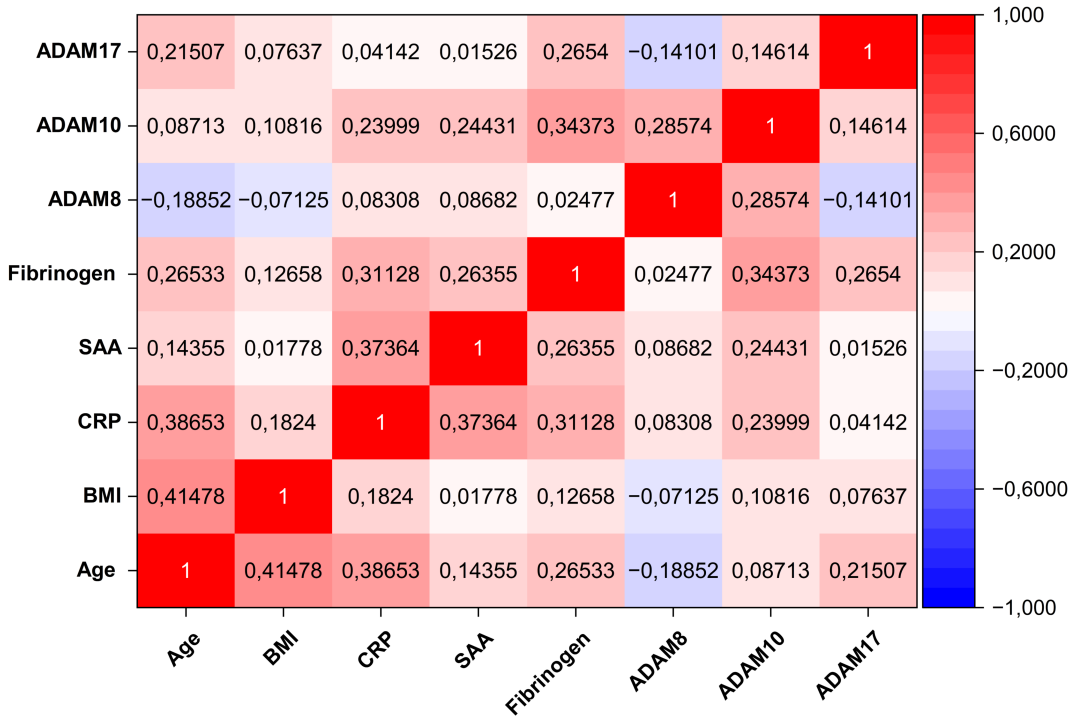

Figure 2. Spearman correlation matrix of demographic variables, acute-phase reactants, and circulating ADAM levels (n=72). The heatmap summarizes Spearman's rank correlation coefficients (ρ) for age, body mass index, C-reactive protein, serum amyloid A, fibrinogen, and circulating ADAM8, ADAM10, and ADAM17 levels. Abbreviations: BMI, body mass index; CRP, C-reactive protein; SAA, serum amyloid A; ADAM, a disintegrin and metalloprotease.

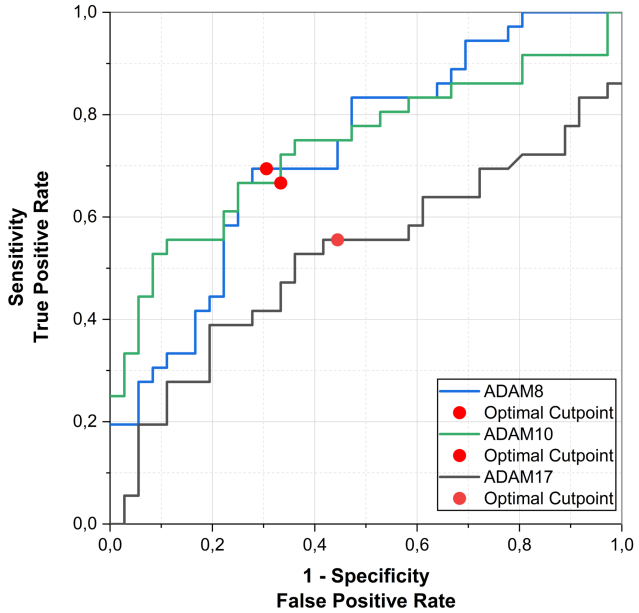

Figure 3. Receiver operating characteristic (ROC) curves of circulating ADAM8, ADAM10, and ADAM17 for discrimination of FMF patients from healthy controls. ROC curves were generated using ADAM8, ADAM10, and ADAM17 concentrations, with FMF defined as the positive state (n=36) and healthy controls as the negative state (n=36). AUC values are presented with standard errors, 95% confidence intervals, and p values. Optimal cut-off values and their corresponding sensitivity and specificity are reported in the text.

DISCUSSION

In this study, circulating levels of ADAM8, ADAM10, and ADAM17 were compared between clinically attack-free FMF patients and healthy controls, and the relationships between these molecules and conventional inflammatory markers were evaluated. Our findings demonstrated that levels of ADAM8 and ADAM10 were significantly increased in clinically attack-free FMF patients, while ADAM17 levels remained unchanged. Importantly, in multivariable binary logistic regression analyses adjusted for age, sex, BMI, and smoking status, ADAM8 and ADAM10 remained independently associated with FMF, whereas ADAM17 did not. Although these results suggest that certain metalloproteinases of the ADAM family may be associated with the inflammatory milieu present in FMF, the cross-sectional design and serum-based measurement approach preclude causal inference or the interpretation of these associations as disease-specific pathophysiological mechanisms. Instead, the observed elevations—together with the significantly higher acute-phase reactants in the FMF group—are more consistent with circulating reflections of intercritical or subclinical inflammatory burden rather than with a direct mechanistic signature. In this context, the present data provide complementary and descriptive information regarding the inflammatory biological background of FMF rather than propose a novel pathogenic mechanism.

Metalloproteinases of the ADAM family contribute to

https://doi.org/10.5455/annalsmedres.2026.01.019

the shaping of inflammatory responses by regulating the ectodomain shedding of numerous cell surface proteins, including cytokines, cytokine receptors, and adhesion molecules [17-19]. The core of FMF pathogenesis involves increased IL-1 release as a result of excessive activation of the pyrin inflammasome, accompanied by neutrophil-dominant systemic inflammation [16,20-22]. Within this framework, the observed increases in ADAM8 and ADAM10 levels in clinically attack-free FMF patients appear more consistent with being circulating reflections of intercritical (chronic/subclinical) inflammatory activity rather than indicators of FMF-specific pathological pathways. Notably, acute-phase reactants were significantly higher in the FMF group, supporting the view that a biochemical inflammatory signal may persist even in the absence of overt clinical attacks.

ADAM8 is a metalloproteinase that is highly expressed in neutrophils and monocytes and plays a role in regulating cell migration and inflammatory tissue responses [23,24]. Increased ADAM8 expression has previously been reported to be associated with activated inflammatory cell responses in autoinflammatory and rheumatologic diseases [12,24]. Given that FMF attacks are characterized by prominent neutrophil-driven inflammation, the persistence of elevated ADAM8 levels even during attack-free periods in our study may be considered biologically plausible. However, the absence of significant correlations between ADAM8 and classical inflammatory markers such as CRP, SAA, and fibrinogen indicates that ADAM8 may not behave as a simple surrogate for the acute-phase response. Rather than excluding biomarker potential, this pattern may suggest that ADAM8 captures a distinct biological dimension of inflammation—particularly neutrophil-related activation or priming—that is not fully represented by conventional systemic markers. Therefore, increased ADAM8 levels may reflect specific aspects of inflammatory cell activation that can persist even when classical acute-phase reactants show limited dynamic range.

ADAM10 is known to play a role in immune system regulation, particularly through Notch signaling–mediated cell–cell interactions and modulation of inflammatory responses [25,26]. The significantly elevated ADAM10 levels observed in FMF patients, together with weak-to-moderate positive correlations with CRP and fibrinogen, suggest that ADAM10 may vary in parallel with inflammatory burden. However, the modest correlation coefficients indicate that ADAM10 is unlikely to be a simple surrogate for the acute-phase response; rather, it may capture additional biological processes that partially overlap with systemic inflammation (e.g., endothelial activation or shedding-related pathways). Accordingly, ADAM10 should be interpreted as a complementary marker reflecting the broader inflammatory environment, not as a standalone indicator of severity. Nevertheless, the relatively modest correlation coefficients and the cross-sectional nature of the study preclude interpreting ADAM10 as a causal or driving mechanism in FMF pathogenesis. Accordingly, the increase in ADAM10 should be regarded as a biochemical reflection of inflammation rather than as direct evidence of a fundamental disease mechanism.

ADAM17 is a key sheddase responsible for the proteolytic release of various transmembrane cytokines and receptors, most notably TNF-α, and plays an important role in inflammatory processes [10,27]. Although the IL-1β axis is central to FMF pathogenesis, TNF-α levels have also been reported to increase, particularly during periods of active inflammation [5,6]. Despite this, no significant difference in ADAM17 levels was observed between FMF patients and healthy controls. From a pathophysiological standpoint, this finding may be biologically plausible: FMF is predominantly driven by the IL-1β/pyrin inflammasome axis, and TNF-related pathways appear to play a comparatively subordinate role in disease pathogenesis [2,4,16]. Unlike TNF-dominant autoinflammatory or autoimmune conditions in which ADAM17-mediated shedding is expected to be more pronounced, the IL-1 central inflammatory milieu of FMF may not sufficiently engage ADAM17 at a systemic level, particularly during intercritical periods [5,6]. Furthermore, colchicine therapy, which attenuates neutrophil-mediated inflammation, may additionally dampen ADAM17 activity in treated patients, potentially narrowing any between-group differences [16]. This finding should be interpreted with caution because the control group had a significantly higher BMI than the FMF group (Table 1), and BMI-related low-grade inflammation may influence circulating inflammatory mediators. To address this issue, we performed multivariable binary logistic regression analyses adjusted for age, sex, BMI, and smoking status. In these analyses, ADAM17 was not independently associated with FMF. Nevertheless, residual confounding cannot be fully excluded. In this context, the absence of a systemic difference does not necessarily rule out a role for ADAM17 in FMF; rather, ADAM17-related effects may be context-dependent, potentially varying according to local tissue environments or specific clinical or genetic subgroups.

Finally, the positive but limited associations observed between ADAM proteins and conventional inflammatory markers indicate that these molecules may, to some extent, parallel the acute-phase response but should not be considered independent indicators that directly reflect the severity of inflammation. These findings support a cautious approach and underscore the need to avoid overinterpretation of the results. Overall, our study provides descriptive, methodologically balanced data on the relationship between ADAM family metalloproteinases and the inflammatory environment in FMF and establishes a conceptual framework for future studies, particularly longitudinal and tissue-level investigations.

Limitations and recommendations

This study has several important limitations. First, the relatively small sample size and the single-center, cross-sectional design limit the generalizability of the findings. Owing to

https://doi.org/10.5455/annalsmedres.2026.01.019

the cross-sectional nature of the study, temporal changes in ADAM levels, dynamics before and after attacks, and causal relationships could not be assessed. In addition, only serum ADAM levels were measured; tissue expression, cellular sources, and analyses of functional activity were not performed, thereby limiting comprehensive understanding of the biological roles of ADAM proteins.

Second, although demographic characteristics were largely comparable, the control group had a significantly higher BMI than the FMF group (Table 1). This difference may have acted as a confounding factor, particularly for molecules potentially influenced by metabolic or adiposity-related inflammatory signals. To address this issue, we performed multivariable binary logistic regression analyses adjusted for age, sex, BMI, and smoking status. In these adjusted models, the associations of ADAM8 and ADAM10 with FMF remained statistically significant, whereas ADAM17 did not. Nevertheless, residual confounding cannot be fully excluded.

Third, all FMF patients were receiving colchicine therapy, making it difficult to distinguish treatment-related modulatory effects from disease-related alterations in inflammatory responses and ADAM levels. Furthermore, although daily colchicine doses ranged from 1 to 2 mg/day across the cohort, the limited variability within this clinically guided dose range precluded a meaningful exploratory analysis of dose–biomarker relationships; this constitutes an additional methodological limitation of the present study. In addition, standardized disease activity indices, such as AIDAI or ISSF, were not available in this cohort, thereby limiting more detailed clinical characterization of disease activity during the attack-free period. Similarly, detailed stratified analyses by variables such as *MEFV* genotype, disease duration, and subclinical inflammation duration could not be performed. Therefore, future studies should adopt larger, multicenter, prospective designs, include BMI-matched and externally validated analyses, incorporate genotype-stratified approaches, and evaluate both attack and intercritical periods, ideally together with tissue-level assessments. Additionally, ROC-derived cut-off values were estimated within the present dataset and were not externally validated; thus, they should be interpreted as exploratory and not directly transferable to clinical decision-making.

CONCLUSION

In conclusion, serum ADAM8 and ADAM10 levels were higher in clinically attack-free FMF patients than those in healthy controls, whereas ADAM17 levels did not differ significantly between the groups. In multivariable analyses adjusted for age, sex, BMI, and smoking status, ADAM8 and ADAM10 remained independently associated with FMF, whereas ADAM17 did not. Nevertheless, these findings should be interpreted cautiously in view of the cross-sectional design, limited sample size, universal colchicine exposure, lack of standardized disease activity indices, genotype heterogeneity, and the possibility of residual confounding. Accordingly, the present results should be considered descriptive and hypothesis-generating rather than directly diagnostic or mechanistic. In this context, the observed alterations in ADAM protein levels may be more appropriately interpreted as circulating reflections of the systemic inflammatory burden present in FMF. Further, larger, longitudinal, externally validated, and mechanistic studies are needed to clarify the biological and clinical relevance of ADAM family proteins in FMF.

Acknowledgements: We thank Recep Tayyip Erdoğan University and Karadeniz Technical University for providing access to academic databases that support access to scientific literature.

Ethics Committee Approval: Recep Tayyip Erdoğan University Non-Interventional Clinical Research Ethics Committee (Approval No: 2025/476, Date: 24.11.2025).

Informed Consent: Written informed consent was obtained from all participants prior to enrollment in the study.

Peer-review: Externally peer-reviewed.

Conflict of Interest: None of the authors has a potential conflict of interest that must be disclosed.

Author Contributions: Conceptualization: E.Y., M.H.Y., and O.C.; Data curation: E.Y., M.H.Y., and O.C.; Formal analysis: E.Y., H.C.Z.; Investigation: E.Y. and H.C.Z.; Methodology: E.Y., M.A., and M.H.Y.; Software: E.Y.; Visualization: M.H.Y.; Project Administration: O.C.; Writing – original draft: E.Y.; Writing – review & editing: M.H.Y., H.C.Z.; and M.A.

Financial Disclosure: This study was not supported by any institution.

Data Availability Statement: The original contributions presented in this study are included in the article; further inquiries can be directed to the corresponding author.

Artificial Intelligence Disclosure: The authors used ChatGPT-4.5 (OpenAI) only for language editing, grammar correction, and improvement of the clarity and readability of the manuscript. Artificial intelligence tools were not used for study design, data collection, statistical analysis, data interpretation, literature interpretation, generation of scientific conclusions, or preparation of original scientific content. All AI-assisted language edits were critically reviewed, verified, and approved by the authors.

REFERENCES

1. Lancieri M, Bustaffa M, Palmeri S, et al. An Update on Familial Mediterranean Fever. *Int J Mol Sci.* 2023;24(11):9584. doi: 10.3390/ijms24119584.
2. Wouters F, Bogie J, Wullaert A, van der Hilst J. Recent Insights in Pyrin Inflammasome Activation: Identifying Potential Novel Therapeutic Approaches in Pyrin-Associated Autoinflammatory Syndromes. *J Clin Immunol.* 2023;44(1):8. doi: 10.1007/s10875-023-01621-5.

https://doi.org/10.5455/annalsmedres.2026.01.019

3. An J, Marwaha A, Laxer RM. Autoinflammatory Diseases: A Review. *J Rheumatol.* 2024;51(9):848-861. doi: 10.3899/jrheum.2023-1209.
4. Migita K, Izumi Y, Fujikawa K, et al. Dysregulated mature IL-1β production in familial Mediterranean fever. *Rheumatology (Oxford).* 2015;54(4):660-665. doi: 10.1093/rheumatology/keu359.
5. Romano M, Piskin D, Kul Cinar O, Sag E. Familial Mediterranean Fever; Recent Advances, Future Prospectives. *Diagnostics (Basel).* 2025;15(7):813. doi: 10.3390/diagnostics15070813.
6. Chaaban A, Yassine H, Hammoud R, et al. A narrative review on the role of cytokines in the pathogenesis and treatment of familial Mediterranean fever: an emphasis on pediatric cases. *Front Pediatr.* 2024;12:1421353. doi: 10.3389/fped.2024.1421353.
7. Hizal M, Tufan A, Mercan R, et al. Interleukin-21 and Interleukin-23 levels in familial Mediterranean Fever before and after treatment: the role of cytokines in disease pathogenesis. *Sci Rep.* 2024;14(1):21351. doi: 10.1038/s41598-024-72736-x.
8. Kilic B, Guler Y, Azman FN, Bostanci E, Ugurlu S. Efficacy and safety of anti-interleukin-1 treatment in familial Mediterranean fever patients: a systematic review and meta-analysis. *Rheumatology (Oxford).* 2024;63(4):925-935. doi: 10.1093/rheumatology/kead514.
9. Lambrecht BN, Vanderkerken M, Hammad H. The emerging role of ADAM metalloproteinases in immunity. *Nat Rev Immunol.* 2018;18(12):745-758. doi: 10.1038/s41577-018-0068-5.
10. Sisto M, Lisi S. Updates on Inflammatory Molecular Pathways Mediated by ADAM17 in Autoimmunity. *Cells.* 2024;13(24):2092. doi: 10.3390/cells13242092.
11. Schumacher N, Rose-John S. ADAM17 Activity and IL-6 Trans-Signaling in Inflammation and Cancer. *Cancers (Basel).* 2019;11(11):1736. doi: 10.3390/cancers11111736.
12. Cook L, Gharzia FG, Bartsch JW, Yildiz D. A jack of all trades - ADAM8 as a signaling hub in inflammation and cancer. *FEBS J.* 2024;291(18):3989-4008. doi: 10.1111/febs.17034.
13. Gómez-Gaviro M, Domínguez-Luis M, Canchado J, et al. Expression and regulation of the metalloproteinase ADAM-8 during human neutrophil pathophysiological activation and its catalytic activity on L-selectin shedding. *J Immunol.* 2007;178(12):8053-8063. doi: 10.4049/jimmunol.178.12.8053.
14. Parmaksız G, Noyan ZA. Can RDW be used as a screening test for subclinical inflammation in children with FMF? Is RDW related to *MEFV* gene mutations?. *Clin Rheumatol.* 2023;42(1):197-202. doi: 10.1007/s10067-022-06358-x.
15. Livneh A, Langevitz P, Zemer D, et al. Criteria for the diagnosis of familial Mediterranean fever. *Arthritis Rheum.* 1997;40(10):1879-1885. doi: 10.1002/art.1780401023.
16. Ozen S, Demirkaya E, Erer B, et al. EULAR recommendations for the management of familial Mediterranean fever. *Ann Rheum Dis.* 2016;75(4):644-651. doi: 10.1136/annrheumdis-2015-208690.
17. Snyder KM, McAloney CA, Montel JS, Modiano JF, Walcheck B. Ectodomain shedding by ADAM17 (a disintegrin and metalloproteinase 17) in canine neutrophils. *Vet Immunol Immunopathol.* 2021;231:110162. doi: 10.1016/j.vetimm.2020.110162.
18. Zhong S, Khalil RA. A Disintegrin and Metalloproteinase (ADAM) and ADAM with thrombospondin motifs (ADAMTS) family in vascular biology and disease. Biochem Pharmacol. 2019;164:188-204. doi: 10.1016/j.bcp.2019.03.033.
19. Kirschke S, Ogunsulire I, Selvakumar B, et al. The metalloprotease ADAM10 generates soluble interleukin-2 receptor alpha (sCD25) in vivo. *J Biol Chem.* 2022;298(6):101910. doi: 10.1016/j.jbc.2022.101910.
20. Dinarello CA. Interleukin-1 in the pathogenesis and treatment of inflammatory diseases. *Blood.* 2011;117(14):3720-3732. doi: 10.1182/blood-2010-07-273417.
21. Park YH, Wood G, Kastner DL, Chae JJ. Pyrin inflammasome activation and RhoA signaling in the autoinflammatory diseases FMF and HIDS. *Nat Immunol.* 2016;17(8):914-921. doi: 10.1038/ni.3457.
22. Van Gorp H, Van Opdenbosch N, Lamkanfi M. Inflammasome-Dependent Cytokines at the Crossroads of Health and Autoinflammatory Disease. *Cold Spring Harb Perspect Biol.* 2019;11(1):a028563. doi: 10.1101/cshperspect.a028563.
23. Edwards DR, Handsley MM, Pennington CJ. The ADAM metalloproteinases. *Mol Aspects Med.* 2008;29(5):258-289. doi: 10.1016/j.mam.2008.08.001.
24. Conrad C, Yildiz D, Cleary SJ, et al. ADAM8 signaling drives neutrophil migration and ARDS severity. *JCI Insight.* 2022;7(3):e149870. doi: 10.1172/jci.insight.149870.
25. Smith TM Jr, Tharakan A, Martin RK. Targeting ADAM10 in Cancer and Autoimmunity. *Front Immunol.* 2020;11:499. doi: 10.3389/fimmu.2020.00499.
26. Rosenbaum D, Saftig P. New insights into the function and pathophysiology of the ectodomain sheddase A Disintegrin And Metalloproteinase 10 (ADAM10). *FEBS J.* 2024;291(13):2733-2766. doi: 10.1111/febs.16870.
27. de Queiroz TM, Lakkappa N, Lazartigues E. ADAM17-Mediated Shedding of Inflammatory Cytokines in Hypertension. *Front Pharmacol.* 2020;11:1154. doi: 10.3389/fphar.2020.01154.

Ann Med Res

Current issue list available at Ann Med Res

Annals of Medical Research

journal page: annalsmedres.org

Retrospective analysis of factors associated with mortality in acute mesenteric ischemia

Sedat Carkit[a], *, Mustafa Karaagac[a]

[a]*Erciyes University, Faculty of Medicine, Department of General Surgery, Kayseri, Türkiye*
**Corresponding author: opdrsedatcarkit@gmail.com (Sedat Carkit)*

MAIN POINTS

- In this single-center, 20-year retrospective cohort of patients undergoing emergency surgery for acute mesenteric ischemia (n=118), the 30-day mortality rate was 76.3%.
- Delayed presentation was common, underscoring the need for earlier recognition and timely surgical intervention.
- Massive intestinal necrosis identified at laparotomy was associated with a marked increase in mortality, underscoring the importance of diagnosis before irreversible ischemia develops.
- Older age and leukocyte count alterations emerged as practical clinical indicators that may aid prognostic assessment at initial presentation.

Cite this article as: Carkit S, Karaagac M. Retrospective analysis of factors associated with mortality in acute mesenteric ischemia. *Ann Med Res*. 2026;33(8):418–425. doi: 10.5455/annalsmedres.2026.01.015.

ABSTRACT

Aim: Acute mesenteric ischemia (AMI) remains one of the most lethal surgical emergencies, with persistently high mortality despite advances in diagnostic imaging and surgical management. Identification of factors associated with early mortality may improve risk stratification and clinical decision-making.

Materials and Methods: This single-center, retrospective observational study included adult patients who underwent emergency surgery for AMI over a 20-year period. Demographic characteristics, presenting symptoms, time to hospital admission, comorbidities, physical examination findings, leukocyte count, and intraoperative findings were analyzed. The primary outcome was 30-day mortality. Survivors and non-survivors were compared using univariate statistical analyses.

Results: A total of 118 patients were included, with a mean age of 64.9 ± 12.5 years; 60.2% were male. The overall 30-day mortality rate was 76.3%. Non-survivors were significantly older than survivors (66.4 ± 12.2 vs. 60.1 ± 12.4 years, p = 0.019). Delayed presentation was strongly associated with mortality: 25.0% of survivors presented within 12 hours compared with 4.4% of non-survivors, whereas presentation after 24 hours was more frequent among non-survivors (82.2% vs. 53.6%, p = 0.002). Leukocyte count categories were significantly associated with mortality (p = 0.034). The presence of massive intestinal necrosis was the strongest predictor of death, identified in 70.0% of non-survivors versus 21.4% of survivors (p < 0.001). Presenting symptoms, physical examination findings, atrial fibrillation, and comorbidity status were not significantly associated with mortality.

Conclusion: Mortality in acute mesenteric ischemia remains exceedingly high and is primarily determined by delayed presentation and the extent of intestinal ischemia. Early diagnosis, prompt surgical intervention, and aggressive management are essential to improving outcomes in this devastating condition.

Keywords: Acute mesenteric ischemia, Mortality risk factors, Intestinal ischemia, Surgical outcomes

Received: Jan 22, 2026 **Accepted:** Jun 08, 2026 **Available Online:** Aug 25, 2026

INTRODUCTION

Acute mesenteric ischemia remains one of the most devastating surgical emergencies affecting the gastrointestinal tract, continuing to carry exceedingly high mortality despite advances in early recognition and timely intervention [1]. The condition arises from an abrupt or progressive reduction in mesenteric blood flow, which may rapidly evolve into intestinal ischemia and transmural necrosis [2]. When diagnosis is delayed, irreversible bowel injury frequently ensues, often compounded by sepsis and multiple organ dysfunction [1]. Given that the clinical course typically begins with nonspecific symptoms, substantial diagnostic delays remain prevalent, particularly among elderly patients and those with significant comorbidities [3].

The etiology of acute mesenteric ischemia is heterogeneous, encompassing distinct pathophysiologic mechanisms including embolic and thrombotic arterial occlusion, nonocclusive mesenteric ischemia, and mesenteric venous thrombosis [4]. This etiologic diversity contributes to considerable variability in clinical presentation and complicates early differentiation

from other causes of acute abdominal pain [5]. Although abdominal pain constitutes the most frequently reported symptom, the classic disproportion between pain severity and physical examination findings is well established as a major source of diagnostic uncertainty [5]. As a consequence, the diagnosis may be overlooked or confirmed only after clinical deterioration, particularly in patients whose initial examination appears deceptively benign [6].

Reported mortality rates for acute mesenteric ischemia range from approximately 50% to 80% [7]. Factors consistently implicated in adverse outcomes include advanced age, delayed hospital presentation, underlying cardiovascular disease, atrial fibrillation, sepsis, metabolic acidosis, and extensive intestinal necrosis [1]. Nevertheless, the relative contribution of these variables and their practical utility for prognostication remain incompletely characterized. In particular, studies comprehensively evaluating the combined impact of presentation timing, physical examination findings, laboratory parameters, and intraoperative observations on mortality within a single, surgically confirmed cohort are notably limited.

Furthermore, existing evidence remains heterogeneous with respect to patient selection, diagnostic pathways, and the spectrum of variables examined; many studies emphasize etiologic classification or advanced laboratory and physiologic markers rather than bedside-applicable parameters obtainable during the initial evaluation. Consequently, the combined prognostic contribution of the timing of presentation, routine clinical findings, simple laboratory stratification (e.g., leukocyte strata), and intraoperative extent of ischemia in a single surgically confirmed AMI cohort remains insufficiently characterized. Defining which readily obtainable clinical and operative features are associated with early mortality in real-world emergency surgical practice may assist clinicians in prioritizing diagnostic escalation and timely operative decision-making [1,6].

Accurate prognostic assessment in acute mesenteric ischemia is critical not only for surgical decision-making but also for counseling patients and their families [8]. Enhanced characterization of clinical and operative markers associated with mortality may facilitate earlier identification of high-risk individuals and support more aggressive diagnostic and therapeutic strategies [9]. In this context, systematic analyses of retrospective clinical data provide an important opportunity to generate real-world evidence that reflects routine practice.

Accordingly, the present study aimed primarily to evaluate associations between routinely available clinical, laboratory, and intraoperative variables and 30-day mortality among adults undergoing emergency surgery for AMI. As a secondary objective, we sought to characterize baseline demographic features, presenting symptoms, admission timing, physical examination findings, and operative characteristics within a surgically confirmed AMI cohort spanning a 20-year period. By focusing on variables routinely accessible during initial assessment and at laparotomy, we aimed to provide pragmatic, real-world evidence to support early risk stratification and guide urgent clinical decision-making in this highly lethal condition.

MATERIALS AND METHODS

Study design

This study was designed as a single-center, retrospective, observational analysis of adult patients who underwent emergency surgery for acute mesenteric ischemia (AMI) at the Department of General Surgery of a tertiary university hospital. Hospital electronic medical records and institutional archived files were systematically reviewed to identify eligible cases over the 20-year study period. As a long-established tertiary-referral university hospital, the institution maintains longitudinal patient records in integrated electronic hospital information systems, supplemented by archived clinical documentation for earlier periods. Only patients with sufficiently complete demographic, clinical, operative, and outcome data were included in the final analysis.

The study protocol was approved by the Erciyes University Faculty of Medicine Ethics Committee (Approval no: 2025/541, Date: 26.11.2025), and all procedures were conducted in accordance with the Declaration of Helsinki [10].

Patient selection criteria

Patients aged 18 years or older who underwent surgical exploration for acute mesenteric ischemia and had adequately documented clinical, laboratory, intraoperative, and outcome data were eligible for inclusion. Inclusion further required that the surgical indication be consistent with acute mesenteric ischemia and that intestinal ischemia or necrosis be assessed intraoperatively.

Patients with incomplete medical records or missing key outcome variables—particularly 30-day mortality data—were excluded from the final cohort.

Study parameters

Data were collected using a standardized extraction form. Demographic variables included age and sex. Clinical presentation was assessed based on the presence of abdominal pain, nausea and vomiting, diarrhea, and melena. Time from symptom onset to hospital admission was categorized as less than 12 hours, 12 to 24 hours, or more than 24 hours. These intervals were selected a priori based on established clinical thresholds widely used in the AMI literature, corresponding to early presentation (fewer than 12 hours), intermediate delay (12–24 hours), and delayed presentation (more than 24 hours)—categories that are recognized to correlate with progressive intestinal ischemia and worsening outcomes [4,7,9]. This categorical approach was adopted to facilitate clinically meaningful interpretation and to enable comparison with prior studies examining the impact of diagnostic delay on mortality in AMI.

https://doi.org/10.5455/annalsmedres.2026.01.015

Comorbidity status was defined as the presence of at least one chronic medical condition, and atrial fibrillation was evaluated as a separate variable. Physical examination findings included abdominal distension, abdominal tenderness, voluntary guarding, and rebound tenderness. Bowel sounds at admission were categorized as hypoactive, hyperactive, or normoactive based on clinical documentation.

Among laboratory parameters, leukocyte count was selected for analysis and stratified according to routine clinical thresholds into three categories: 0–10,000/μL, 10,001–20,000/μL, and greater than 20,000/μL [11].

Intraoperative findings focused on the extent of intestinal ischemia. Massive intestinal necrosis was recorded as a distinct variable and defined, on the basis of operative reports, as transmural ischemia or necrosis involving multiple intestinal segments and/or bowel that the operating surgeon deemed to necessitate extensive resection because of widespread nonviable intestine. Classification was based on intraoperative documentation of bowel viability and the extent of ischemic involvement; however, standardized measurements of bowel length were not consistently available across all cases.

The primary outcome measure was 30-day mortality, defined as death occurring during the index hospitalization or within 30 days after admission.

Study power

Given the retrospective nature of the study, an a priori sample size calculation was not performed. A post hoc power analysis was instead conducted to assess the adequacy of the available sample. Based on the observed difference in prevalence of massive intestinal necrosis between survivors and non-survivors (21.4% vs. 70.0%), the sample of 118 patients provided statistical power exceeding 90% to detect the observed difference at a two-sided alpha level of 0.05, supporting the study's ability to identify clinically meaningful differences in the primary outcome.

Statistical analysis

All statistical analyses were performed using SPSS version 22.0 (IBM Corp., Armonk, NY, USA). Continuous variables are presented as mean ± standard deviation and were compared using the independent-samples t-test under the assumption of normality. Categorical variables are summarized as frequencies and percentages, and compared using the Pearson chi-square test; the likelihood ratio chi-square test is applied where appropriate, particularly for variables with multiple categories or low expected cell counts. A two-sided p-value of less than 0.05 was considered statistically significant.

Multivariable logistic regression was not performed. Given the retrospective design, the relatively limited number of survivors (n = 28), and the associated risk of model overfitting with multiple covariates, multivariable modeling was deemed methodologically inappropriate for the reliable identification of independent risk factors. The analysis was therefore intentionally restricted to univariate comparisons to explore associations between individual clinical, laboratory, and intraoperative variables and 30-day mortality.

RESULTS

General demographic characteristics

A total of 118 patients with acute mesenteric ischemia were included in the study. The mean age of the cohort was 64.9 ± 12.5 years (range, 35–89 years), with 71 patients(60.2%)being male and 47 (39.8%) female. The overall 30-day mortality rate

Table 1. Baseline clinical and presenting characteristics of patients with acute mesenteric ischemia (n = 118).

Variable	n (%) / Mean ± SD
Age, years	64.9 ± 12.5 (range: 35--89)
Sex	
Male	71 (60.2%)
Female	47 (39.8%)
Presenting Symptoms	
Abdominal pain	115 (97.5%)
Nausea/vomiting	74 (62.7%)
Diarrhea	18 (15.3%)
Melena	12 (10.2%)
Symptom Duration Prior to Admission	
< 12 hours	11 (9.3%)
12--24 hours	18 (15.3%)
> 24 hours	89 (75.4%)
Comorbidities	
Any comorbidity	95 (80.5%)
Atrial fibrillation	35 (29.7%)
Physical Examination Findings	
Abdominal distention	41 (34.7%)
Tenderness	101 (85.6%)
Guarding	73 (61.9%)
Rebound tenderness	37 (31.4%)
Bowel Sounds on Admission	
Hypoactive	94 (79.7%)
Hyperactive	11 (9.3%)
Normoactive	13 (11.0%)
Leukocyte Count (Categorical)	
0--10,000 /μL	11 (9.3%)
10,001--20,000 /μL	63 (53.4%)
> 20,000 /μL	44 (37.3%)
Intraoperative Findings	
Massive intestinal necrosis	69 (58.5%)
Outcome	
30-day mortality	90 (76.3%)

Note: Continuous variables are presented as mean ± standard deviation, whereas categorical variables are expressed as number (%). Age refers to the age at hospital presentation. Symptom duration represents the time interval from symptom onset to hospital admission. Massive intestinal necrosis was defined as transmural ischemia involving extensive segments of the intestine. Thirty-day mortality includes both in-hospital deaths and deaths occurring within 30 days of admission.

https://doi.org/10.5455/annalsmedres.2026.01.015

Table 2. Univariate analysis of clinical, laboratory, and intraoperative factors associated with 30-day mortality in acute mesenteric ischemia (n = 118).

Variable	Survivors (n=28)	Non-survivors (n=90)	Test statistic	p-value
Age (years) (mean ± SD)	60.07 ± 12.35	66.38 ± 12.19	t = 2.38	**0.019**
Sex				
Male Female	20 (71.4%) 8 (28.6%)	51 (56.7%) 39 (43.3%)	χ^2 = 1.94	0.163
Abdominal pain				
Present Absent	27 (96.4%) 1 (3.6%)	88 (97.8%) 2 (2.2%)	χ^2 = 0.16	0.692
Nausea--vomiting				
Present Absent	20 (71.4%) 8 (28.6%)	54 (60.0%) 36 (40.0%)	χ^2 = 1.19	0.275
Diarrhea				
Present Absent	4 (14.3%) 24 (85.7%)	14 (15.6%) 76 (84.4%)	χ^2 = 0.03	0.870
Melena				
Present Absent	3 (10.7%) 25 (89.3%)	9 (10.0%) 81 (90.0%)	χ^2 = 0.01	0.913
Symptom duration				
<12 h 12--24 h >24 h	7 (25.0%) 6 (21.4%) 15 (53.6%)	4 (4.4%) 12 (13.3%) 74 (82.2%)	χ^2 = 12.92	**0.002**
Atrial fibrillation				
Present Absent	7 (25.0%) 21 (75.0%)	28 (31.1%) 62 (68.9%)	χ^2 = 0.38	0.536
Comorbidity				
Present Absent	21 (75.0%) 7 (25.0%)	74 (82.2%) 16 (17.8%)	χ^2 = 0.71	0.399
Abdominal distension				
Present Absent	6 (21.4%) 22 (78.6%)	35 (38.9%) 55 (61.1%)	χ^2 = 2.87	0.090
Abdominal tenderness				
Present Absent	25 (89.3%) 3 (10.7%)	76 (84.4%) 14 (15.6%)	χ^2 = 0.41	0.524
Guarding (defense)				
Present Absent	15 (53.6%) 13 (46.4%)	58 (64.4%) 32 (35.6%)	χ^2 = 1.07	0.301
Rebound tenderness				
Present Absent	9 (32.1%) 19 (67.9%)	28 (31.1%) 62 (68.9%)	χ^2 = 0.01	0.918
Bowel sounds				
Hypoactive Hyperactive Normoactive	23 (82.1%) 2 (7.1%) 3 (10.7%)	71 (78.9%) 9 (10.0%) 10 (11.1%)	χ^2 = 0.22	0.897
WBC count				
0--10,000 10,001--20,000 >20,000	0 (0.0%) 18 (64.3%) 10 (35.7%)	11 (12.2%) 45 (50.0%) 34 (37.8%)	LR = 6.77	**0.034**
Massive necrosis				
Present Absent	6 (21.4%) 22 (78.6%)	63 (70.0%) 27 (30.0%)	χ^2 = 20.75	**<0.001**

Note: Data are presented as mean ± standard deviation for continuous variables and as number (%) for categorical variables. Comparisons between survivors and non-survivors were performed using the independent-samples t test for continuous variables and the Pearson chi-square test for categorical variables; the likelihood ratio test was applied where appropriate. Survivors were defined as patients alive at 30 days after admission, whereas non-survivors included in-hospital deaths and deaths occurring within 30 days. All p values are two-sided, and a p value <0.05 was considered statistically significant.

https://doi.org/10.5455/annalsmedres.2026.01.015

was 76.3%, with 90 deaths occurring within the first 30 days of admission (Table 1).

Clinical characteristics

Abdominal pain was the most frequently reported presenting symptom, identified in 115 patients (97.5%), followed by nausea and vomiting in 74 patients (62.7%), diarrhea in 18 patients (15.3%), and melena in 12 patients (10.2%). With respect to the interval between symptom onset and hospital admission, 11 patients (9.3%) presented within the first 12 hours, 18 patients(15.3%)between 12 and 24 hours, and the majority (89 patients, 75.4%) presented after more than 24 hours (Table 1).

Most patients had at least one comorbid condition (n = 95; 80.5%), with atrial fibrillation identified in 35 patients (29.7%). On physical examination, abdominal distension was present in 41 patients (34.7%), abdominal tenderness in 101 (85.6%), guarding in 73 (61.9%), and rebound tenderness in 37 (31.4%). Bowel sounds at presentation were classified as hypoactive in 94 patients (79.7%), hyperactive in 11 (9.3%), and normoactive in 13 (11.0%) (Table 1).

Laboratory parameters

Laboratory evaluation showed leukocyte counts of 0–10,000/μL in 11 patients (9.3%), 10,001–20,000/μL in 63 patients (53.4%), and >20,000/μL in 44 patients (37.3%) (Table 1).

Factors affecting mortality

Univariate analyses compared survivors (n = 28) and non-survivors (n = 90) with respect to 30-day mortality. The mean age of non-survivors (66.38 ± 12.19 years) was significantly greater than that of survivors (60.07 ± 12.35 years; p = 0.019). The sex distribution did not differ significantly between the two groups (Table 2).

No significant associations were identified between mortality and individual presenting symptoms, including abdominal pain, nausea and vomiting, diarrhea, or melena. In contrast, symptom duration was significantly associated with mortality (p = 0.002). Presentation within the first 12 hours was substantially more frequent among survivors (25.0%) than non-survivors (4.4%), whereas delayed presentation exceeding 24 hours was markedly more prevalent among non-survivors (82.2% vs. 53.6%) (Table 2).

Neither atrial fibrillation nor overall comorbidity burden was significantly associated with mortality. Among physical examination findings, abdominal distension was observed more frequently in non-survivors (38.9%) than in survivors (21.4%); however, this difference did not attain statistical significance (p = 0.090). Remaining physical examination findings and bowel sound patterns were likewise not significantly associated with mortality (Table 2).

With regard to laboratory parameters, leukocyte count categories were significantly associated with mortality (p = 0.034). Notably, no survivors had leukocyte counts in the 0–10,000/μL range; this category encompassed 11 non-survivors (12.2%). Massive intestinal necrosis was strongly associated with mortality: it was identified in 70.0% of non-survivors compared with 21.4% of survivors (p < 0.001) (Table 2).

DISCUSSION

In this retrospective study, we systematically examined the clinical, laboratory, and intraoperative factors associated with 30-day mortality in patients undergoing emergency surgery for acute mesenteric ischemia. The principal findings demonstrate that mortality remains exceedingly high in this patient population and is significantly associated with advanced age, delayed hospital presentation, marked leukocyte count alterations, and the intraoperative presence of massive intestinal necrosis [7,12]. In contrast, the nature of presenting symptoms, several physical examination findings, and certain comorbid conditions appeared to have limited value in demonstrating significant univariate associations with mortality.

The observed 30-day mortality rate of 76.3% in our cohort is consistent with the high mortality ranges reported in the literature [13]. Despite advances in diagnostic imaging and surgical techniques, acute mesenteric ischemia remains one of the most lethal abdominal emergencies, largely due to delays in diagnosis and treatment. In our series, approximately three-quarters of patients presented to the hospital more than 24 hours after symptom onset, a finding that likely contributed substantially to the unfavorable outcomes [14]. Delayed presentation is well known to facilitate progression from potentially reversible ischemia to irreversible intestinal necrosis, thereby diminishing the effectiveness of surgical intervention [9].

Age was significantly associated with mortality in our analysis [15]. The significantly higher mean age among non-survivors may be attributed to diagnostic delays and reduced physiological reserve in elderly patients. Age-related factors such as atherosclerotic vascular disease, cardiac rhythm disturbances, and coexisting systemic illnesses may predispose older individuals to compromised mesenteric perfusion and reduced tolerance to ischemic injury [16]. These findings underscore the importance of maintaining a low threshold for initiating advanced diagnostic evaluation and prompt surgical assessment in elderly patients with suspected acute mesenteric ischemia.

Evaluation of presenting symptoms revealed that abdominal pain was almost universally present; however, none of the common symptoms—including abdominal pain, nausea/vomiting, diarrhea, or melena—was significantly associated with mortality. This observation suggests that the prognostic value of clinical presentation in acute mesenteric ischemia is limited, supporting the well-described concept of a dissociation between pain severity and physical examination findings [17]. Rather than symptom intensity, the duration

https://doi.org/10.5455/annalsmedres.2026.01.015

and extent of ischemic injury appeared to be more closely associated with outcome [18].

Symptom duration was one of the clinical variables most strongly associated with mortality in this study [19]. Patients presenting within the first 12 hours demonstrated markedly higher survival rates, highlighting once again the critical importance of early diagnosis and timely surgical intervention. Conversely, the dramatic increase in mortality among patients presenting after 24 hours clearly reflects the time-dependent nature of acute mesenteric ischemia [20]. This finding emphasizes the need for heightened clinical suspicion among emergency physicians and primary care providers when evaluating patients with unexplained severe abdominal pain, particularly in high-risk populations [5].

Neither the presence of atrial fibrillation nor the overall burden of comorbid disease was significantly associated with mortality in our cohort. Although atrial fibrillation is widely recognized as a major risk factor for mesenteric embolism, its lack of association with short-term mortality in this study suggests that postoperative outcomes may be more closely related to the extent of ischemic injury and delays in intervention than to the underlying etiology [21]. Similarly, the lack of a significant association between comorbidity status and mortality suggests that the acute local and systemic consequences of mesenteric ischemia may outweigh the impact of chronic underlying diseases in the early postoperative period.

Among physical examination findings, abdominal distension was more frequent among non-survivors, although the difference did not reach statistical significance. Other signs of peritoneal irritation, including tenderness, guarding, and rebound tenderness, were not associated with mortality. These findings indicate that classical signs of an acute abdomen do not consistently carry prognostic significance in acute mesenteric ischemia [7]. This may be explained by the fact that peritoneal signs often develop late in the disease course and may be subtle or absent during the early, potentially reversible stages of ischemia [6].

With regard to laboratory parameters, only the categorical distribution of leukocyte counts showed a significant association with mortality. The presence of low leukocyte counts among non-survivors may reflect advanced sepsis or a suppressed bone marrow response in late-stage disease [22]. Nevertheless, leukocyte levels alone appear insufficient as reliable prognostic markers and should be interpreted in conjunction with clinical findings and intraoperative assessments.

The most striking finding of this study was the strong association between intraoperative massive intestinal necrosis and mortality [13]. The identification of massive necrosis in 70% of non-survivors suggests that the extent of bowel ischemia is strongly associated with adverse outcomes [1]. Massive necrosis not only necessitates more extensive bowel resection but is also associated with severe sepsis, an increased risk of short bowel syndrome, and multiorgan failure [23]. This observation highlights the critical importance of meticulous intraoperative assessment of bowel viability and supports consideration of staged procedures, including planned second-look operations, in selected patients [24].

Limitations

Several limitations of this study should be acknowledged. The retrospective, single-center design limits causal inference and introduces the potential for selection bias. Moreover, because clinical symptoms and physical examination findings were extracted retrospectively from medical records, information bias cannot be excluded. Several examination findings, including abdominal tenderness, guarding, and rebound tenderness, are inherently subjective and may have been documented variably by different clinicians during the prolonged study period, potentially limiting consistency and standardization of measurements. Additionally, because the study encompasses a 20-year period, temporal changes in diagnostic imaging, surgical techniques, perioperative intensive care practices, and institutional management strategies may have influenced patient outcomes. These changes could not be systematically adjusted for in this analysis and may have introduced unmeasured variability in mortality estimates over time. Furthermore, a standardized etiological classification of AMI subtypes (arterial embolism, arterial thrombosis, mesenteric venous thrombosis, and non-occlusive mesenteric ischemia) was not consistently available throughout the study period, precluding reliable subgroup analyses. Given the heterogeneity of AMI pathophysiology and prognosis, future studies incorporating systematic etiological stratification may improve risk characterization and prognostic precision. Likewise, standardized intraoperative measurements of the extent of bowel involvement were not consistently available, limiting objective quantification of massive intestinal necrosis. Another important limitation is the absence of a multivariable regression analysis. Although multivariable modeling was considered, the relatively small number of survivors (n=28) and the associated risk of overfitting limited the robustness of such analyses. Consequently, the associations identified in this study should be interpreted as univariate observations rather than as independent predictors of mortality, and potential confounding effects between variables cannot be excluded. In particular, clinically relevant factors such as age, delayed presentation, and the extent of intestinal necrosis may be interrelated, and the independent prognostic contribution of delayed presentation could not be reliably distinguished within the present analytical framework. Therefore, the present findings indicate associations with mortality rather than causal or independent prognostic relationships. Future multicenter studies with larger cohorts are warranted to enable robust multivariable analyses and more reliable identification of independent mortality predictors in AMI. Nevertheless, this series spans a 20-year period and includes surgically confirmed cases of acute mesenteric ischemia, providing a robust dataset

https://doi.org/10.5455/annalsmedres.2026.01.015

that reflects real-world clinical practice.

CONCLUSION

This study demonstrates that mortality from acute mesenteric ischemia remains unacceptably high and appears to be strongly associated with time to presentation and the extent of intestinal ischemia. Advanced age, delayed hospital admission, marked alterations in leukocyte levels, and the presence of massive intestinal necrosis were the variables most strongly associated with short-term mortality. These findings underscore the pivotal importance of early recognition, prompt surgical decision-making, and aggressive management strategies in patients with suspected acute mesenteric ischemia.

Ethics Committee Approval: The study protocol was approved by the Erciyes University Faculty of Medicine Ethics Committee (Approval no: 2025/541, Date: 26.11.2025).

Informed Consent: Informed consent was waived by the Ethics Committee due to the retrospective design of the study and the use of anonymized data.

Peer-review: Externally peer-reviewed.

Conflict of Interest: The authors have no conflicts of interest to declare.

Author Contributions: Conception and design: S.C., M.K.; Administrative support: M.K.; Provision of study materials or patients: S. C.; Collection and assembly of data: S.C., Data analysis and interpretation: M.K. Manuscript writing: S.C., M.K.; Final approval of manuscript: S.C., M.K. The authors are accountable for all aspects of the work and for ensuring that questions related to the accuracy or integrity of any part of the work are appropriately investigated and resolved.

Financial Disclosure: None.

Availability of Data and Materials: The datasets used and/or analysed during the current study are available from the corresponding author on reasonable request.

Artificial Intelligence Disclosure: During the preparation of this manuscript, the authors used Claude Sonnet 5 (Anthropic), an artificial intelligence-based language model, to improve the language and readability of the text. After using this tool, the authors reviewed and edited the content as necessary and take full responsibility for the content of the publication.

REFERENCES

1. Tamme K, Reintam Blaser A, Laisaar KT, et al. Incidence and outcomes of acute mesenteric ischaemia: a systematic review and meta-analysis. *BMJ Open.* 2022;12(10):e062846. doi: 10.1136/bmjopen-2022-062846.
2. Lendzion RJ, Frahm-Jensen G, Keck J. Acute Mesenteric Ischemia. *Clin Colon Rectal Surg.* 2022;35(3):227-236. doi: 10.1055/s-0042-1743283.
3. Niang FG, Faye I, Ndong A, et al. Acute mesenteric ischemia: A case report. *Radiol Case Rep.* 2023;19(1):150-152. doi: 10.1016/j.radcr.2023.10.011.
4. Kärkkäinen JM, Acosta S. Acute mesenteric ischemia (part I) - Incidence, etiologies, and how to improve early diagnosis. *Best Pract Res Clin Gastroenterol.* 2017;31(1):15-25. doi: 10.1016/j.bpg.2016.10.018.
5. Nuzzo A, Peoc'h K, Vaittinada Ayar P, et al. Improving clinical suspicion of acute mesenteric ischemia among patients with acute abdomen: a cross-sectional study from an intestinal stroke center. *World J Emerg Surg.* 2023;18(1):37. doi: 10.1186/s13017-023-00505-8.
6. Bala M, Catena F, Kashuk J, et al. Acute mesenteric ischemia: updated guidelines of the World Society of Emergency Surgery. *World J Emerg Surg.* 2022;17(1):54. doi: 10.1186/s13017-022-00443-x.
7. Sinz S, Schneider MA, Graber S, et al. Prognostic factors in patients with acute mesenteric ischemia-novel tools for determining patient outcomes. *Surg Endosc.* 2022;36(11):8607-8618. doi: 10.1007/s00464-022-09673-1.
8. Evola G, Vacante M, Evola FR, et al. Clinical Features and Outcomes of Patients with Acute Mesenteric Ischaemia in a Retrospective Study. *Chirurgia (Bucur).* 2025;120(5):583-592. doi: 10.21614/chirurgia.3127.
9. Sumbal R, Ali Baig MM, Sumbal A. Predictors of Mortality in Acute Mesenteric Ischemia: A Systematic Review and Meta-Analysis. *J Surg Res.* 2022;275:72-86. doi: 10.1016/j.jss.2022.01.022.
10. World Medical Association. World Medical Association Declaration of Helsinki: ethical principles for medical research involving human subjects. *JAMA.* 2013;310(20):2191-4. doi: 10.1001/jama.2013.281053.
11. Memet O, Zhang L, Shen J. Serological biomarkers for acute mesenteric ischemia. *Ann Transl Med.* 2019;7(16):394. doi: 10.21037/atm.2019.07.51.
12. Cui X, Chen Y, Guan G, Luo F, Zhang Z. Tricky acute mesenteric ischemia: what can we do? *Gastroenterol Rep (Oxf).* 2025;13:goaf067. doi: 10.1093/gastro/goaf067.
13. Kundan M, Chebrolu H, Muniswamppa C, et al. Outcomes of Management of Patients with Acute Mesenteric Ischemia: A Prospective Study. *Niger J Surg.* 2021;27(1):16-21. doi: 10.4103/njs.NJS_54_20.
14. De Pietro R, Martin J, Tradi F, et al. Prognostic factors after acute mesenteric ischemia: which patients require specific management? *Int J Colorectal Dis.* 2023;38(1):242. doi: 10.1007/s00384-023-04540-4.
15. Magnus L, Lejay A, Philouze G, et al. Mortality and Delays of Management of Acute Mesenteric Ischemia: The Need of a Dedicated Program. *Ann Vasc Surg.* 2023;91:28-35. doi: 10.1016/j.avsg.2022.12.070.
16. Vrba R, Řezáč T, Špička P, et al. Acute mesenteric ischaemia in the elderly - results of combined endovascular and surgical treatment. Primary study. *Sci Rep.* 2025;15(1):74. doi: 10.1038/s41598-024-84026-7. Erratum in: *Sci Rep.* 2025;15(1):7063. doi: 10.1038/s41598-025-91657-x.
17. Florim S, Almeida A, Rocha D, Portugal P. Acute mesenteric ischaemia: a pictorial review. *Insights Imaging.* 2018;9(5):673-682. doi: 10.1007/s13244-018-0641-2.
18. Martini V, Lederer AK, Fink J, et al. Clinical characteristics and outcome of patients with acute mesenteric ischemia: a retrospective cohort analysis. *Langenbecks Arch Surg.* 2022;407(3):1225-1232. doi: 10.1007/s00423-021-02423-2.
19. Harmantepe AT, Dulger UC, Gonullu E, et al. A method for predicting mortality in acute mesenteric ischemia: Machine learning. *Ulus Travma Acil Cerrahi Derg.* 2024;30(7):487-492. doi: 10.14744/tjtes.2024.48074.
20. Ozturk S, Unver M, Ozdemir M, et al. Prognostic factors in acute mesenteric ischemia and evaluation with multiple logistic regression analysis effecting morbidity and mortality. *Pol Przegl Chir.* 2020;93(1):25-33. doi: 10.5604/01.3001.0014.5824.
21. Gnanasekaran P, Ranjith N, Viswam D, Rajavel K, Ravikumar PR. Complex case of acute mesenteric ischemia in a patient with atrial fibrillation: A radiologic -surgical collaboration for timely intervention. *Bioinformation.* 2024;20(12):1922-1926. doi: 10.6026/9732063002001922.

https://doi.org/10.5455/annalsmedres.2026.01.015

22. Augène E, Lareyre F, Chikande J, et al. Platelet to lymphocyte ratio as a predictive factor of 30-day mortality in patients with acute mesenteric ischemia. *PLoS One.* 2019;14(7):e0219763. doi: 10.1371/journal.pone.0219763.
23. Bourcier S, Klug J, Nguyen LS. Non-occlusive mesenteric ischemia: Diagnostic challenges and perspectives in the era of artificial intelligence. *World J Gastroenterol.* 2021;27(26):4088-4103. doi: 10.3748/wjg.v27.i26.4088.
24. Matsune Y, Aoki T, Tashiro Y, et al. Intraoperative Assessment of Bowel Viability Using Indocyanine Green Fluorescence and Doppler Ultrasound in Incarcerated or Threatened Bowel Obstruction. *Am Surg.* 2026;92(2):619-621. doi: 10.1177/00031348251378905.

https://doi.org/10.5455/annalsmedres.2026.01.015